AHTD TRC TRANSPORTATION RESEARCH COMMITTEE

TRC8705

The Development of ROADHOG: A Flexible Pavement Overlay Design Procedure

R. P. Elliott, K. D. Hall, N. T. Morrison, K. S. Hong

Final Report

1990

FINAL REPORT

TRC-8705
NDT OVERLAY DESIGN

The Development of ROADHOG
A Flexible Pavement Overlay Design

by

Robert P. Elliott, Kevin D. Hall

Neal T. Morrison, and Kong Soon Hong

Conducted by

Arkansas Highway and Transportation Research Center
Department of Civil Engineering
Engineering Experiment Station
University of Arkansas

in cooperation with

Arkansas State
Highway and Transportation Department

and

U.S. Department of Transportation
Federal Highway Administration

Report No. UAF-AHTRC-90-001

University of Arkansas
Fayetteville, Arkansas 72701

November, 1990

Technical Report Documentation Page

1. Report No. FHWA/AR-91-003	2. Government Accession No.	3. Recipient's Catalog No.
4. Title and Subtitle TRC-8705, NDT OVERLAY DESIGN The Development of ROADHOG A Flexible Pavement Overlay Design Procedure		5. Report Date November 1990
		6. Performing Organization Code
7. Author(s) Elliott, R.P., Hall, K.D., Morrison, N.T. and Hong, K.S.		8. Performing Organization Report No. UAF-AHTRC-90-001
9. Performing Organization Name and Address Arkansas Highway and Transportation Research Center Department of Civil Engineering University of Arkansas Fayetteville, Arkansas 72701		10. Work Unit No. (TRAIS)
		11. Contract or Grant No. TRC-8705
12. Sponsoring Agency Name and Address Arkansas State Highway & Transportation Department Materials and Research Division P. O. Box 226 Little Rock, Arkanss 72203		13. Type of Report and Period Covered Final Report
		14. Sponsoring Agency Code

15. Supplementary Notes

Study Conducted in cooperation with the U.S. Department of Transportation, Federal Highway Administration

16. Abstract

A flexible pavement overlay thickness design procedure was developed. The procedure follows the AASHTO structural number approach to flexible pavement design and uses the structural deficiency concept in selecting the overlay thickness. The subgrade resilient modulus (M_r) and existing pavement structural capacity (effective structural number or SN_{eff}) are determined from NDT data obtained using a falling weight deflectometer. M_r is calculated using the deflection measured 3 feet from the FWD center of loading. This method of calculation is based on ILLI-PAVE finite element pavement analyses and was selected following an evaluation of various available NDT back calculation methods. SN_{eff} is determined from the difference between the deflections at the center of loading and the deflection at a distance form the center equal to the total pavement thickness. The SN_{eff} determination method was developed under this study.

The complete procedure is programmed for use on an IBM PC, XT, AT, or any compatible system having at least one floppy drive and a minimum of 364K of available RAM. The program is user friendly and runs interactively. It is menu-driven and features on-line help facilities.

17. Key Words Overlay Design, Flexible Pavement, Deflection Analysis, Non-destructive Testing, Effective Structural Number	18. Distribution Statement No restrictions

19. Security Classif. (of this report)	20. Security Classif. (of this page)	21. No. of Pages	22. Price

Form DOT F 1700.7 (8-72)

Reproduction of completed page authorized

ACKNOWLEDGEMENTS/DISCLAIMER

This report is based on the findings of Project TRC-8705, NDT Overlay Design.

TRC-8705 is sponsored by the Arkansas State Highway and Transportation Department and the U.S. Department of Transportation, Federal Highway Administration.

The contents of this report reflect the view of the authors who are responsible for the facts and the accuracy of the data presented herein. The contents do not necessarily reflect the official views or policies of the Arkansas State Highway and Transportation Department or the Federal Highway Administration. This report does not constitute a standard, specification, or regulation.

SI CONVERSION FACTORS

1 inch = 25.4 mm

1 foot = 0.305 m

1 pcf = 16 kg/m^2

1 psi = 6.9 kN/m^2

1 ksi = 6.9 MN/m^2

1 lb = 4.45 N

TABLE OF CONTENTS

LIST OF TABLES

LIST OF FIGURES

Figure		Page

CHAPTER 1

PROJECT OVERVIEW

1.1 INTRODUCTION

In recent years, highway programs nationwide have shifted their emphasis from new construction to rehabilitation, maintenance and preservation. With this shift, a major deficiency in pavement design technology became more significant. That deficiency was the lack of practical, proven design procedures for selecting the thickness of pavement overlays. The need for a flexible pavement overlay design procedure was particularly significant in Arkansas where, except for Interstate pavements, most highways have flexible pavements.

TRC-8705, Development of a Flexible Pavement Overlay Design Procedure Utilizing Nondestructive Testing Data, was initiated to correct the deficiency. As originally envisioned, TRC-8705 would develop an NDT (nondestructive testing) based overlay design procedure using mechanistic pavement design principles (Figure 1.1). As such major activities of the project as originally proposed were the development of design and analysis algorithms and the selection of performance transfer functions.

However, as the study progressed, the procedure development was shifted from a mechanistic base to an empirical (structural number) base. Two factors were responsible for the shift. The first factor was the difficulties encountered in the use of backcalculation procedures for determining modulus values for the various pavement layers. These difficulties demonstrated the magnitude of the mechanistic undertaking and clearly showed that the complete development of a mechanistic design procedure would not be possible within the limits of the project time and funding. The second and more decisive factor was the publication of the 1986 AASHTO Guide for Design of Pavement Structures (1).

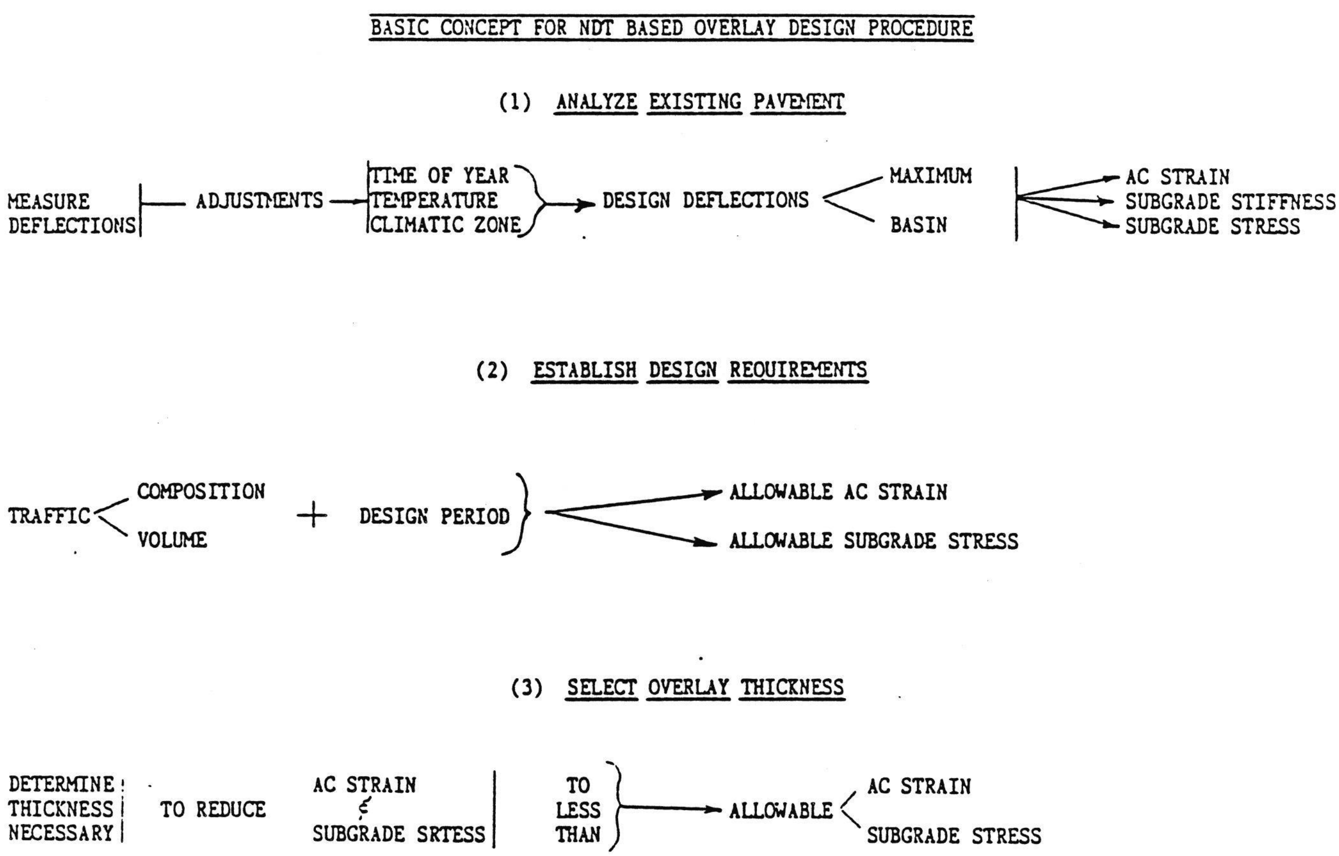

Figure 1.1 Overlay Design Concept as Initially Envisioned.

From the beginning, the major objective of the project was to develop a practical, easy to use design procedure that was compatible with other AHTD pavement design practices and that consistently produced reasonable design thicknesses. AHTD designs pavements using the AASHTO Guide. When the 1986 Guide became available, AHTD began to transition to it from the previous Guide. Unlike the previous Guide, the 1986 Guide contained procedures for overlay design. These were not complete but they did provide a framework around which a complete design procedure could be developed that would be compatible with the new pavement portions of the Guide and, thus, be compatible with AHTD's other pavement design practices. Consequently, with the approval of the Project Subcommittee, the study was redirected during the second year to the development of an NDT overlay design procedure following the general approach presented in the 1986 AASHTO Guide.

1.2 AASHTO OVERLAY APPROACH

The AASHTO approach to flexible pavement design uses a Structural Number (SN) to refelct the combined structural contribution of all the pavement layers. SN is defined by the equation:

$$SN = a_1 D_1 + a_2 D_2 + a_3 D_3 \qquad \text{(Eq 1.1)}$$

where

a_i = structural layer coefficient for the surface (1), base (2), and subbase (3),

D_i = thicknesses of the surface (1), base (2), and subbase (3).

For overlay design, the 1986 Guide uses SN in a structural deficiency approach to design. In its simplest terms, the structural deficiency approach states that the overlay required is simply the difference between the total structure needed and the structure that currently exists. The Guide expresses this with the following equation:

$$SN_{OL} = SN_y - F_{RL}SN_{eff} \qquad \text{(Eq 1.2)}$$

where

SN_{OL} = required structural number of the overlay

SN_y = total structural number required to carry future trasffic

F_{RL} = remaining life factor (discussed in detail in Chapter 5)

SN_{eff}= effective structural number of the existing pavement.

The thickness of the overlay is determined using the relationship:

$$D_{OL} = SN_{ol}/a_{ac}$$

where a_{ac} is the structural layer coefficient for the asphalt concrete overlay material.

Within this general approach, the major components lacking for a complete, workable design procedure were specific methodologies for determining SN_{eff} and the subgrade resilient modulus needed for determining SN_y. Other componenets also needed to be examined and/or modified for practical use. In particular, the remaining life factor needed to be studied. As a result, the major activities under the study after the shift in direction was the selection and/or development of procedures for determining the subgrade modulus (Chapter 3) and SN_{eff} (Chapter 4).

1.3 PROCEDURE DEVELOPMENT

A flow diagram of a complete overlay design procedure that follows the general approach from the 1986 AASHTO Guide was developed. As illustrated in Figure 1.2, a complete procedure would consider original construction data and past performance data as well as NDT data in the selection of the overlay thickness. It was recognized from the beginning that the procedure developed

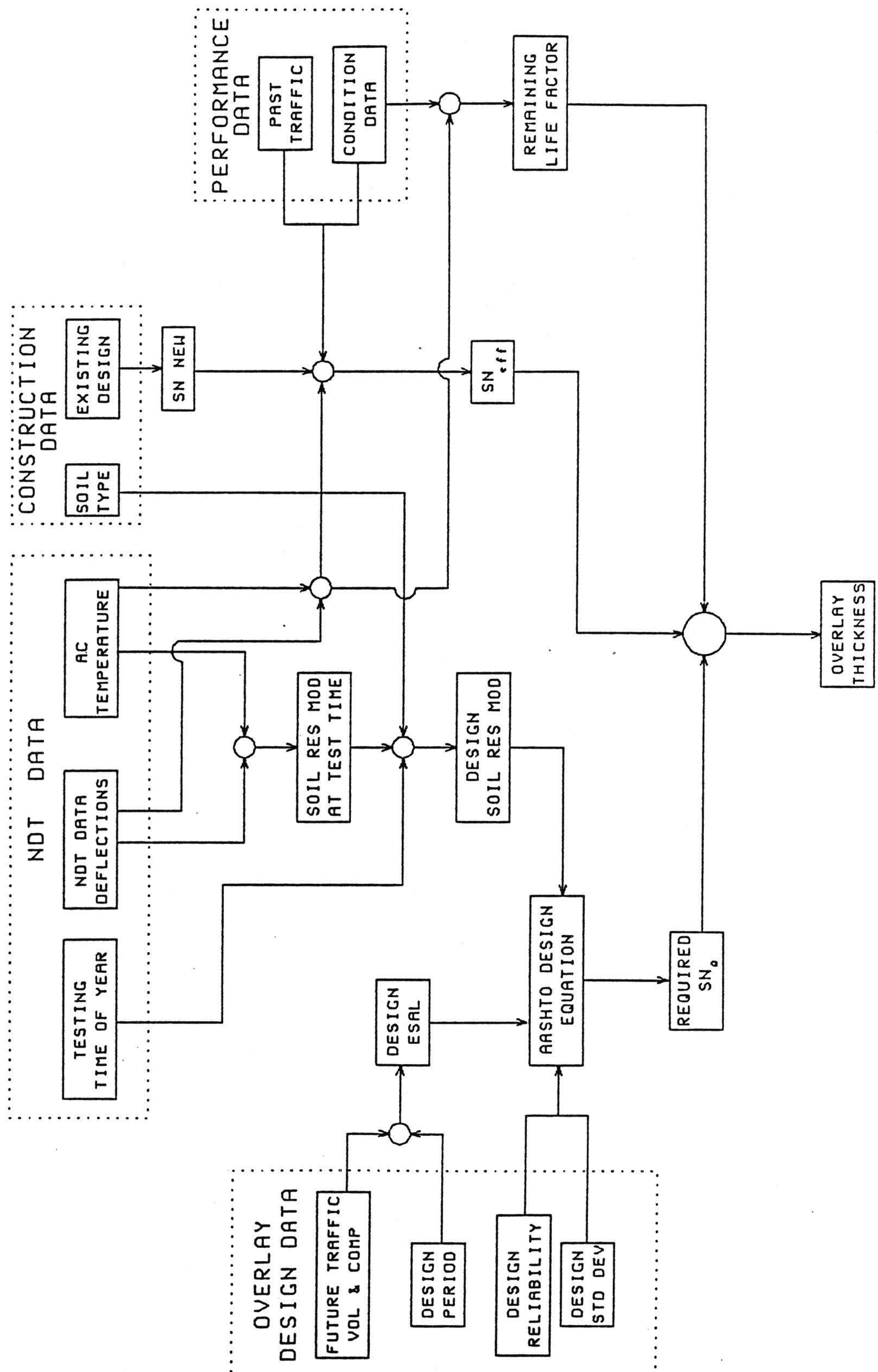

Figure 1.2 Flow Diagram for AASHTO Based Overlay Design Procedure.

under the study would not encompass all of the flow lines. In particular, the development of procedures for the consideration of construction and past performance data went beyond the scope of the study. Nevertheless, the conceptual interaction of these data were included on the flow diagram for completeness; and this flow diagram served as the basis for development and programming the final design procedure.

The design procedure was programmed in a modular fashion with each major function performed in a separate module. This was done to facilitate modification of the program when improved methods become available in the future. The programming was done in Clipper (2). Clipper was selected becasue it provided the capability to produce a user friendly format and a stand-alone, executable program that could be used on any PC compatible computer with minimal hardware requirements and no additional software requirements.

The completed design procedure was named ROADHOG to designate that it is a roadway design tool that was developed at the Univerity of Arkansas (the Razorbacks). Figure 1.3 shows the primary program modules of ROADHOG as they relate to the flow diagram in Figure 1.2. Besides the modules illustrated in Figure 1.3, the complete program contains two additional modules, XFORM and OUTPUT, that perform input/output functions and necessary data manipulations. The following are brief descriptions of the modules.

XFORM - The FWD used by AHTD stores the NDT data in an ASCII format on a floppy disk; XFORM reads this data and transform it into a database file (dBASE format) that can be used by the other modules.

SNEFF - This module uses the NDT data to calculate SN_{eff} at each NDT test location. Chapter 4 documents the development of the procedure used for the calculation.

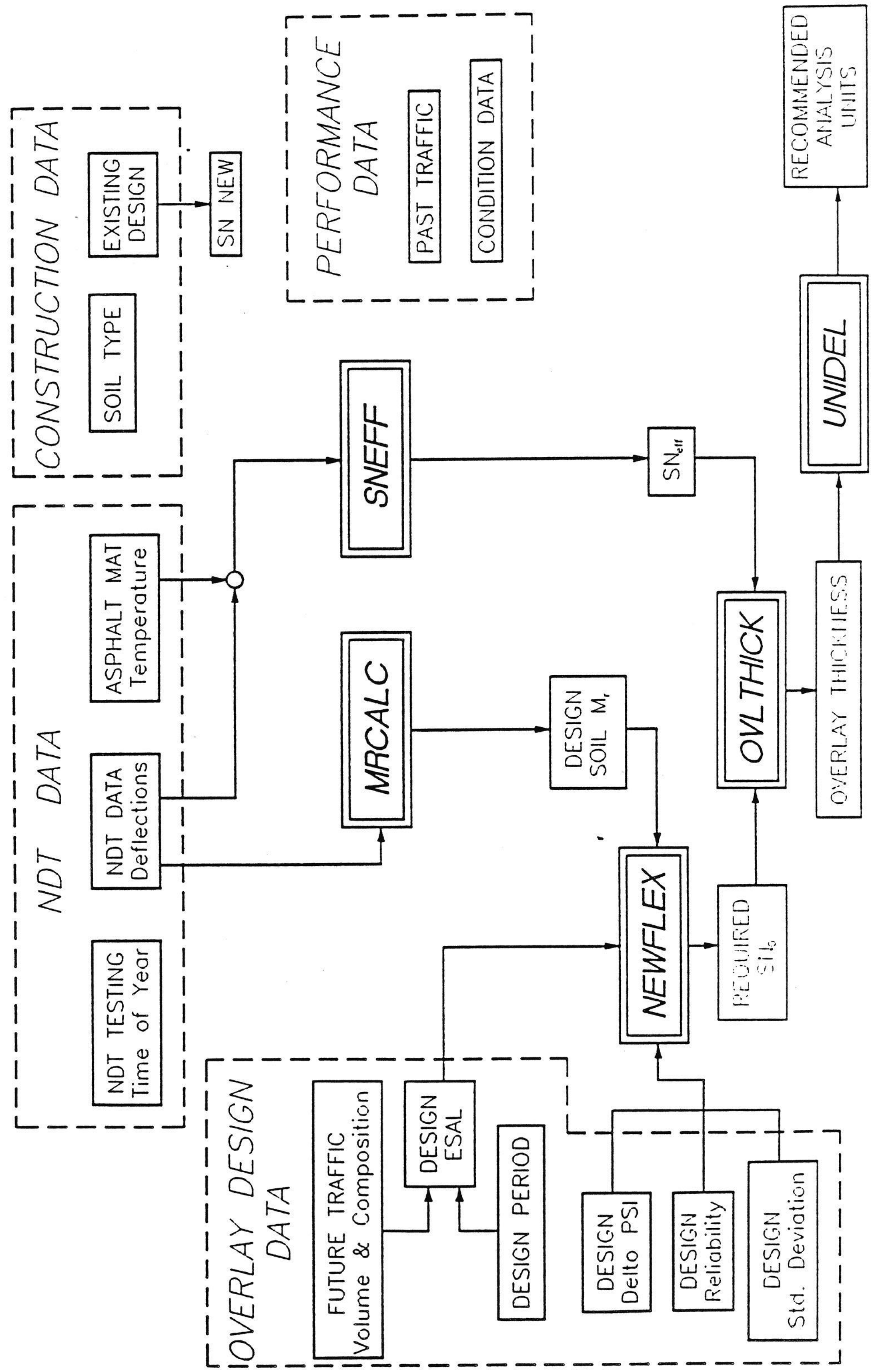

Figure 1.3 Flow Diagram for the ROADHOG Overlay Design Program.

MRCALC - The subgrade resilient modulus at each test location is calcualted in this module. The method of calculation and its development is presented in Chapter 3.

NEWFLEX - This module contains the AASHTO pavement design performance equation. It is used to determine SN_y for each test location using the subgrade modulus from MRCALC and the required performance data input by the designer.

OVLTHICK - The required overlay thickness at each test location is calculated in this module.

UNIDEL - This module analyzes the point-by-point overlay thicknesses from OVLTHICK to divide the overlay project into subprojects. This aids the designer in developing a "balanced" design that uses different overlay thicknesses according to what is needed in various areas. Details of UNIDEL are discussed in Chapter 6.

CHAPTER 2

TRANSFER FUNCTIONS FOR MECHANISTIC DESIGN

2.1 INTRODUCTION

As discussed in Chapter 1, TRC-8705 was initiated with the intent to develop a mechanistic based overlay design procedure. However, as the study progressed, the procedure development was shifted from a mechanistic base to an empirical, structural number base. Nevertheless, before the shift, a significant amount of effort was devoted to reviewing and identifying appropriate transfer functions that could be used in a mechanistic design procedure. This chapter is devoted to documenting that effort. The reader should keep in mind that none of the material discussed in this chapter was used in the design procedure developed.

2.2 THE MECHANISTIC CONCEPT OF DESIGN

Procedures for the structural design of pavement systems are generally categorized as either empirical or theoretical. In the pure empirical procedure, the design is based solely on experience and the past performance of existing pavements. Consequently, use of the empirical procedure is limited to materials, thicknesses, loadings, etc. for which experience and performance data are available. Theoretical procedures, on the other hand, are based on the analysis of the effects of traffic generated stresses, strains, and deformations on the behavior of the pavement materials. In concept at least, the theoretical approach is more widely applicable to designs, materials, and conditions for which experience is not available. However, the analytical complexity of the pavement system and its environment prevents the development of a "totally theoretical" procedure.

The mechanistic concept of pavement design provides an avenue for integrating the empirical and theoretical approaches. This marriage of approaches is accomplished through the use of Transfer Functions. A Transfer Function relates traffic generated structural response (stresses, strains, and deformations) to the number of load applications (18K ESAL's) a pavement can carry to some state of failure. The stresses, strains, and deformations are determined from a theoretical structural analysis. The number of load applications to failure are established from the analysis of past performance (empirical data) and supplemented, where necessary, with laboratory material behavioral relationships. This paper examines various Transfer Functions for use in mechanistic design procedures and develops recommendations for selecting appropriate Transfer Functions for practical design.

2.3 MODEL DEPENDENCY OF TRANSFER FUNCTIONS

In examining, selecting, and using Transfer Functions, it must be recognized that the Transfer Functions from various sources should not be compared directly but must be viewed either in general terms or within the context of the procedures for which they were developed. Transfer Functions serve as a bridge between "real world" performance and the structural model that serves as the basis of the design procedure. Since the stresses, strains, and deformations predicted for a given pavement situation are not identical for all structural models, the relationships between structural response and pavement life (i.e.the Transfer Function) must also be different.

As a result, Transfer Functions must be recognized as being "model dependent"; and Transfer Functions from one design procedure should not be used directly in another procedure without a thorough determination of applicability and compatibility. The general format and types of Transfer Functions, however, can be used.

2.4 TYPES OF TRANSFER FUNCTIONS

In the mechanistic approach to pavement design, a combination of materials and thicknesses is selected that limits the load-induced stresses, strains and deformations to levels that are tolerable for the volume and composition of traffic expected over the life of the pavement. This requires an identification of the critical structural responses (stress, strain, and/or deformation) and the determination of their relationships to pavement performance. These critical response-performance relationships constitute the design Transfer Functions.

For Full Depth asphalt concrete (AC) and conventional (AC surface on a granular base/subbase) flexible pavements, two structural response parameters are generally accepted as being critical. These are the maximum tensile strain at the bottom of the AC layer and the maximum structural response (stress or strain) at the top of the subgrade. These are generally selected because they relate to the two most prevalent load-related distress types - fatigue cracking in the AC layer (AC tensile strain) and subgrade rutting (subgrade response). Transfer Functions based on these response parameters serve as the basis for the four more well known mechanistic design procedures - 1) FHWA's VESYS procedure (3), 2) PDMAP developed under the National Cooperative Highway Research Program Project 1-10B (4), 3) The Asphalt Institute's (TAI) procedure (5), and 4) the Shell design procedure (6).

A third structural response for which Transfer Functions are available is surface deflection. Deflection has been used as the basis for overlay design (7) but has not been used in mechanistic design procedures for new construction. Nevertheless, it has several advantages over the other two parameters that make it an attractive choice as a design criterion and worthy of examination. First, deflection is the one structural response parameter that is easily visualized and readily measured under prototype loading conditions. Consequently design engineers can relate to and understand a deflection-based design procedure more easi+y. Secondly, the deflection measurements on completed sections give immediate "feedback" on at least a portion of the design approach. Thirdly, strong relationships exist between surface deflection and the other response parameters. Analysis algorithms reported by Thompson and Elliott (8) and Gomez and Thompson (9) show that both subgrade response and AC strain can be predicted with good accuracy using deflection measurements. A deflection based procedure would therefore also reflect a consideration of these two parameters.

2.5 FATIGUE FUNCTIONS

Fatigue Transfer Functions reflect the fatigue behavior of AC. This behavior has been studied by many investigators mostly by subjecting laboratory mixture specimens to repeated applications of load until some failure state has been reached. A variety of testing methods and failure definitions have been used by the different researchers. The method of test and the failure definition have been found to have some influence on the test results. Nevertheless, researchers agree that the general form of the fatigue relationship in terms of asphalt strain is:

$$\log N = K + n \log (1/eac) \qquad \text{(Eq 2.1)}$$

where

N = number of load applications to failure

eac = maximum tensile strain in the asphalt

K & n = constants determined by testing.

At least one researcher (10) has found that a single relationship of this form adequately describes the fatigue behavior of a given mix regardless of test temperature and the resulting mix stiffness. Nevertheless many other researchers (4, 11, 12, 13) have found that the dynamic stiffness modulus (Eac) of the specimen also influences the fatigue test results. Based on this, a more general form of the fatigue relationship is:

$$\log N = K + n \log (1/eac) + b \log (1/Eac) \qquad \text{(Eq 2.2)}$$

Two general types of fatigue testing are used. These are: 1) controlled stress tests in which the magnitude of stress is held constant throughout the test and 2) controlled strain tests in which strain is held constant. Of these, the controlled stress test results in the shorter fatigue life and is more severe. This is due to the change in specimen stiffness that occurs as the testing proceeds. During the testing, the stiffness slowly decreases. To maintain a constant stress with the decreasing stiffness, the load induced strain must increase. Conversely, under the constant strain test, the stress level (and therefore applied loading) must decrease as the test proceeds.

Several researchers have investigated the implications of this effect relative to pavement design. Finn (14) concluded that the constant strain test should be used for relatively thin (<5") asphalt surfacings and that the constant stress test should be used for thicker surfacings. Pell (15) reached essentially the same conclusion. He found that the constant strain test was appropriate for asphalt thicknesses of 2 inches or less and that the constant stress test was appropriate for thicknesses of 6 inches or greater.

Regardless of which test is appropriate at any particular thickness, these results suggest that one fatigue relationship may not be appropriate for all thicknesses. For practical design purposes, it may be necessary to develop two Fatigue Transfer Functions, one for Full Depth AC pavements and another for conventional (AC over granular base) flexible pavements.

The influence of type of test on the fatigue relationship also demostrates that the laboratory fatigue results cannot be used directly for design purposes. In actual pavements, there is a continuous variation in the load conditions, in the AC stiffness (Eac), and in the subgrade support. Consequently, the behavioral relationships are quite complex and never approach either a constant strain or a constant stress condition. A more practical approach that has been used (16) is to assume the basic fatigue equation relationship (Eq 2.2), adopt values for the "n" and "b" constants based on laboratory results, and determine an appropriate k value from analysis of actual pavement performance data.

However, even this may not be entirely appropriate since the "n" and "b" values themseleves may be influenced by the testing conditions and definition of failure. For example, Pell (15) has shown that the value of "n" is greater under constant strain conditions than under constant stress. He also has found that "n" is affected by the definition used for failure. For the same mixture, the "n" coefficient for applications to crack initiation was found to be greater than the "n" coefficient when crack propagation through the specimen was included. Since the failure of a pavement would appear to be more closely related to the propagated crack than to crack initiation, this would suggest that the "n" coefficient for pavement performance purposes may be somewhat less than the coefficient determined by laboratory fatigue tests. The AC surfacing in real pavements, therefore, may be somewhat more sensitive to strain level than laboratory fatigue testing would suggest.

This was also demonstrated by work reported by Van Dijk (17). Van Dijk tested various mixes in a wheel tracking machine and monitored the strains and load applications to various stages of "failure". He then developed fatigue equations from the data. His work showed that the "n" coefficient based on surface cracking was always less than the "n" coefficient based on hairline cracking at the bottom of the AC layer (a condition similar to typical laboratory "failure"). He also found both "n" coefficients to be less than that found when testing the same mixes by normal laboratory fatigue methods. For a dense graded mix similar to those typically used in the U.S., he found "n" to be 4.23 for hairline cracking at the bottom and 2.66 for cracking at the surface.

Nevertheless, laboratory testing must be relied upon to give some indication of the appropriate "n" and "b" values. Bonnaure et al. (11) reviewed the results of laboratory fatigue testing conducted by many researchers throughout Europe. On the basis of their review, they proposed fatigue relationships in which "n" is equal to 5 and "b" is equal to 1.8 for controlled strain testing and 1.4 for constant stress conditions. Their constant strain relationship (n = 5, b = 1.8) is used as the Fatigue Transfer Function in the Shell (6) design procedure.

The TAI (18) design procedure uses a Fatigue Transfer Function in which "n" equals 3.29 and "b" equals 0.854. This relationship was developed by Finn (4). Finn selected the "n" and "b" values from reported laboratory fatigue relationships. He subsequently analyzed pavement data from selected sections of loops 4 and 6 of the AASHO Road Test. From the analysis, he established a K value based on the number of load repetitions those pavements carried prior to the appearance of fatigue cracking over approximately 20% of their surface area.

The AASHO Road Test flexible pavements were also analyzed by Elliott and Thompson (19). For their analysis, they used "n"coefficients of 3.16 and 3.29 and "b" coefficients of .854, 1.4 and 1.8. The combination of "n" equal to

3.16 and "b" equal to 1.4 was found to provide the best fit to the performance data.

In the same paper, Elliott and Thompson developed "n" coefficients for conventional flexible pavements using the AASHO Road Test deflection equations with their ILLI-PAVE asphalt strain algorithm. This analysis produced "n" coefficients of 2.92 and 3.27 for terminal Present Serviceablity Indexes of 2.5 and 1.5 respectively.

In another research study, Elliott and Herrin (20) examined the relative fatigue characteristics of dense graded mixes using a relationship developed by Maupin and Freeman (21) between the split tensile strength of an asphalt mix and its laboratory fatigue properties. Maupin and Freeman's work indicates that the "n" coefficient can be predicted with reasonable accuracy by the equation:

$$n = .0374\ ST - .744 \qquad \text{(Eq 2.3)}$$

where

ST = the split tensile strength in psi.

Elliott and Herrin used this relationship to estimate the "n" coefficient for 9 mixes used by the Illinois Department of Transportation. The values found ranged from 1.89 to 5.90 with a mean value of 3.50.

Other estimates of the "n" coefficients can be made using procedures developed by Cooper and Pell (22). Their procedures estimate the fatigue equation for a mix based on the volumetric asphalt content and the ring and ball softening point of the asphalt. Using the Cooper and Pell procedures with mix data reported by Elliott and Herrin (20), the "n" coefficients for the 9 Illinois mixes were estimated to range from 3.28 to 4.53.

These values compare favorably with the values obtained from laboratory fatigue tests on a similar mix as reported by Shurma and Larson (23). This mix was an AC surface course commonly used in Pennsylvania. The fatigue testing was performed by TAI. The "n" coefficients found ranged from 3.51 when tested at 85 F to 3.92 at 55 F.

2.6 FATIGUE FUNCTION SENSITIVITY ANALYSIS

The research cited above indicates that the appropriate "n" coefficient for typical dense graded AC mixes would be in the range of 3.0 to 4.0. To check the significance of any one particular value, a sensitivity analysis was conducted using "n" coefficients ranging from 2.8 to 5.0. For this sensitivity analysis, the "b" coefficient was held constant at 1.4.

The analysis was conducted in two phases. In the first phase, fatigue equations were established based on analyses of the performance of the Loop 4 AASHO Road Test pavements. These were established using the techniques reported by Elliott and Thompson (19). The second phase involved selecting AC design thicknesses for three levels of traffic using the developed fatigue relationships.

The results of the "n" coefficient sensitivity study is shown in Figure 2.1. The design thickness is seen to be more sensitive to the strain level as the "n" coefficient decreases (greater difference in thickness between low and high traffic volumes). It is also seen that the thickness at higher traffic volumes is influenced more by the "n" coefficient than is the thickness at lower volumes.

A similar analysis was conducted relative to the value of the "b" coefficient. For this analysis, the "n" coefficient was set at 3.0. The results of this study are shown in Figure 2.2. Again, the greater AC thicknesses are found to be more sensitive to the value of the "b" coefficient. However, since the thickness at each traffic level generally decreases with increasing "b"

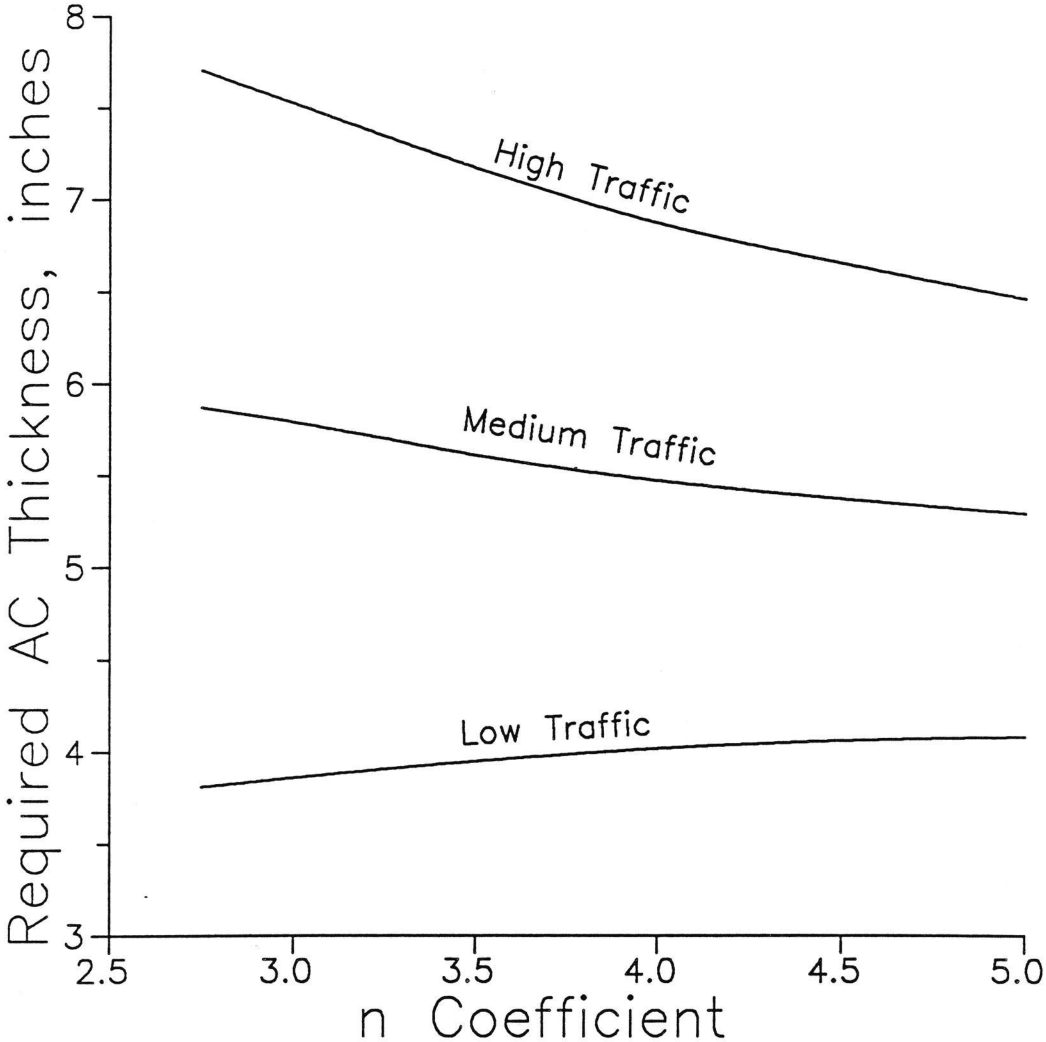

Figure 2-1. Sensitivity of Design Thickness to "n" in the Fatigue Transfer Function.

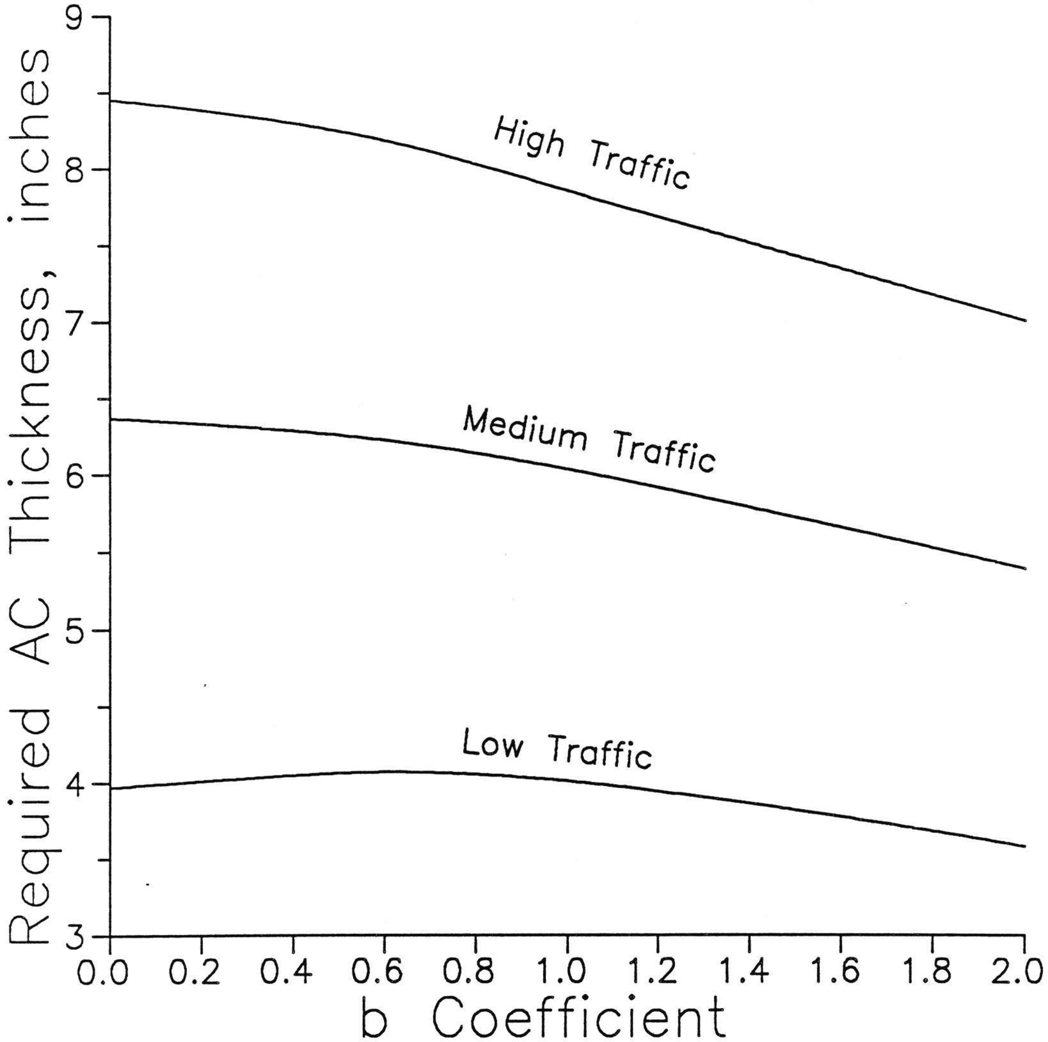

Figure 2-2. Sensitivity of Design Thickness to "b" in the Fatigue Transfer Function.

value, the relative sensitivity (thickness difference from high to low traffic) to strain level is not as great for "b" as it is for "n".

Based on these two sensitivity analyses, 3.0 would appear to be a practical value to use for "n" in developing Fatigue Transfer Functions. As shown in Figure 2.1, this value would provide strong sensitivity to traffic loading and the load induced strain. It would also be in the range indicated by the rresearch discussed above.

There is less guidance as to an appropriate practical value for "b". Howeever, the real significance in the value selected is in the thickness differential it produces going from low to medium to high traffic. In this regard, Figure 2.2 shows little difference as "b" changes. An appropriate value, therefore, might be 0.0 which in effect eliminates Eac from the equation and simplifies the Transfer Function.

2.7 SUBGRADE FUNCTION

The concept of limiting the load-induced subgrade stress or strain has long been recognized as a valid flexible pavement design criterion. This concept served as the basis for the CBR design procedure that was in general use for many years and that is still used by some agencies.

The purpose of the subgrade Transfer Function is to control the development of permanent subgrade deformation and the corresponding appearance of rutting at the pavement surface. Knutson et al. (24) studied the permanent deformation behaviour of several cohesive soils finding that the behavior could be modeled by the equation:

$$ep = AN^b \qquad \text{(Eq. 2.4)}$$

In this equation, ep is the permanent strain after N applications of stress; and A and b are coefficients determined by testing. The b coefficient was found to vary between 0.1 and 0.2 depending upon soil type. The A coefficent was found to be a function of the ratio of applied stress to the soil's "threshold stress" (the stress level above which permanent deformation was found to accumulate rapidly). The "threshold stress" is approximatly equal to the unconfined compressive stress.

In other research on the permanent deformation behavior of cohesive soils, Poulsen and Stubstadt (25) found a strong correlation between the soils' resilient modulus and the "permissible" deviator stress. (The "permissible" deviator stress was the stress level that resulted in 2 percent permanent strain after 100,000 applications.) The stress-resilient modulus relationship was found to change very little when numbers of load applications other than 100,000 were used. This lack of sensitivity to numbers of load applications is consistent with the low b coefficients for Eq 2.4 found by Knutson et al. The stress-resilient modulus relationship is also consistent with the A coefficient being a function of the stress ratio. There exists a strong correlation between the unconfined compressive strength and a soil's resilient modulus (9). Consequently, unconfined compressive strength could be substitued for resilient modulus in the Poulsen and Stubstadt's deviator stress-resilient modulus relationship. This would result in a stress ratio relationship.

Most currently used mechanistic design procedures use a Transfer Function that relates subgrade vertical strain to pavement life. The general form of the Transfer Functions used in these procedures is:

$$\log N = k + a \log (1/ez) \qquad \text{(Eq 2.5)}$$

where

ez = the load-induced vertical strain at the top of the subgrade

k & a = constants determined from analysis.

Barker et al. (26) reported a comparative study of the Subgrade Strain Transfer Functions that have been reported by various researchers around the world. The Transfer Functions that they studied, as well as several additional ones reported in the literature (5, 6, 32, 43) were examined as a part of this study. Of particular interest are the Transfer Functions used in the Shell, TAI, and Kentucky design procedures. The Shell and Kentucky functions form upper and lower bounds for the functions reported; and the TAI function more or less fits through the middle of the functions.

For comparison purposes, a subgrade vertical strain Transfer Function was developed through analysis of data from Loop 4 of the AASHO Road Test. This analysis was conducted using the approach previously reported by Elliott and Thompson (19) except that the log of subgrade strain was used instead of subgrade deviator stress. The developed equation is shown in Figure 2.3 together with the Shell, TAI, and Kentucky Transfer Functions.

The subgrade Transfer Function, however, need not be linked to subgrade vertical strain. The research reported by Poulsen and Stubstadt (25) and by Knutson et al. suggests that a stress based Transfer Function would be appropriate. Similarly, in reporting on the development of South Africa's mechanistic design procedure, Walker et al. (27) stated a preference for a function based on shear stress. A later paper by Maree and Freeme (28) indicated that South Africa had adopted a strain based function but expressed dissatisfaction with its use.

Chou (29) has suggested developing a Transfer Function based on a stress factor. He defines the stress factor as a function of the subgrade deviator stress and the depth within the subgrade. The subgrade is divided into layers and the average deviator stress is determined for each layer. The stress factor is the summation of the products of deviator stress and layer thickness.

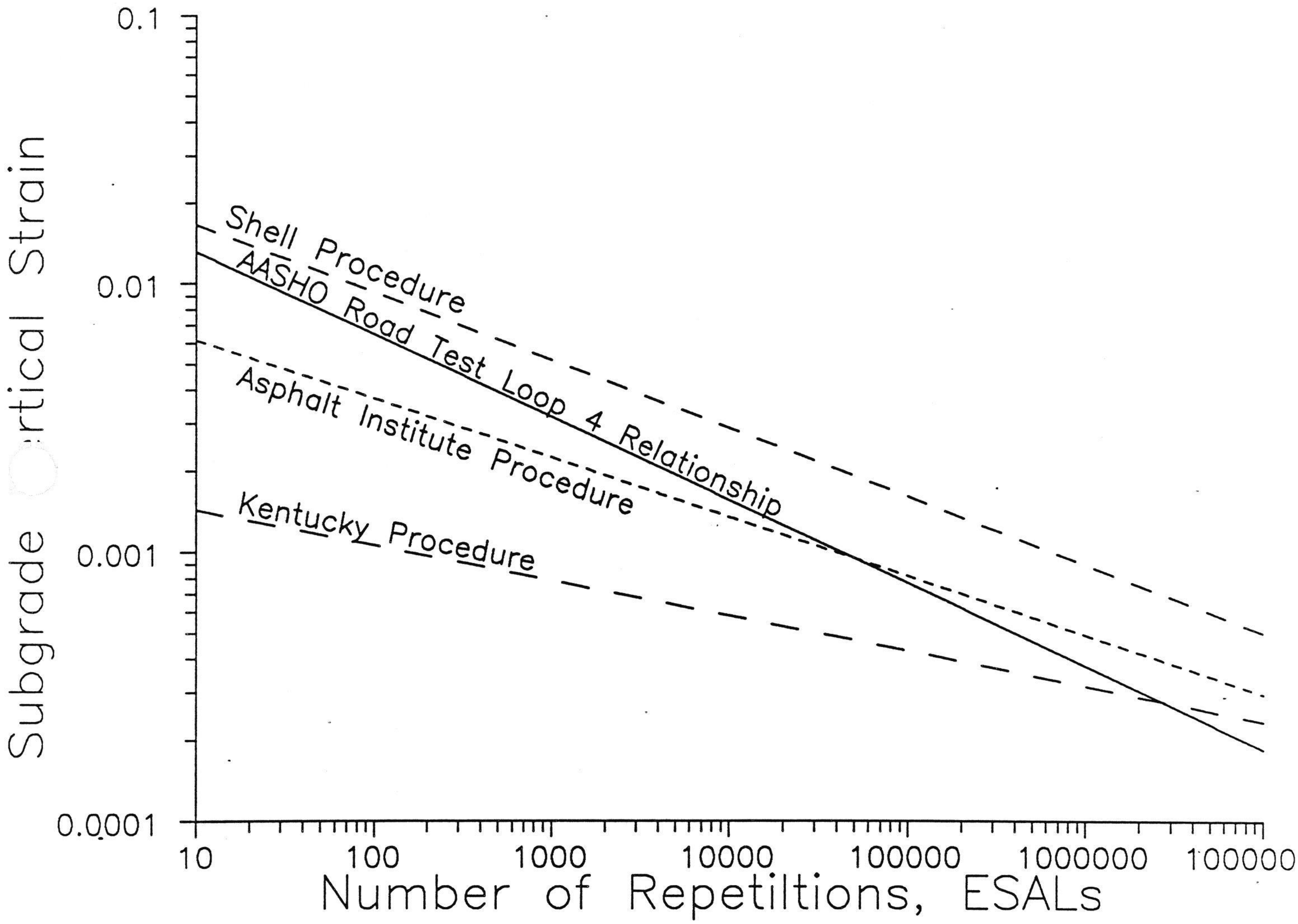

Figure 2-3 Comparison of Various Subgrade Strain Transfer Functions.

Elliott and Thompson (16) investigated Chou's stress factor relative to the stress dependent finite element structural model ILLI-PAVE. They found that the stress factor could be reliably predicted by using the top of subgrade deviator stress alone. They subsequently combined this finding with Knutson et al. research findings (24) and developed a subgrade stress ratio Transfer Function concept. In this concept the Transfer Function has the form:

$$\log N = k + a\,Sr \qquad \text{(Eq 2.6)}$$

where

Sr = stress ratio, subgrade deviator stress divided by the unconfined compressive strength

k & a = constants determined from analysis.

For comparison purposes, Transfer Functions were developed based on both the subgrade strain and the subgrade stress ratio concepts using the data from Loop 4 of the AASHO Road Test. The following lists the developed equations, their correlation coefficients (R), and their standard errors of estimate.

STRAIN TRANSFER FUNCTION

$$\log N = -4.97264 + 3.204 \log (1/ez) \qquad \text{(Eq 2.7)}$$

R = .891 Std. Err. = .253

STRESS RATIO TRANSFER FUNCTION

$$\log N = 7.25573 - 5.179\,Sr \qquad \text{(Eq 2.8)}$$

R = .908 Std. Err. = .233

The stress ratio equation is seen to have a higher correlation coefficient and a lower standard error of estimate. Although the differences are not significant, they do suggest that a stress ratio Transfer Function would be at least as reliable as one based on subgrade strain. This being the case, the stress ratio Transfer Function appears to be the more practical. Pavement engineers are generally more attuned to thinking in terms of stress and stress ratios than they are to strain. Also, the unconfined compressive strength is a soil property familiar to all engineers that is readily measured.

2.8 DEFLECTION FUNCTIONS

Numerous investigators have studied the relationship between surface deflection and pavement life. Some of the more fully developed relationships are presented here. It should be noted that these are not truly Transfer Functions since they are based on measured deflections rather than deflections predicted by a structural model. It should also be noted that the studies reported are all based on deflections measured using the Benkelman beam (or other very similar device). The Benkelman beam is used to measure the surface deflection at the point of loading as produced by a dual tired, single axle normally loaded to 18,000 pounds. The measurements are taken either at creep speed (<2 mph) or as the rebound from a stopped position. As a result, the Benkelman beam deflection is generally greater than the deflection produced by the same load when traveling at normal highway speeds. They are also greater than the deflections measured using a dynamic test device (e.g. Road Rater or FWD) which are generally comparable to normal highway deflections. Studies made during the AASHO Road Test (30) indicate that the deflection at highway speeds is about 60% of the Benkelman beam deflection.

From the viewpoint of mechanistic pavement design, it is not surprising that strong relationships have been found between pavement life and surface deflections. Analyses of the predicted structural responses of a wide range of pavement designs on an equally wide range of subgrades (19) have shown strong correlations between surface deflection and each of response parameters generally considered in pavement design Transfer Functions (i.e. AC radial strain and subgrade vertical strain and/or stress ratio). Consequently, surface deflection is a single parameter that relates to both of the response parameters generally accepted as critical to flexible pavement design.

The pavement life-deflection relationships that are perhaps the most well known and documented were developed from the AASHO Road Test (30). These relationships are quite significant since most pavement design procedures currently used in the U.S. are based on the Road Test data. The Road Test deflection equations, therefore, relate directly to current design practice and experience. These equations for deflections measured in the spring of the year are shown in Figure 2.4.

Lister and Kennedy (31) reported on extensive studies conducted by the Transportation and Road Research Laboratory in England that relate pavement life to measured deflections. The relationships found are shown on Figure 2.5 for granular base and bituminous stablized base pavements, respectively. It should be noted that these relationships are based on 7000 pound wheel load deflections.

Considerable deflection-pavement life research has also been conducted in Canada. Figure 2.6 shows a comparison of various relationships identified both in Canada and by U.S., Australian, and British researchers. The design criteria adopted as a result of analysis of these relatonships (44) is shown in Figure 2.7.

The Asphalt Institute (TAI) developed a deflection based procedure for selecting the thickness of overlay to be placed on an existing flexible pavement. In developing the procedure, Kingham (33) examined numerous deflection-performance relaltionships. Figure 2.8 shows the relationships considered by Kingham in comparison with the one used as the basis for the TAI overlay design procedure.

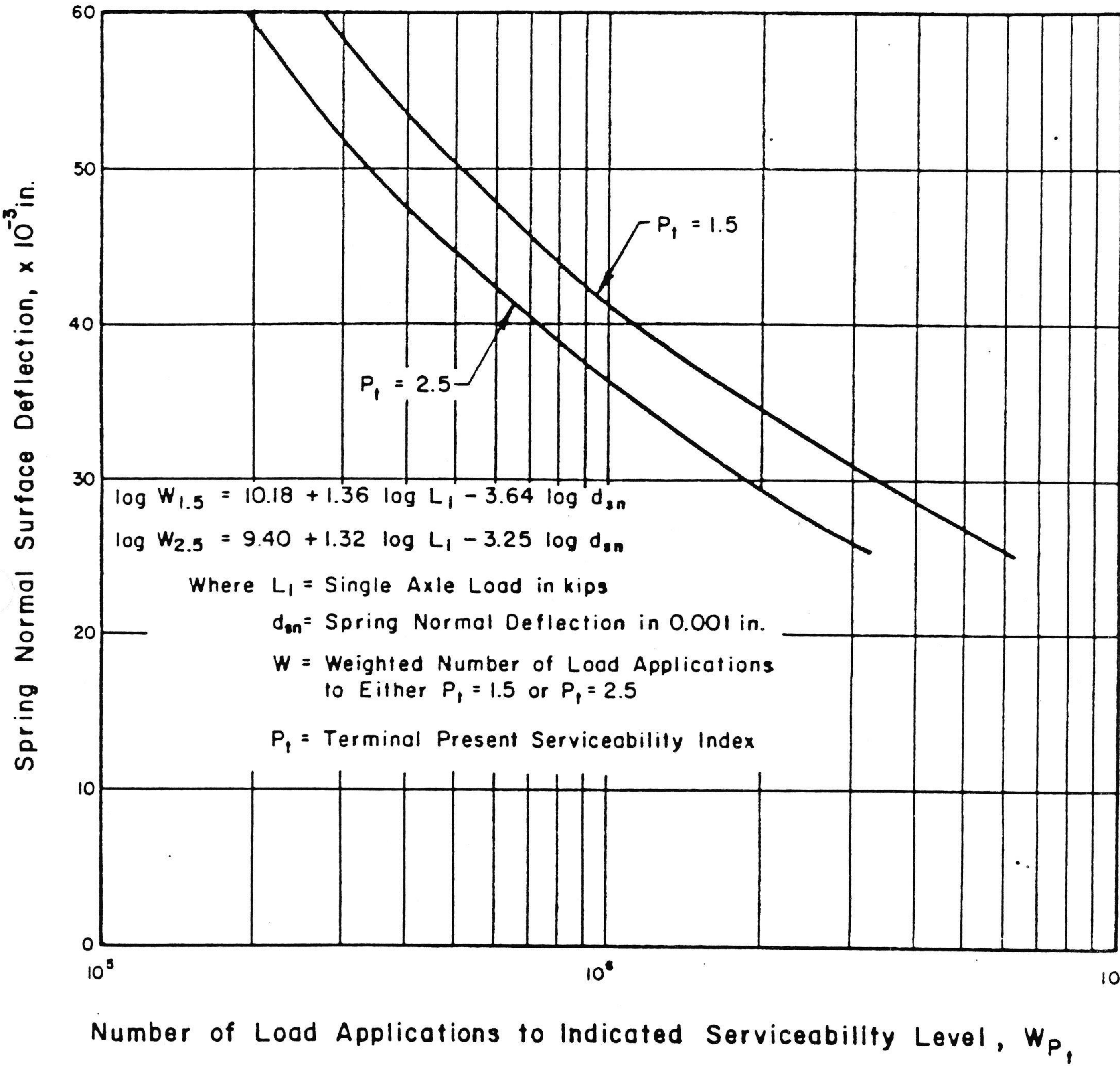

Figure 2-4. Deflection Based Performance Equations from the AASHO Road Test (Ref 40).

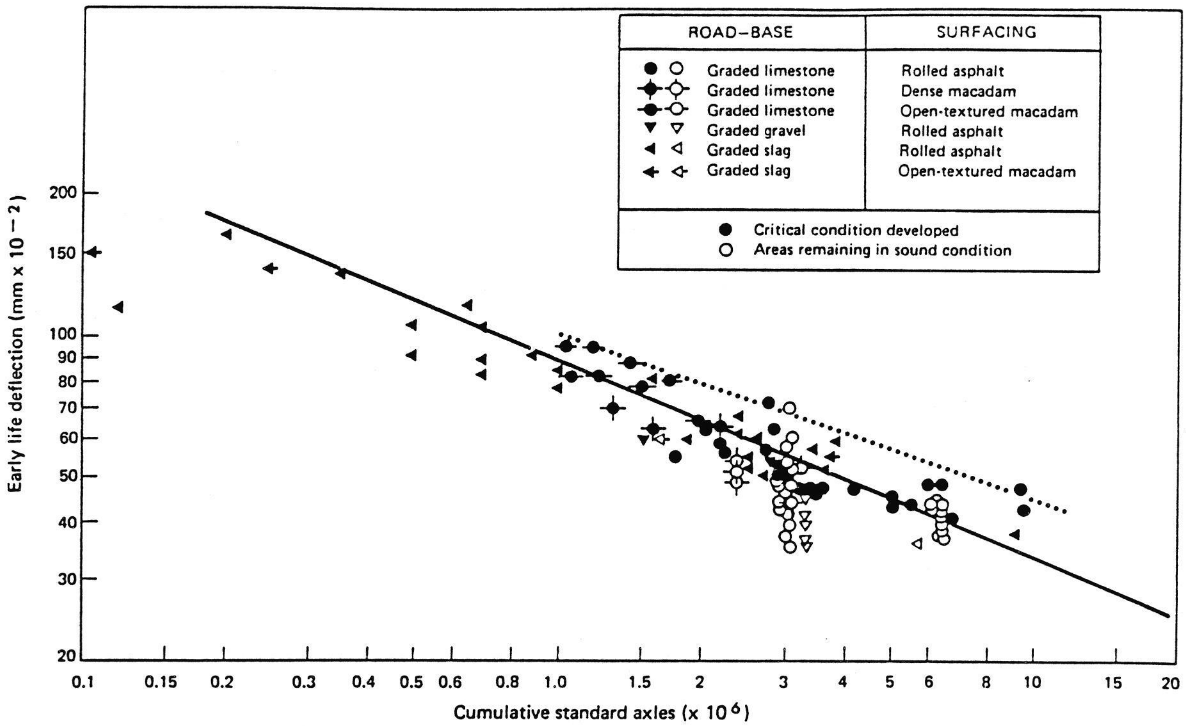

RELATION BETWEEN EARLY LIFE DEFLECTION AND CRITICAL LIFE FOR PAVEMENTS WITH GRANULAR BASES

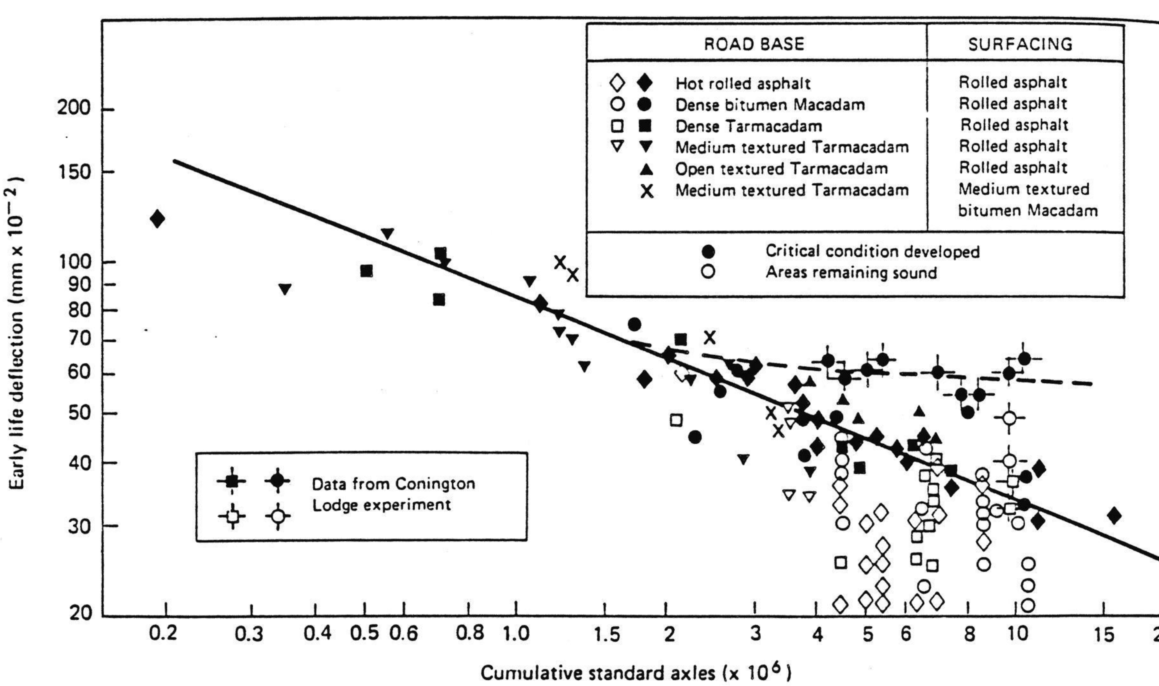

RELATION BETWEEN EARLY LIFE DEFLECTION AND CRITICAL LIFE FOR PAVEMENTS WITH BITUMEN AND TAR BOUND BASES

Figure 2-5. Deflection versus Life Relationship for Flexible Pavements in Great Britain (Ref 31).

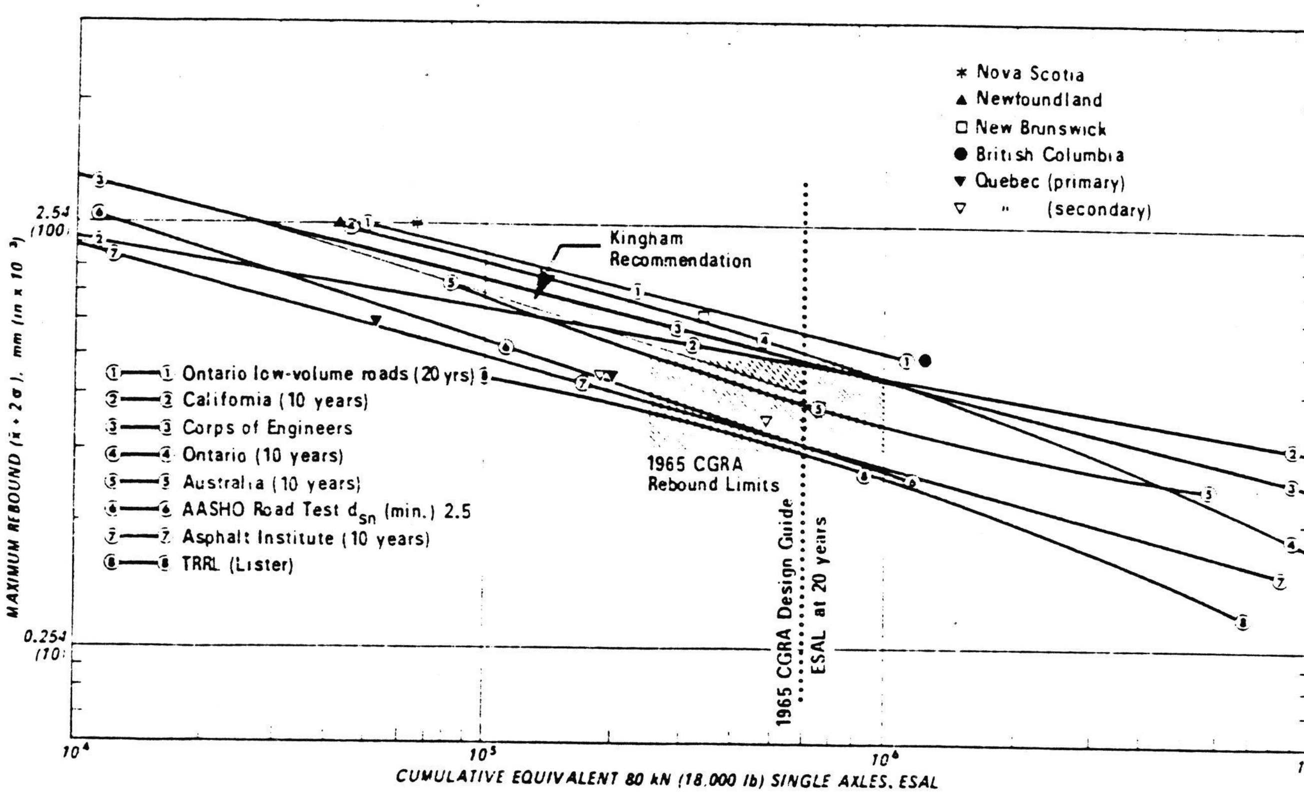

Figure 2-6. Deflection-Life Relationships Examined by Canada (Ref 44).

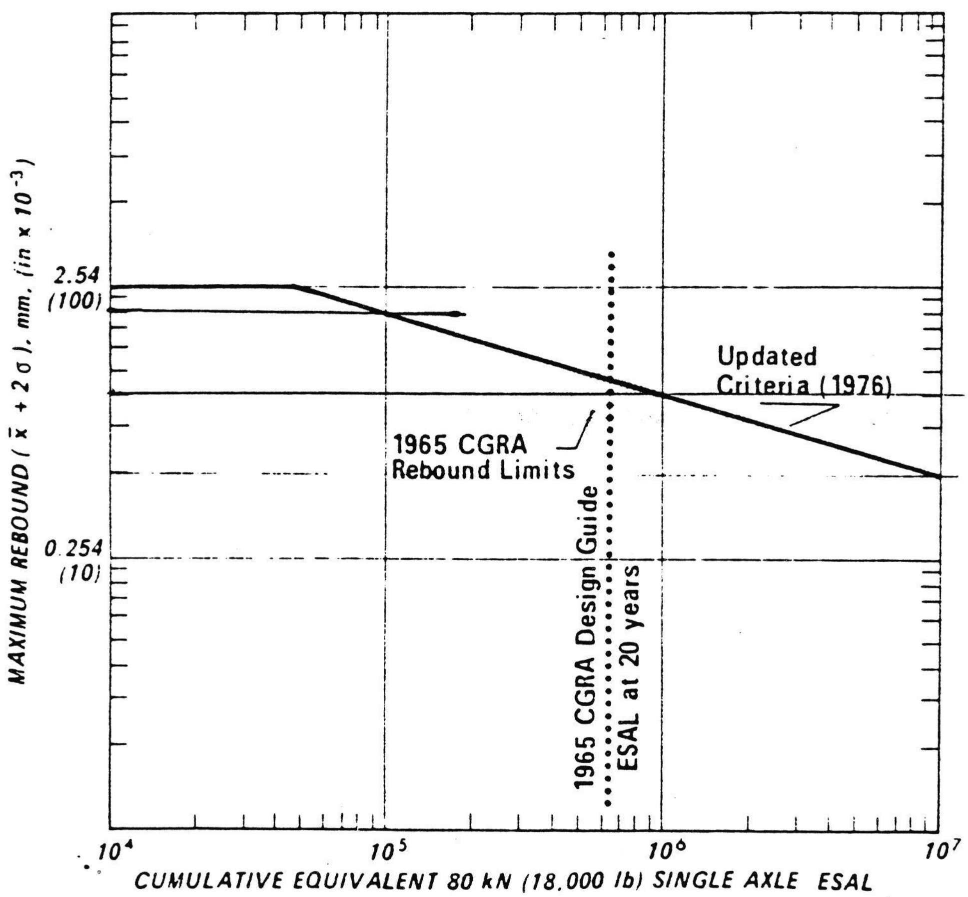

Figure 2-7. Canadian Deflection Based Design Transfer Function (Ref 44).

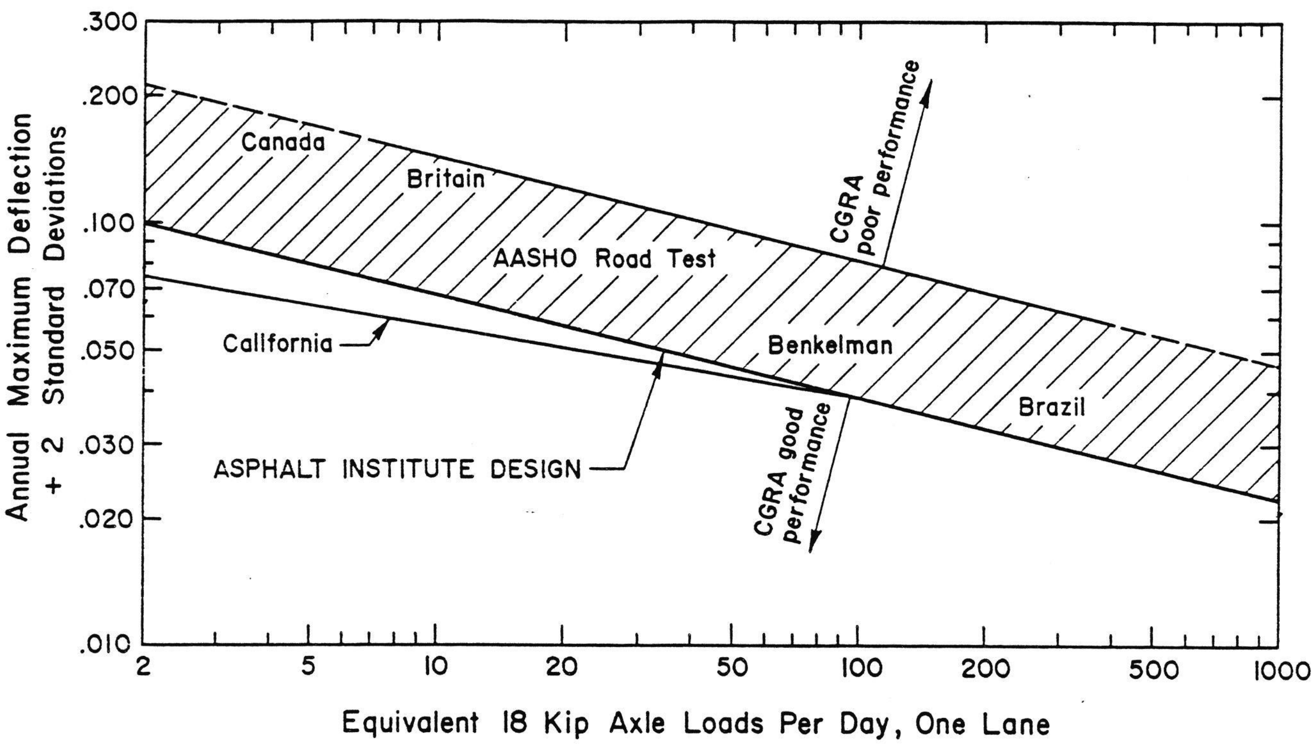

Figure 2-8. Comparison of Various Deflection Based Transfer Functions Compiled by Kingham (Ref 33).

2.9 SELECTION OF TRANSFER FUNCTIONS

The process of selecting Transfer Functions for use in a mechanistic design procedure must consider accuracy, reliability, and practicality. The procedures developed to date (3, 4, 5, 6) have used two Transfer Functions - one for AC fatigue and one for subgrade response. However, as discussed previously, a single relationship based on deflection might also be considered.

From a practical standpoint, the single deflection based Transfer Function is quite attractive. As mentioned earlier, a design based on deflection is more readily appreciated by a practicing engineer since deflection is the one response parameter that can be easily measured. Also, if the procedure is to be presented and used in a chart or nomograph form, the single relationship will reduce the number of charts. This will lessen the design complexity making the procedure "user friendly" and more acceptable in routine practice.

The deflection relationship, however, must accurately reflect the relative effects of both of the other two response parameters. To accomplished this, two deflection-pavement life relationships must be established. These would be based on the two typical Transfer Functions and on relationships between deflection and the other response parameters. The deflection Transfer Function then would be established by examining these relationships and selecting the critical portions of each. Figure 2.9 illustrates the resulting Transfer Function.

The accuaracy of the pavement life predictions will be lessened somewhat with the deflection Transfer Function since deflection does not correlate perfectly (R = 1.0) with the other response parameters. Therefore, substitution of deflection for those parameters will add some error in the prediction capability. However, analysis of ILLI-PAVE structural response predictions shows that the correlations between deflection and the other critical response par-

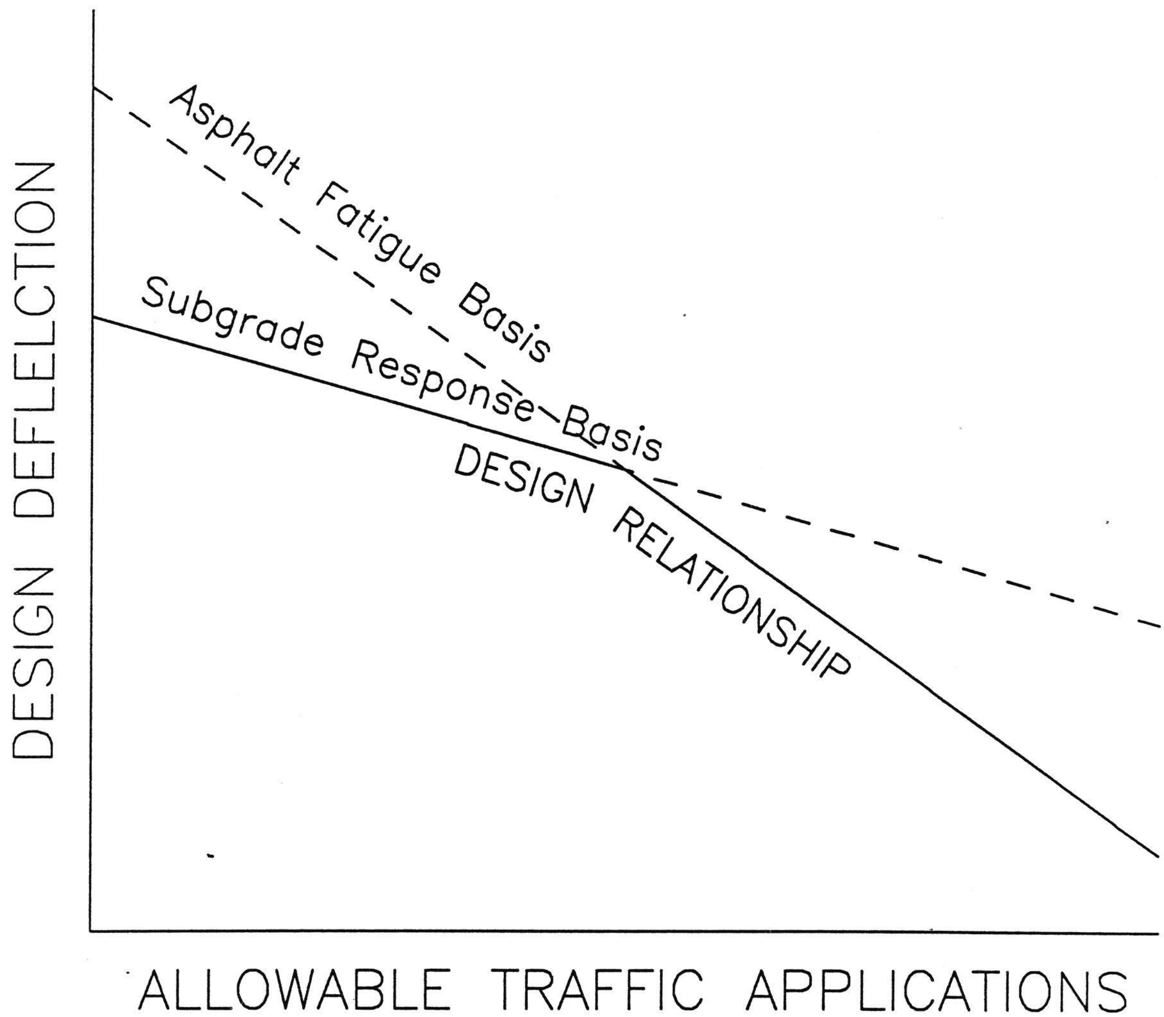

Figure 2-9. Illustration of Deflection Based Transfer Function Considering Both Fatigue and Subgrade Rutting for Mechanistic Design.

ameters are strong (for asphalt strain R = .86, for subgrade stress ratio R = .91). Consequently, the error introduced by using deflection in place of these parameters will be relatively small. Judgement would have to be exercised as to whether the other advantages gained by the use of a deflection Transfer Function outweigh the loss in accuracy.

If the design procedure is to be presented in a chart or nomograph form, the advantages are believed to be quite significant; and the deflection approach may be appropriate. However, if the procedure is to be computerized, there appears to be little advantage to the simplification gained by the use of a deflection based Transfer Function.

2.10 CONCLUSIONS RELATIVE TO TRANSFER FUNCTIONS

On the basis of this examination of Transfer Functions, the following conclusions have been made.

1) Transfer Functions are model dependent. They relate pavement performance to predicted structural response. since the predicted response is not identical for all structural models, the relationship will be different.
2) Transfer Functions for mechanistic design of asphalt pavements should represent the two most predominate load related failure modes - fatigue cracking in the AC layer and surface rutting due to overstressing the subgrade.
3) The two failure modes can be represented adequately by a single Transfer Function based on surface deflection. This would appear to be a particularly attractive alternative if the design procedure is to be presented in the form of design charts and nomographs.
4) The more conventional approach is to use two Transfer Functions,

one representing each failure mode.

5) The general form of the Fatigue Function is:

$$\log N = K + n \log (1/eac) + b \log (1/Eac) \quad \text{(Eq 2.2)}$$

6) A practical approach for determining the values for the constants (K, n, and b) in the Fatigue Function is to select reasonable values for n and b and then to develop a value for K using actual pavement performance data. In this respect, analyses presented in this paper suggest that 3.0 for n and 0.0 for b are reasonable and practical values for the dense graded AC mixes typically used in Arkansas and much of the U.S.

7) One Fatigue Function may not be appropriate for all AC thicknesses. For practical design purposes, it may be necessary to develop two Fatigue Functions, one for Full Depth AC pavements and another for conventional (AC over granular base) flexible pavements.

8) Subgrade Functions have generally been based on the load induced vertical strain at the top of the subgrade (Eq 2.5). However, stress ratio (i.e. subgrade deviator stress to unconfined compressive strength) offers an alternate basis (Eq 2.6) that was found to be at least as reliable and, from a practical standpoint, may be preferred.

CHAPTER 3

DETERMINATION OF SUBGRADE RESILIENT MODULUS

Subgrade support has long been recognized as a fundamental parameter that must be considered in any rational pavement design process. In recent years, pavement researchers and designers have adopted resilient modulus (M_r) as the measure of subgrade support that most influences the performance of a pavement and the property, therefore, that should be included in design. In fact, the 1986 AASHTO Guide adopted M_r as the measure of subgrade support that is used in the design of flexible pavements. The selection of an appropriate method for determining the M_r of the existing subgrade was largest single activity under this study.

The methods investigated all involved the use of NDT data and are commonly referred to as "back calculation" procedures. The term "back calculation" refers to a process by which the elastic moduli of pavement layers are estimated from the results of a nondestructive deflection test. The estimation requires the use of a structural model of the pavement system. This phase of the project began with a review of the structural models used for flexible pavement analysis followed by a review of the various back calculation methods that have been proposed and used. Several methods were subsequently evaluated using NDT data from the project.

3.1 STRUCTURAL MODELS FOR FLEXIBLE PAVEMENTS

In the mechanistic design of flexible pavements, the engineer must pay close attention to two major modes of failure: rutting, which is generally regarded as being the result of excessive vertical compressive stresses at the top of the subgrade, and fatigue cracking in the asphalt concrete, which is caused by repetitive radial tensile strains at the bottom of the bituminous layer (Figure 3.1). The way in which these and other critical conditions are limited is determined by a reasonable prediction of the magnitude of the load responses (stresses, strains and displacements) prior to the actual construction of the pavement. These estimates can be obtained by using a mathematical model subjected to hypothetical boundary and surface loading conditions similar to those expected in the field. The most commonly used model is the one developed through elastic layer theory.

Layered elastic models require the assumption that all of the materials in the system have linear stress versus strain curves, and therefore constant moduli of elasticity. It is also assumed that the elastic properties of the layers are sufficiently defined in terms of elasticity by their Young's moduli and Poisson's ratios. The following is brief review of the historical development of elastic layer theory.

3.1.1 Boussinesq's Theory

In 1883, Joseph Boussinesq published his equations for solving for the stresses and displacements in a single layer soil deposit produced by a static point load applied normal to its surface (45). The soil mass was assumed to be homogeneous, isotropic, linearly elastic, and of infinite depth. The three dimensional coordinate system used in Boussinesq's analysis is shown in Figure 3.2. Equations 3.1 through 3.3 are for determining the change in the horizontal and vertical normal stresses at any point in the system due to a point load applied at the origin (ground surface).

$$\Delta P_x = \frac{P}{2\pi}\left\{\frac{3x^2 z}{L^5} - (1-2\mu)\left[\frac{x^2 - y^2}{Lr^2(L+z)} + \frac{y^2 z}{L^3 r^2}\right]\right\} \quad \text{(Eq 3.1)}$$

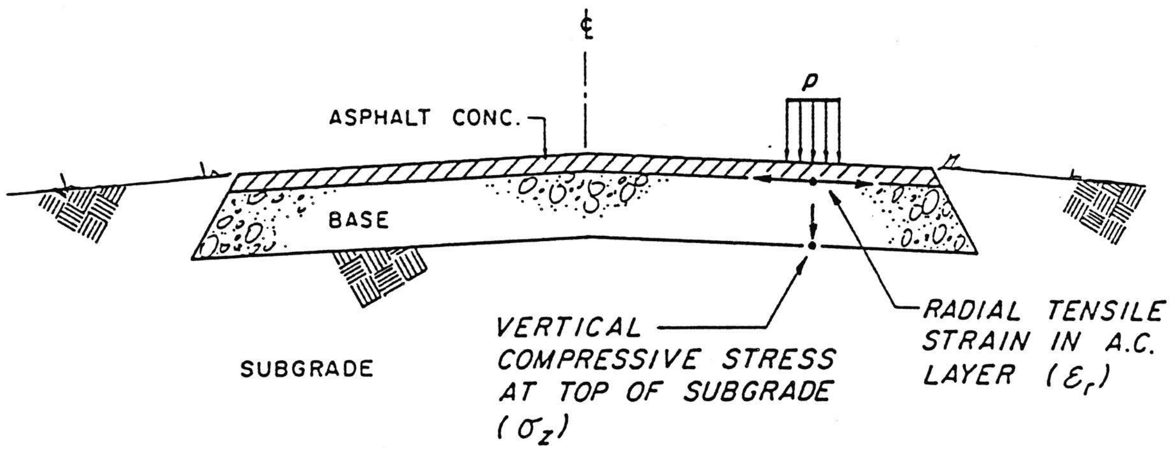

Figure 3.1 Load Stresses and Strains Generally Considered Critical in Mechanistic Design.

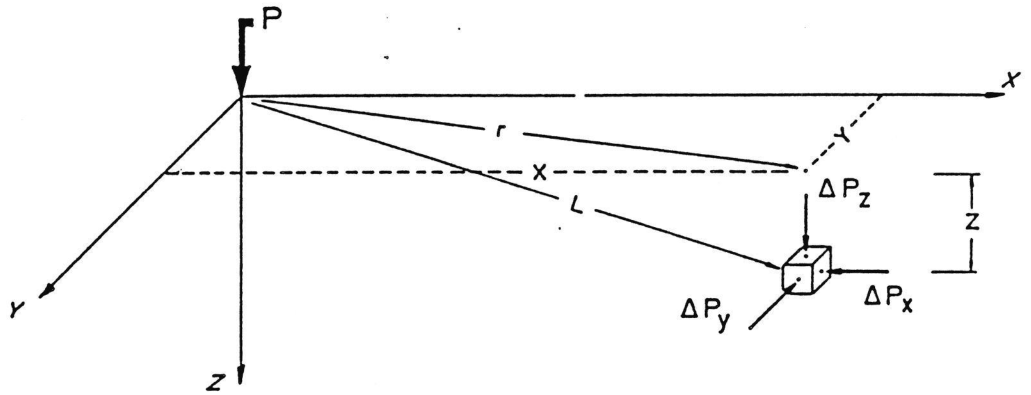

Figure 3.2 Coordinate System and Element Used in Boussinesq's Analysis.

$$\Delta P_y = \frac{P}{2\pi}\left\{\frac{3y^2z}{L^5} - (1-2\mu)\left[\frac{y^2-x^2}{Lr^2(L+z)} + \frac{x^2z}{L^3r^2}\right]\right\} \quad \text{(Eq 3.2)}$$

$$\Delta P_z = \frac{3P}{2\pi}\frac{z^3}{(r^2+z^2)^{5/2}} \quad \text{(Eq 3.3)}$$

Since these equations were originally presented, they have been adapted to solve other types of loading problems. For example, Love (46) integrated Boussinesq's displacement equations to derive expressions to solve for the vertical displacement of the surface due to a uniformly loaded circular area, which are presented as equations 3.4a and 3.4b. In these, attention is given as to whether the bearing area is rigid or flexible because its stiffness affects the distribution of stresses in the system.

Flexible Bearing Area:

$$W = \frac{2(1-\mu^2)pr}{E} \quad \text{(Eq 3.4a)}$$

Rigid Bearing Area:

$$W = \frac{\pi(1-\mu^2)pr}{2E} \quad \text{(Eq 3.4b)}$$

where

W = surface deflection

p = uniformly distributed static pressure

r = radius of the bearing area

E = modulus of elasticity of the soil

u = Poisson's ratio of the soil

Boussinesq's theory represented a major breakthrough and is still in use today. However, it has few direct applications in pavement engineering since it considers only a single layer of "infinite" depth.

3.1.2 Burmister's Theory for a Two Layer System

The apparent need for a methodology for analyzing multi-layer systems was partially fulfilled in 1943 when D. M. Burmister presented his equations with which the stresses and displacements in a two layer system could be estimated (47,48). Using the mathematical theory of elasticity, he derived these equations based on the following assumptions:

1. The layers were assumed to be homogeneous, isotropic and linearly elastic in order to make Hooke's law valid.
2. The surface reinforcing layer was considered to be weightless, of finite thickness, and of infinite lateral extent; the subgrade layer was assumed to extend infinitely in both the lateral and downward directions.
3. The surface of the reinforcing layer was assumed to be free of normal and shearing stresses outside of the loaded area, and the stresses and displacements in the subgrade layer were assumed to be zero at infinite depth.
4. The two layers were assumed to be in continuous contact at the interface, and that the subgrade provided continuous, uniform support for the reinforcing layer.
5. Continuity required the assumption that the normal stresses, and the horizontal and vertical displacements at the interface be equal.
6. The Poisson's ratio of the layers was assumed to be 0.5.

Except for numbers 1 and 6, these assumptions and continuity conditions are generally satisfied in most types of flexible pavement construction, and, as will be discussed later, are quite similar to those used in contemporary computer based models.

Figure 3.3 shows a typical two layer elastic system subject to a uniform static pressure applied through a circular plate. Burmister's equations for determining the surface settlement due to a uniform pressure are presented below. These equations are the same as equations 3.4 with Poisson's ratios of 0.5, further modified by the settlement coefficient (Fw), which can be obtained from Figure 3.4.

Flexible Bearing Area

$$W = \frac{1.5\,pr\,F_w}{E_2} \qquad \text{(Eq 3.5a)}$$

Rigid Bearing Area

$$W = \frac{1.18\,pr\,F_w}{E_2} \qquad \text{(Eq 3.5b)}$$

where

W = surface settlement

p = uniformly distributed static pressure

r = radius of the bearing area

E_2= Young's modulus of subgrade layer

F_w= settlement coefficient

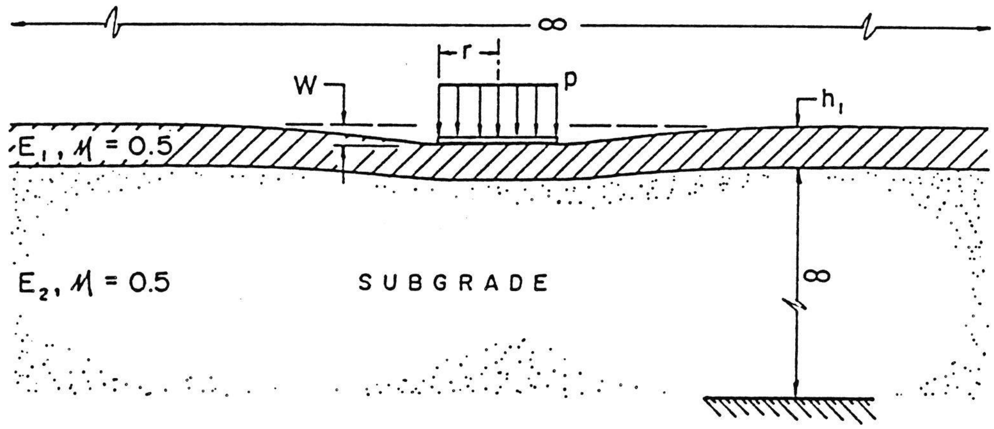

Figure 3.3 Typical Two-Layer Elastic System Pavement Idealization.

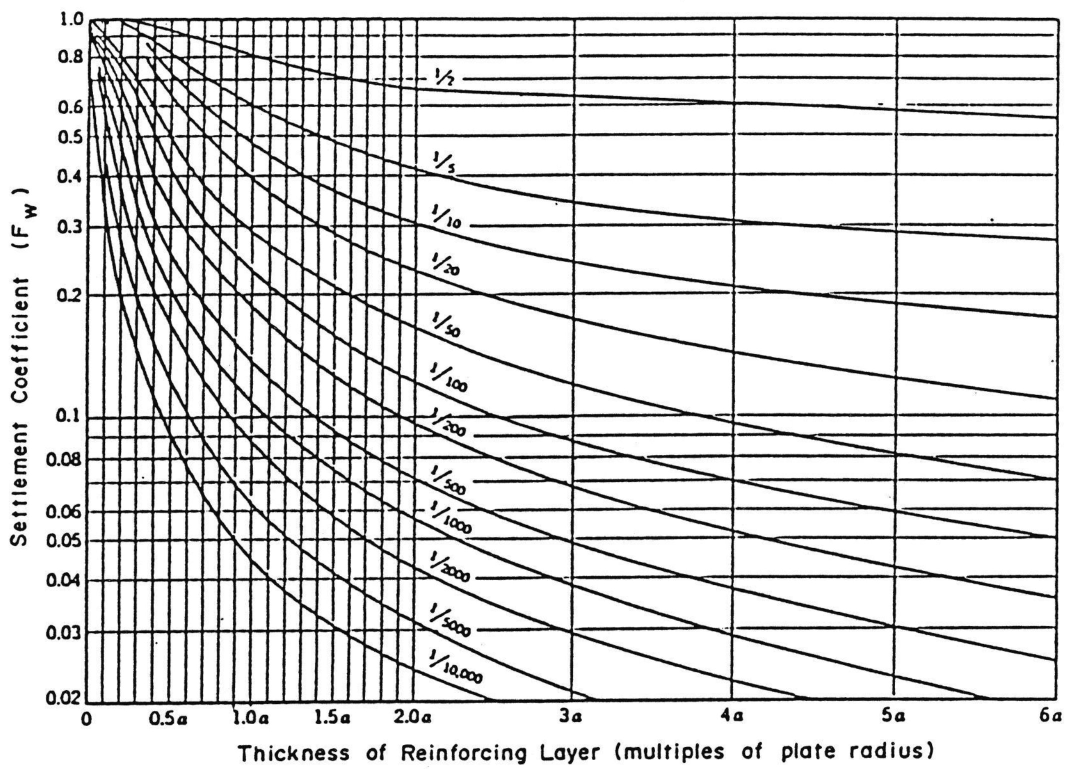

Figure 3.4 Burmister's Influence Chart for Two Layer System (Ref 47).

The settlement coefficient accounts for the effect of the reinforcing layer (pavement) on the surface settlement. It is a function of the basic ratios of the radius of the bearing area to the thickness of the reinforcing layer (r/h_1), and the elastic modulus of the subgrade layer to that of the reinforcing layer (E_2/E_1).

3.1.3 Other Elastic Theories of Two and Three Layer Systems

In addition to Burmister's work, a number of other response analysis techniques were developed prior to 1960. Theories for two and three layer systems are shown in Tables 3.1 and 3.2, respectively (49).

3.1.4 Multilayer Elastic Theory and Computers

With the advent of high speed computers, the full potential of elastic layer theory in its application to flexible pavement analysis was realized. Computer codes can perform the numerous, complex calculations required in multilayer elastic theory quickly and accurately. Modern procedures use the theory of elasticity in much the same way as Burmister used it to derive his equations. However, Burmister was limited to two and three layer systems in order to avoid undue complexity. The computerized techniques are capable of addressing more layers and variables in the system.

In this type of analysis, the pavement is modelled in an axisymmetric cylindrical coordinate system, with an element of stress as shown in Figure 3.5. The stress tensor for the element in matrix form is:

$$\sigma^{i}(r,\theta,z) \equiv \begin{bmatrix} \sigma^{i}_{rr} & \sigma^{i}_{r\theta} & \sigma^{i}_{rz} \\ \sigma^{i}_{r\theta} & \sigma^{i}_{\theta\theta} & \sigma^{i}_{\theta z} \\ \sigma^{i}_{rz} & \sigma^{i}_{\theta z} & \sigma^{i}_{zz} \end{bmatrix} \qquad \text{(Eq 3.6)}$$

Table 3.1 Elastic Theories for Two-Layered Systems.

Author	Assumed Condition of the Layers	Assumed Condition at the Interface	Form of Loading	Parameters Used	Stresses and Deflections Determined	Comments
Westergaard (1926)	Elastic plate on a subgrade acting as a series of parallel, vertical, independent springs.	Discontinuous	Uniform, circular	Modulus of subgrade reaction (i.e. spring constant)	Tensile stresses at three points on the surface of the plate	The subgrade is unrealistic, and stresses in the subgrade are not considered.
Hogg (1938)	Elastic plate on a semi-elastic subgrade	Discontinuous	Uniform, circular	Young's modulus and Poisson's ratio for the subgrade	Tensile stresses in the plate	Extension of Westergaard's theory.
Fox (1948)	Elastic layer on a semi-infinite elastic subgrade	Discontinuous	Uniform, circular	a/h, E1/E2	All stresses in the pavement and subgrade	Extension and numerical evaluation of Burmister's work.
Hank and Scrivner (1948)	Elastic layer on a semi-infinite elastic subgrade	Discontinuous	Uniform, circular	a/h, E1/E2	Stresses at both sides of the interface	Extension and numerical evaluation of Burmister's work.
Pickett and Ai (1948)	Elastic plate on a semi-infinite elastic subgrade	a) Discontinuous b) No horizontal displacement at the interface	Uniform, circular	a/h and functions of E1/E2, m1, and m2	All stresses and deflections in the subgrade	Mainly applicable to Concrete pavements.
Odemark (1949)	Elastic plate on a semi-infinite elastic subgrade	Discontinuous	Uniform, circular	a/h and functions of E1/E2, m1, and m2	Deflections at the surface and radial stress at the bottom of the upper layer	

Table 3.2 Elastic Theories for Three-Layered Systems.

Author	Assumed Condition of the Layers	Assumed Condition at the Interface	Form of Loading	Parameters Used	Stresses and Deflections Determined	Comments
Burmister (1945)	Two elastic layers on a semi-infinite elastic subgrade	a) Continuous b) Discontinuous	Bessel function	a/h2, h1/h2, E1/E2, and E2/E3	Deflection at the second interface	A method of calculating all of the stresses is given, but no numerical evaluation of the deflections or stresses.
Hank and Scrivner (1948)	Two elastic layers on a semi-infinite elastic subgrade	Continuous	Uniform, circular	a/h2, h1/h2, E1/E2, and E2/E3	All of the stresses at the first surface	Extension and numerical evaluation of Burmister's equations for the first interface.
Acum and Fox (1951)	Two elastic layers on a semi-infinite elastic subgrade	Continuous	Uniform, circular	a/h2, h1/h2, E1/E2, and E2/E3	Vertical and radial stresses at both interfaces	Extension and numerical evaluation of Burmister's equations for the vertical and radial stresses.
Jeuffroy and Bachelez (1957)	Elastic plate on an elastic layer on a semi-infinite elastic subgrade	Discontinuous at the first interface, continuous at the second	Uniform, circular	h2/a, h1(E1)/a(6E2), (E2-E3)/(E2+E3)	w1, rr1, and zz2	

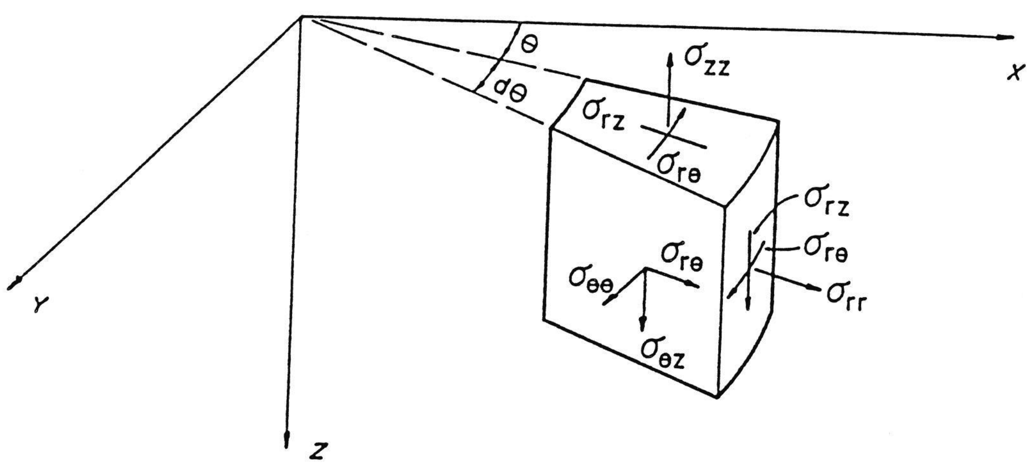

Figure 3.5 Axisymmetric Cylindrical Coordinate System and Element of Stress.

Similarly, the displacement vector is:

$$u^i(r,\theta,z) \equiv \begin{bmatrix} u_r^i \\ u_\theta^i \\ u_z^i \end{bmatrix} \qquad \text{(Eq 3.7)}$$

In the notation used, (i) is the layer number which ranges from 1 to (N), the number of layers (including the subgrade). The equations of stress and displacement for the layer in question are derived and presented by Schiffman (50), along with the applicable boundary and surface loading conditions.

As mentioned previously, the assumptions of this version of the theory are similar to those used by Burmister, with the exception of assumptions numbered 4 and 6. Assumption 4 required that the layers be considered in continuous contact at the interface and that the subgrade provide continuous, uniform support for the reinforcing layer (47). Although the new model still requires that the subgrade provide continuous uniform support, the degree of bond at the layer interfaces can be varied in some procedures. In the program BISAR, for example, the bond can be rated from zero (full friction) to 1000 (frictionless) at any interface. The elastic layer program ELSYM5 assumes that full adhesion is developed at all interfaces of the system with one exception: if a rigid layer exists at finite depth, the interface between the subgrade and the rigid layer can be designated as frictionless or fully adhered.

Burmister's sixth assumption requires that the Poisson's ratio of all of the layers be assigned the value 0.5 (47). The computer codes enable the user to choose a Poisson's ratio depending on the layer material. Table 3.3 lists some typical values of Poisson's ratio for common paving materials.

Problems involving multiple wheel loads, multiple layers, varying degrees of interface friction, and finite subgrade thicknesses can be solved using an elastic layer program such as BISAR or ELSYM5. The general input required by

Table 3.3 Typical Poisson's Ratios fo Paving Materials (Ref 51).

Material Type	Range	Value
Portland Cement Conc.	.15 - .20	0.15
Asphalt Concrete	.25 - .35	0.35
Cement Stabilized Base	.20 - .30	0.30
Asphalt Stabilized Base	.25 - .35	0.35
Unbound Granular Base	.20 - .50	0.40
Granular Subgrade	.30 - .50	0.40
Clayey or Silty Subgrade	.40 - .50	0.45
Lime Treated Subgrade		0.40

these programs are the number of layers, the thickness and elastic properties of each layer, the interface conditions (if applicable), and the location and intensity of the load(s). From these geometric and physical data, the program can estimate the stress, strain and displacement at any point within the system.

3.1.5 Finite Element Method

The finite element method is a numerical approach to the analysis of solids. This theory requires that the subject solid be discretized into a network of elements to be manipulated and analyzed in a computer environment (51). The principles of statics, dynamics, thermodynamics, etc. can be applied with the appropriate boundary conditions to each interacting element. Then, the behavior of all or part of the model can be examined by looking at the responses of the elements in the desired area.

The type of element of primarily used in flexible pavement analyses is the axisymmetric ring element. It is a two dimensional element which, when rotated about an axis of symmetry, produces a solid of revolution. Similarly, when a series or group of these elements are rotated, a solid of the desired size and shape is produced. The model used in this research is a right cylindrical solid of revolution as shown in Figure 3.6.

The strain-displacement relationship for an axisymmetric element in matrix form is (52):

$$\xi = du = \begin{bmatrix} \frac{\partial}{\partial r} & 0 \\ 0 & \frac{\partial}{\partial z} \\ \frac{1}{r} & 0 \\ \frac{\partial}{\partial z} & \frac{\partial}{\partial r} \end{bmatrix} \begin{bmatrix} u & v \end{bmatrix} \qquad \text{(Eq 3.8)}$$

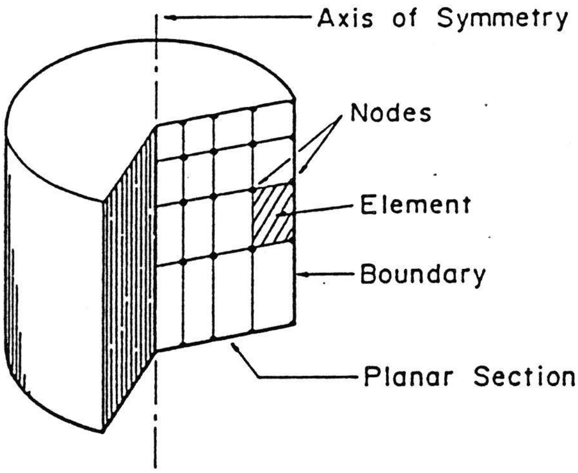

Figure 3.6 Cylindrical Solid of Revolution Model of Pavement System Typically Used in Finite Element Analyses.

The stress-strain relationship in matrix form for an isotropic continua is (52):

$$\sigma = \mathbf{E}\epsilon$$

where

$$\mathbf{E} = \frac{E}{(1+v)e_2}\begin{bmatrix} e_1 & v & v & 0 \\ v & e_1 & v & 0 \\ v & v & e_1 & 0 \\ 0 & 0 & 0 & e_3 \end{bmatrix} \qquad \text{(Eq 3.9)}$$

$$e_1 = 1 - v \;,\quad e_2 = 1 - 2v \;,\quad e_3 = \frac{e_2}{2}$$

A finite element based computer program solves for the stresses, strains and displacements for the elements of an axisymmetric solid using these basic equations. A typical axisymmetric element of stress is shown in Figure 3.7.

One of the major disadvantages of the finite element method at this time is the sophisticated computing facilities required to operate it. For a model of significant size, a great deal of memory is required to store the vast amount of working data. In addition, it requires a very fast machine to solve the problems in a reasonable amount of time. However, these problems will become secondary as small computing systems develop more capacity and speed.

The primary advantage of the finite element method is its versatility. Models of many sizes and shapes can be analyzed, as well as those with unique material properties and loading conditions. Using the ANSYS finite element package, for example, a model with stress dependent elastic properties, and a dynamic loading condition can be created, thus eliminating some of the major drawbacks of the elastic layer theory.

3.2 REVIEW OF BACK CALCULATION METHODS USED IN THE PAST

Modulus back calculation from a static plate load test became possible with the equations of Boussinesq. Using the equations of Boussinesq and Burmister, estimates of layer moduli can be obtained by using the results of a static plate loading test (ASTM D1196-64) (53). In these methods, only the

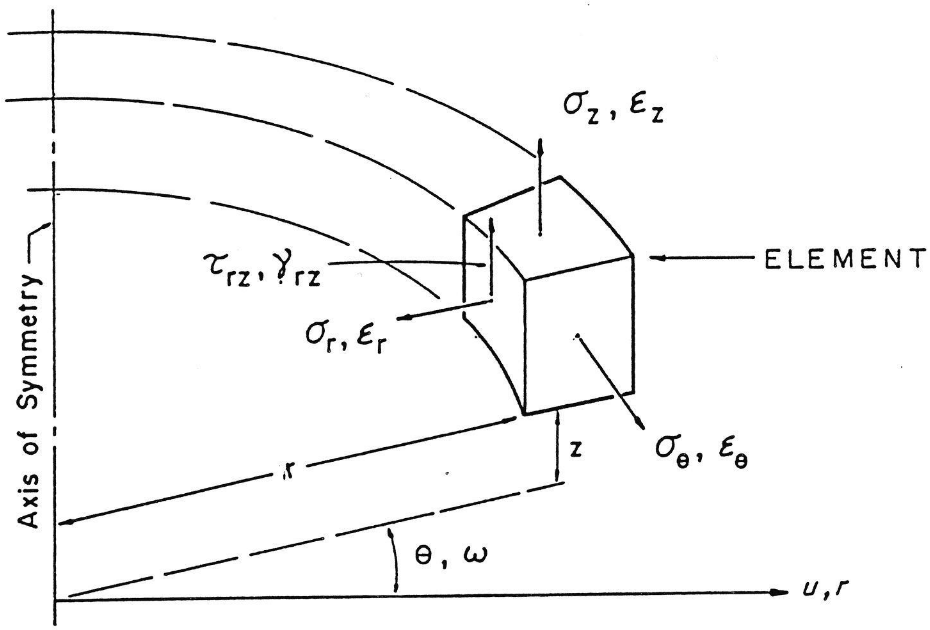

Figure 3.7 Finite Element Axisymmetric Ring Element.

deflection at the center of the loading plate is used for moduli prediction.

Modulus back calculation of a single, semi-infinite soil layer can be done directly using forms of Boussinesq's equations integrated for a uniformly loaded circular area (46). The deflection from the load test can be substituted into either equation 3.4a or 3.4b, depending on the nature of the loading plate. The equations are repeated here in a rearranged form such that the elastic modulus of the subgrade (E) is the dependent variable.

Flexible Bearing Area:

$$E = \frac{2(1-\mu^2)pr}{W} \qquad \text{(Eq 3.4a)}$$

Rigid Bearing Area:

$$E = \frac{\pi(1-\mu^2)pr}{2W} \qquad \text{(Eq 3.4b)}$$

Burmister's theory has also been used in back calculation. When using Burmister's equations for a two layer system (47) to back calculate moduli, two deflection tests are required: one on the subgrade, and one on the pavement-subgrade system. The subgrade modulus (E_1) is obtained exactly as above (Eq 3.4a or b); then, using either Equation 3.5a or b (shown below rearranged), the settlement coefficient (F_w) is solved for as follows:

Flexible Bearing Area:

$$F_w = \frac{WE_2}{1.5\,pr} \qquad \text{(Eq 3.5a)}$$

Rigid Bearing Area:

$$F_w = \frac{WE_2}{1.18\,pr} \qquad \text{(Eq 3.5b)}$$

After (E_2) and (F_W) have been obtained, the next step requires an influence chart like the one shown in Figure 3.4. Using the known values of (F_W) and (h_1), the ratio (E_2/E_1) can be obtained from the graph, and, since (E_2) is known, (E_1) can be solved.

3.3 BACK CALCULATION USING VIBRATORY TESTS

The use of vibratory tests to investigate the mechanical properties of soils and paving materials began in Germany between 1928 and 1939 (54). Shortly after World War II, Swedish engineers were able to compute the elastic modulus of a uniform clay based on wave velocities (55). After 1948, most of the developments in vibration testing were influenced by Van der Poel and Nijboer. Working for the Shell Laboratories, they developed a heavy vibrator which became known as the "Dutch Shell Vibrator" (56).

Two different types of vibrating machines were used in this type of testing after 1950. A heavy vibrator, which operated at frequencies of 5 to 60 cycles per second (c/s), was capable of penetrating a depth of up to 10 meters. With three eccentric masses revolving on synchronized axes, the heavy vibrator could generate a sinusoidal transient load with a peak impulse of up to 2000 kg applied to the surface of the pavement through a 30 cm diameter circular plate (56). A light vibrator was used for generating higher frequencies (up to 3000 c/s), but at the expense of penetrating power, which was only about 10 cm (56). The impulse load using the light vibrator was negligible, and was not measured. For both vibrators, wavelengths were measured through the use of an electronic pick-up shifted along a measuring tape with the vibrator at its origin.

One criticism of the heavy vibrator in its simulation of a moving wheel load was that it applied the same rate of loading to all of the layers of a pavement, regardless of depth. In reality, the loading is much longer and of a lower intensity for the deeper layers than it is for those above because of the conical dispersion of a moving wheel load. Soil and other materials in the road have mechanical properties that are directly related to the rate of loading (55).

Using the wavelength (L), and the frequency (n) of the vibrations, the velocity (v) of the waves could be calculated, thus:

$$v = nL \qquad \text{(Eq 3.10)}$$

The dynamic modulus (E_d) of an elastic material can be computed by the following equation (57):

$$E_d = 2(1+u)d\ v^2 \qquad \text{(Eq 3.11)}$$

where (d) is the density of the medium, and (u) is its Poisson's ratio. The variable (v) in this equation refers to the velocity of shear waves as opposed to Rayleigh waves.

One of the more difficult tasks in this type of analysis is choosing the proper frequency and wavelength for a particular layer in a multilayered system. Jones (58) established guidelines for the correct interpretation of wave velocity data.

3.4 MODERN NONDESTRUCTIVE DYNAMIC TESTING DEVICES

After the work of Van der Poel and Nijboer, there emerged a new breed of nondestructive dynamic testing devices, such as the Dynaflect, the Road Rater, and the Falling Weight Deflectometer (FWD). These devices are completely self contained and trailer mounted for easy transport. This section will describe the FWD in detail since it is the device currently used by the Arkansas Highway and Transportation Department, and will give cursory descriptions of the Dynaflect and Road Rater.

3.4.1 The Dynatest Falling Weight Deflectometer

Interest in dynamic plate loading tests increased in the 1960's when researchers from Denmark began extending the development of the French falling ball deflectometer (59,60). The new device, called the falling weight deflectometer (FWD), applied a single impulse load similar to that of a moving wheel load.

The modern version of the Dynatest FWD (model 8000) is shown in Figure 3.8. It is capable of producing a load pulse from 1500 to 27,000 pounds with a duration of approximately 25 to 30 milliseconds. The peak load is measured by a load cell above the loading plate, which is 11.82 inches in diameter (61). The peak deflection of the pavement surface is measured by a series of seven seismic geophones located on a straight line radiating from the center of the loading plate. The first geophone is located at the center of the plate, and the remaining sensors can be placed at any radius up to 7.4 feet (61). According to the manufacturer of the FWD, the measured deflections are typically within one percent (+/- 0.04 mils) of the actual deflection, and the measured loads are within one percent (+/- 22.5 pounds) of the actual load (61).

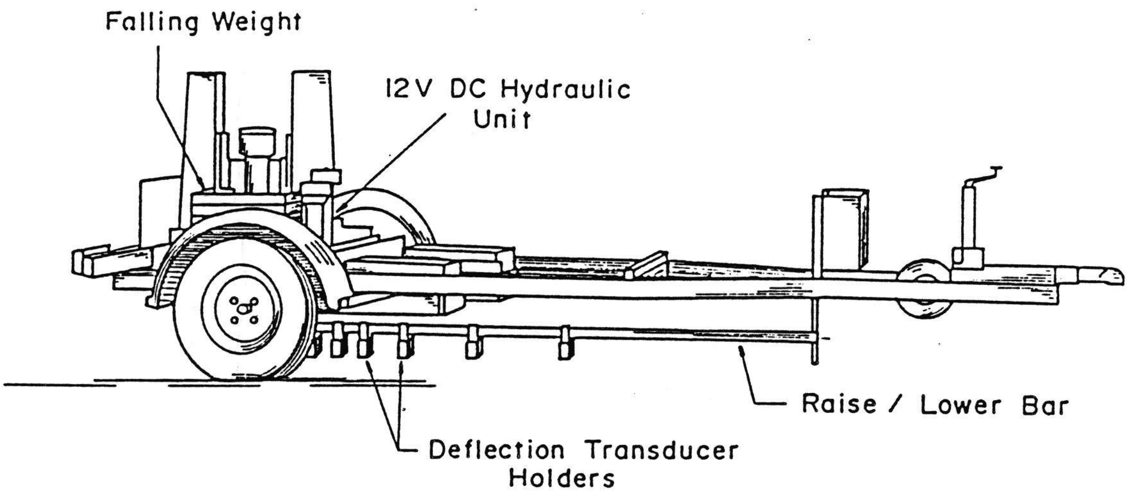

Figure 3.8 Typical Falling Weight Deflectometer (Ref 60).

The actions of the FWD are intended to simulate the effect of a moving wheel load on a pavement. This is important because all mechanistic design procedures are geared toward limiting the strains at critical points due to this type of load. Several studies indicate that this device generates load responses that are comparable to those produced by a moving wheel (60,62). However, like the Shell vibrator, but unlike a moving wheel, the FWD applies the same rate of loading to all of the pavement layers.

3.4.2 Other Nondestructive Dynamic Testing Devices

The falling weight deflectometer is the primary testing device of this research project. However, there are other devices used today in similar applications, such as the Dynaflect and the Road Rater. These two devices are similar to the Shell vibrator because they also produce a sinusoidal load.

The Dynaflect applies a steady-state harmonic load with a peak-to-peak amplitude of 1000 pounds through two steel wheels which are twenty inches apart. The peak-to-peak deflections are measured by five geophones spaced twelve inches apart with the first one being located between the two wheels.

The Road Rater Model 400 generates a simple harmonic load with a 160 pound vibrating weight. The frequency of the vibrations can be varied from 5 to 100 Hz; the load is transmitted to the surface of the pavement through two, four by seven inch rectangular steel plates which are 10.5 inches apart. The peak-to-peak deflections are measured by four geophones spaced twelve inches apart with the first one being located between the two plates. The peak load is calculated according to the following equation (63):

$$F_{peak} = 0.0511\ w\ f^2\ D \qquad \text{(Eq 3.12)}$$

where:

w = weight, pounds

f = frequency, Hz

D = peak-to-peak displacement, inches.

Details of these and other devices and comparisons thereof are available elsewhere (64,65).

3.5 TECHNIQUES FOR BACK CALCULATION OF SUBGRADE MODULUS

3.5.1 Iterative Back Calculation Programs.

Since no exact solution is available for solving for a set of layer moduli from known deflections and layer thicknesses, iterative techniques were developed in the late 1970's. Researchers at Cornell University began to manually "fit" real deflection basins with synthetic basins using layered elastic theory (66). Soon, computer codes were developed to generate moduli and perform iterations.

The individual steps of this type of iterative analysis are illustrated in Figure 3.9 and are briefly described here. The logic is representative of the two iterative computer programs used in this research, BISDEF and FPEDD1. More detailed descriptions of these programs and their operation are available elsewhere (52,67,68,69)

<u>Step 1</u>. Figure 3.10 illustrates the general input data required for the analysis of a conventional flexible pavement. The inputs include the peak load (P), the radius of the loading plate (a), the number of deflection sensors (n), the sensor radii (r_i), and the surface deflections (d_i). For each layer, the component material and thickness are required along with modular data in the form of maximum, minimum and seed moduli. At the user's option, BISDEF and FPEDD1 will generate all three of these modular values automatically. Tables 3.4 and 3.5 show the default values for the two programs. BISDEF uses the values shown for the seed moduli of

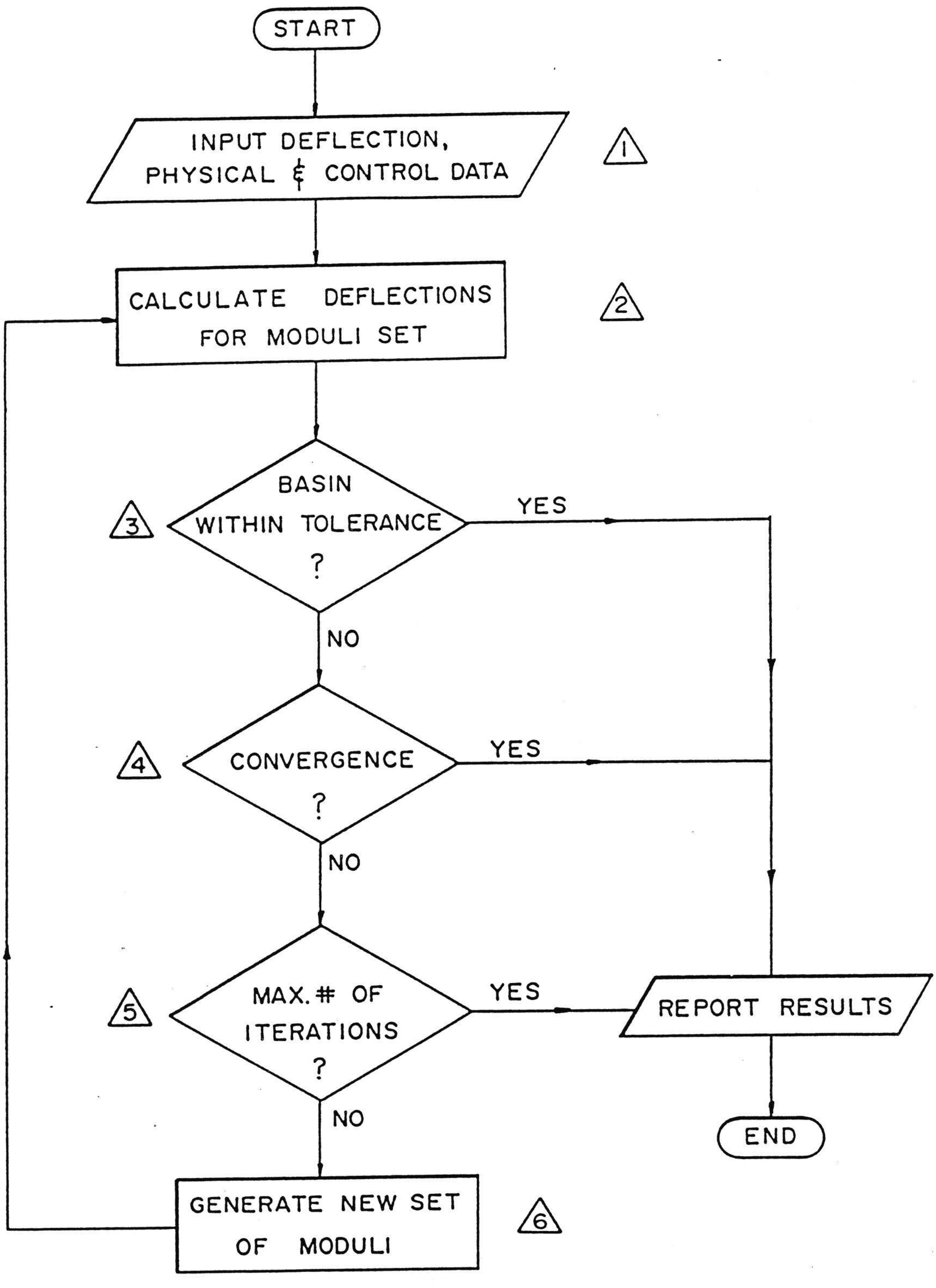

Figure 3.9 General Flow Diagram for Iterative Back Calculation Programs.

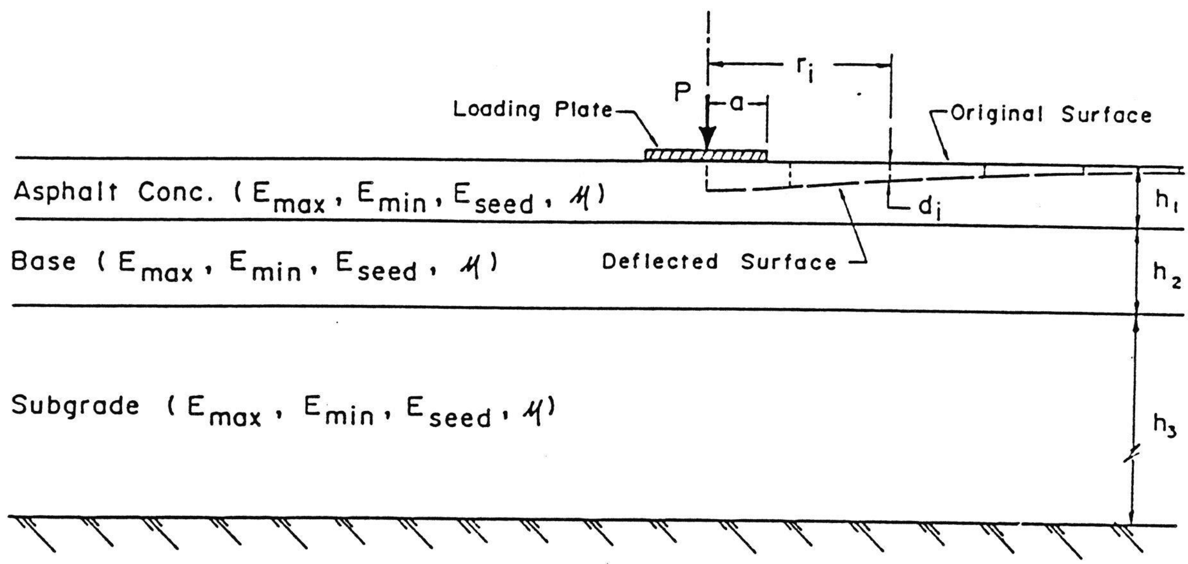

Figure 3.10 General Input Required for Back Calculation.

Table 3.4 Default Moduli Seed and Ranges Used by BISDEF (Ref 51).

	Moduli (ksi)		
Material	Minimum	Maximum	Seed
Asphalt Conc.	200	1000	350
P. C. Concrete	2500	7000	3500
High Quality Stabilized Base	500	2500	1000
Stabilized Base	100	1000	300
Granular Base	5	150	30
Rigid Boundary	--	--	1000

Table 3.5 Default Moduli Ranges Used by FPEDD1 (Ref 51).

	Moduli (ksi)	
Material	Minimum	Maximum
Asphalt Conc.	80	1100
P. C. Concrete	2000	6500
Stabilized Base	80	300
Granular Base	20	70
Granular Subbase	10	70

surface and base materials, and an empirical algorithm for the subgrade seed modulus and range. FPEDD1 uses the default ranges shown in Table 3.5, and empirical algorithms for generating the seed moduli of all of the pavement layers.

Step 2. After the input data have been read, a deflection basin is synthesized using an elastic layer subroutine for the seed moduli on the first iteration, and for adjusted moduli on subsequent iterations (see Step 6). In this step, the model pavement is subjected to a load similar in magnitude to that produced by the NDT device when the deflection data were acquired. The computed deflections are stored for later use. BISDEF uses the layered elastic program BISAR, and FPEDD1 uses ELSYM5 for this step.

Step 3. The calculated and actual deflections are compared based on some statistical parameter. Both programs use the absolute sum of the percent error in the deflections at each sensor as calculated by the following equation:

$$ABSE = \sum_{i=1}^{n} \left| \frac{(d_{mi} - d_{ci})\ 100}{d_{mi}} \right| \qquad \text{(Eq 3.13)}$$

where

ABSE = absolute sum of error, percent

n = the number of sensors

d_{mi} = measured deflection at sensor i

d_{ci} = calculated deflection at sensor i

If the ABSE is within a prespecified tolerance, the program will terminate and the moduli of the current iteration are reported as being the actual moduli. BISDEF fixes this tolerance ten percent.

The FPEDD1 tolerance may be set by the user, but it has an optional default of two percent.

<u>Step 4</u>. If the test in Step 3 fails, and one or more iterations has passed, Step 4 checks for convergence. BISDEF compares the moduli of the current iteration with those of the previous one. If the moduli seem to have converged, the program will terminate. The tolerance for this step in BISDEF is fixed at ten percent. FPEDD1 checks the individual (computed) deflections, and the moduli of the surface, base and subbase for convergence. The user may specify an acceptable tolerance, but default values are available. They are 0.05 mils for the deflections, four (4) percent for the surface course, three (3) percent for intermediate layers, and 0.05 percent for the subgrade.

<u>Step 5</u>. As a time consideration, both programs will terminate after a specified number of iterations. This value is fixed at three (3) iterations for BISDEF and is variable for FPEDD1 (default = 10).

<u>Step 6</u>. If the tests of Steps 3 through 5 fail, both programs will adjust the layer moduli within the limits of the specified ranges, and another iteration will be performed starting with Step 2. Iterations will continue until the program is terminated by Steps 3, 4 or 5.

There are a number limitations in this type of procedure, some of which will be discussed in the Section 3.6 entitled EFFECTS OF SIMPLIFYING ASSUMPTIONS.

3.5.2 ELMOD

The computer program ELMOD (Evaluation of Layer Moduli and Overlay Design) is another popular approach to modulus back calculation. The first part of the program calculates layer moduli, the function of interest here; then, if the user wishes, it will perform a remaining life analysis and an overlay design. ELMOD was developed by the manufacturers of the Falling Weight Deflectometer, and is compatible only with FWD data.

For back calculating elastic moduli, ELMOD uses integrated forms of Boussinesq's equations and Odemark's method of equivalent thicknesses (62). This method is more direct and faster than the previously described iterative procedures. The basic assumption in the method of equivalent thicknesses is that the stresses, strains, and deflections below a particular interface are dependent on the stiffnesses and thicknesses of the layers above. In effect, this transforms a layered structure into a semi-infinite, single layer, to which Boussinesq's equations are easily applied (62).

3.5.3 Back Calculation Using Response Algorithms.

In 1985, Elliott and Thompson (19) presented response algorithms which were developed using data generated from the ILLI-PAVE finite element pavement model. ILLI-PAVE model is a unique response analysis tool in that pavements with both linear and nonlinear materials can be analyzed.

Two types of algorithms were developed: design response algorithms to serve as a basis for developing a design procedure, and analysis algorithms for evaluating existing pavements. Such equations were developed for predicting a number of pavement properties. The only ones of interest here are the pavement analysis algorithms for predicting subgrade resilient moduli.

The algorithms were derived using multivariate regression analysis in which the desired pavement parameter was the dependent variable, and the remaining significant effects were independent variables on the right side of the equation. In the equations presented here, the subgrade "breakpoint" resilient modulus (E_{ri}) is the dependent variable. Each equation will yield E_{ri}, but will not necessarily give the same value since each one uses a different approach.

$$\log E_{ri} = 7.61 + .17\,T_{ac} - 2.14(\log T_{bse})/T_{ac} - .18(\log E_{ac})T_{ac} - 3.82\,\log D_0 \qquad \text{(Eq 3.14)}$$

$$\log E_{ri} = 5.89 - .11\,T_{ac} + .066(\log E_{ac})T_{ac} - 1.95(\log D_0) - .148\,\text{AREA} \qquad \text{(Eq 3.15)}$$

$$\log E_{ri} = 25.035 - 5.245\,D_3 + .286\,D_3^2 \qquad \text{(Eq 3.16)}$$

where

T_{ac} = thickness of the asphalt surface,

T_{bse} = thickness of the granular base,

E_{ac} = estimated elastic modulus of asphalt,

D_0 = deflection at the center of the plate, mils

AREA = deflection basin parameter

$= 6*(D_0 + 2*D_1 + 2*D_2 + D_3)/D_0$

The deflection basin parameter is calculated using the surface deflections at 0, 1, 2 and 3 feet (D_0, D_1, D_2 and D_3, respectively). These particular radii originated from the sensor spacing on the NDT device used at the University of Illinois at the time that these equations were developed. The correlation coefficients (R) for the above equations are 0.889 for Eq 3.14, 0.984 for Eq 3.15, and 0.990 for Eq 3.16.

In the regression analysis, data from 192 different pavement configurations were used. The asphalt concrete thicknesses varied from 3 to 8 inches, the base thicknesses varied from 4 to 18 inches, and there were four levels of subgrade modulus - 1 ksi, 3.02 ksi, 7.68 ksi, and 12.34 ksi (69).

Three different material models were used in the analysis. The asphalt concrete was assumed to have a constant modulus of elasticity, the granular base was assumed to be "stress hardening," and the cohesive subgrade was assumed to be "stress softening." The typical "stress dependent" models for the behavior of these materials are shown in Figures 3.11 and 3.12.

Another advantage of the ILLI-PAVE model is the stress adjustment feature which accounts for the limited shear strength of fine grained soils and unbound granular bases. This prevents the program from predicting stresses in excess of the strength of the material. Details of this procedure are available elsewhere (69,70).

3.6 EFFECT OF ASSUMPTIONS ON BACKCALCULATED M_R

Even though steady progress has been made in modulus back calculation, there remain several weak links within the procedures that compromise their accuracy. The most significant of these are:

1. The models used are based on static loading conditions, thus ignoring dynamic load effects;
2. The subgrade layer in some models is assumed to be semi-infinite in depth and in any case the depth is generally not known.

The effect of these were investigated since they were believed to be at least partially responsible for difficulties encountered in the evaluation of the back calculation methods. They are other assumptions that are also believed to limit the accuracy of the back calculation. However, these do not appear to present as significant a limitation on back calculation and were not evalu-

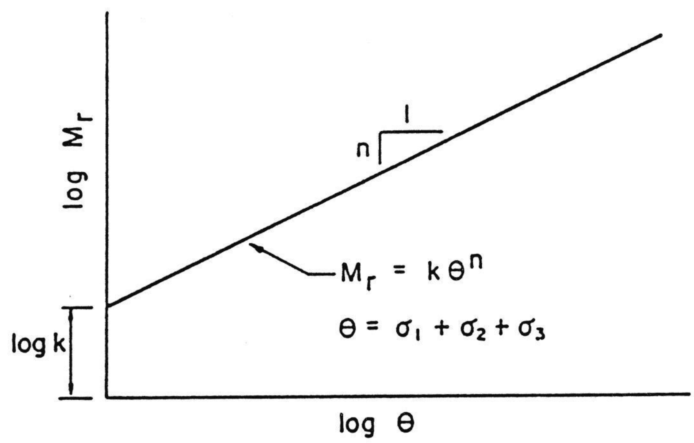

Figure 3.11 Typical Stress Dependent Behavior of Granular Base Materials.

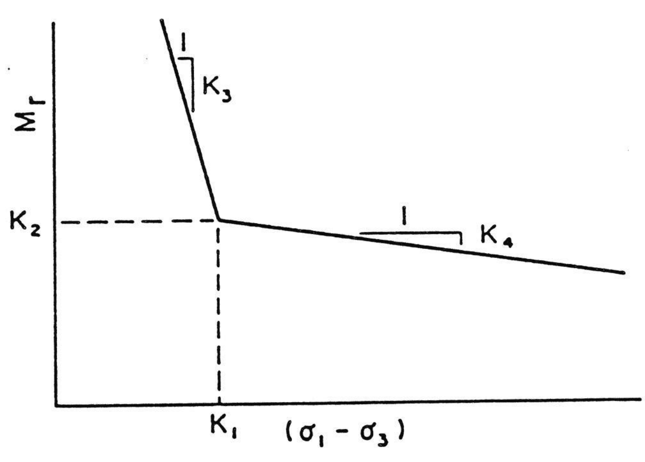

Figure 3.12 Typical Stress Dependent Behavior of Cohesive Soils.

ated. These include the assumptions that the layers are linear elastic, isotropic, homogeneous and infinite in lateral extent.

One of the primary reasons for these simplifications is the limited power and capacity of small, affordable computing systems. A superminicomputer employing the finite element method can overcome many of these limitations, but, as of now, this type of system is out of the reach of most practicing engineers. Hopefully, as personal computers become more powerful, a more realistic model will become available.

3.6.1 Method of Investigation

In order to look more closely at the problems created by static loads and indefinite subgrade depths, the finite element method was employed. Using the ANSYS finite element package, a layered model with varying layer thicknesses was developed. The model was then subjected to both dynamic and static loading conditions, and the surface deflections were recorded. From the results of these analyses, the effects of the type of loading and subgrade thickness could be evaluated.

The ANSYS finite element system was used to generate the pavement model and loading mechanism. The dynamic analysis was intended to simulate the response of a conventional flexible pavement to the load generated by a Dynatest Model 8000 Falling Weight Deflectometer (FWD). For the purposes of this investigation, all of the materials were assumed to be linearly elastic, isotropic and homogeneous. Their properties are listed in Table 3.6, which includes the material properties of the components of the FWD loading plate.

The pavement system is modelled as an axisymmetric solid of revolution; this type of solid is defined as a three dimensional body developed by the rotation of a planar section about an axis (19). The planar section used

Table 3.6 Material Properties Used in ANSYS Analyses.

Material	Modulus of Elasticity	Poisson's Ratio	Density
Asphalt Concrete	400,000 psi	0.35	145 pcf
Granular Base	30,000	0.40	130
Subgrade Soil	7,000	0.40	100
Rubber	1,100	0.40	---
Polyethylene	123,000	0.30	---
Steel	29,000,000	0.30	---

here is shown in Figure 3.13, and, when rotated about its y-axis, the desired solid is produced. In this model, there are 306 elements and 340 nodes that make up the pavement and subgrade. There are an additional 12 elements and 15 nodes that represent the loading plate, which is illustrated in detail in Figure 3.14. The plate is actually a composite of three materials: rubber, polyethylene, and steel; the materials, their properties and the plate dimensions accurately represent those of an actual FWD bearing plate.

Eight different pavement systems were analyzed. Four had 2 inches of asphalt concrete over 8 inches of granular base and four different depths to bedrock (100, 300, 500 and 700 inches); four others had 4 inches of asphalt over 12 inches of base with the same four bedrock depths. For all of the different configurations, the top two rows of elements (Figure 3.12) were used for asphalt concrete, the next four were the granular base, and the remaining elements represented the subgrade soil. When the model was extended to various depths, the subgrade elements were adjusted proportionately (i.e., the elements nearer the surface absorbed less of the extra depth than those below it). This technique is consistent with the recommendations of Duncan, et al. (72).

Another material property that was considered in the model was damping. The paving materials were assumed to have a composite damping ratio of approximately five percent which has been used in previous in studies in this area (73). In order to include damping in the ANSYS model, two variables (and) had to be selected for the following equation (73):

$$\xi = \alpha/4\pi f + \beta\pi f \qquad \text{(Eq 3.17)}$$

where

ξ = damping ratio,

α = material damping coefficient,

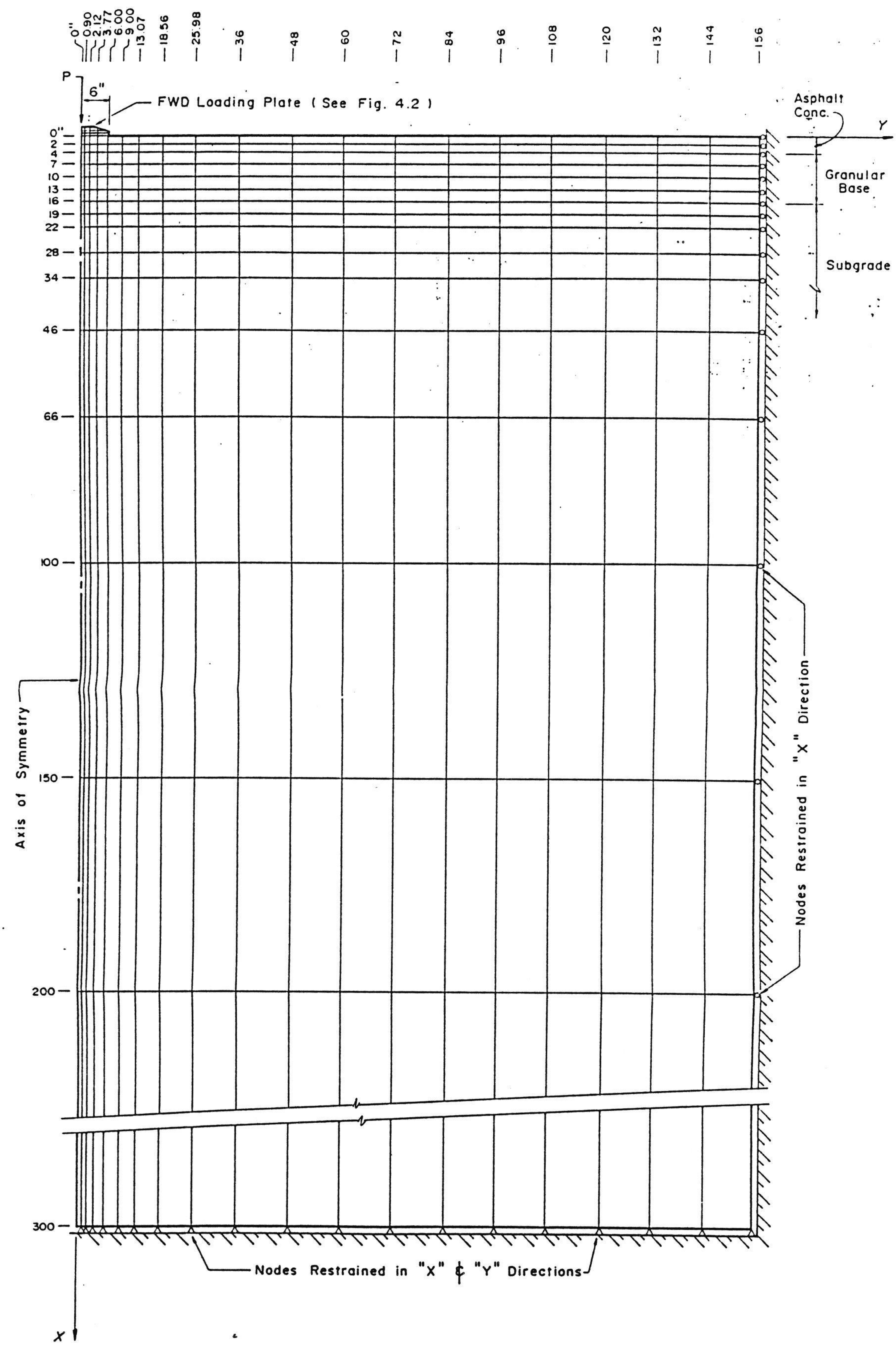

Figure 3.13 Pavement Model Used in ANSYS Finite Element Analysis.

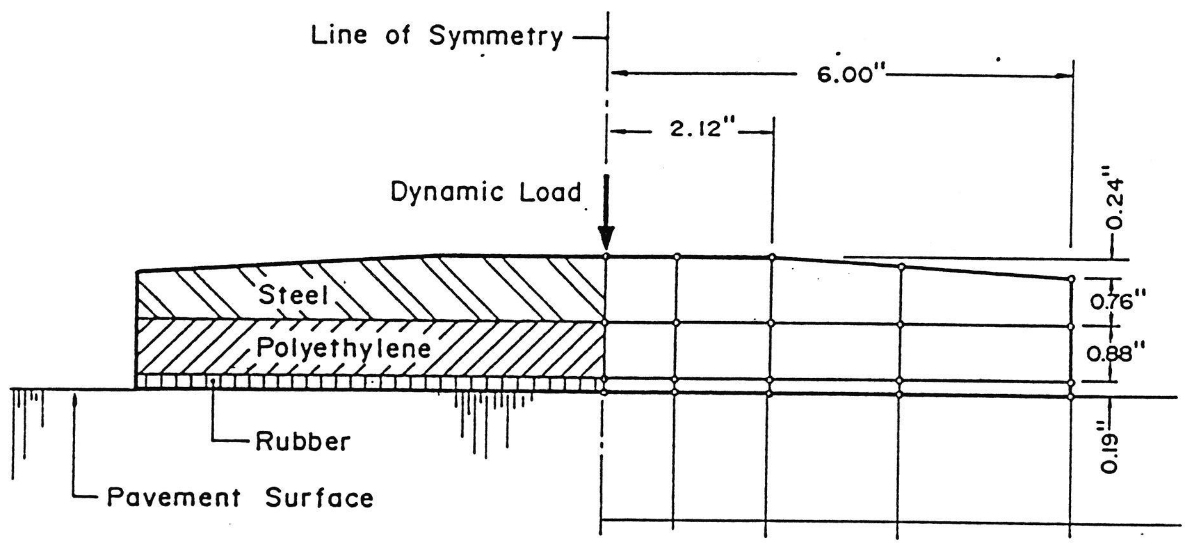

Figure 3.14 FWD Loading Plate Model Used in ANSYS Finite Element Analysis.

β = structural damping coefficient,

f = fundamental frequency of pavement.

For most pavements, the first fundamental frequency (f) falls between 8 and 18 Hz (75). In order for ( ) to be near the target of 5 percent, a material damping coefficient ( ) of 5 and a structural damping coefficient ( ) of 0.0005 were chosen. Figure 3.15 shows the two components of Eq 3.17 and their combined effect. The selected coefficients yield a damping ratio of roughly 5 percent in the range of resonant frequencies that are likely to be encountered.

The boundary conditions are the same as those that have been used in the past in finite element models of this type (72). Referring to Figure 3.13, the boundary conditions are as follows:

1. The nodes at the right boundary are restrained in the "x" direction, but allowed to move vertically.
2. The nodes at the bottom of the subgrade layer are restrained in both the "x" and "y" directions, indicating that full friction is developed at the subgrade - rigid boundary interface.
3. Along the line of symmetry (the y-axis), the nodes are unrestrained, but, because of the symmetrical loading, they will only move vertically.
4. The common nodes at the layer interfaces do not allow the layers to move relative to one another; thus, it was assumed that full friction was developed at these interfaces.

In order to simulate the impulse of a falling weight, a transient point load with a total duration of 30 milliseconds (msec) was used. It acts at the middle of the loading plate, or, as is the case of a symmetrical load, along the line of symmetry. Since the plane is rotated 360 degrees, the total

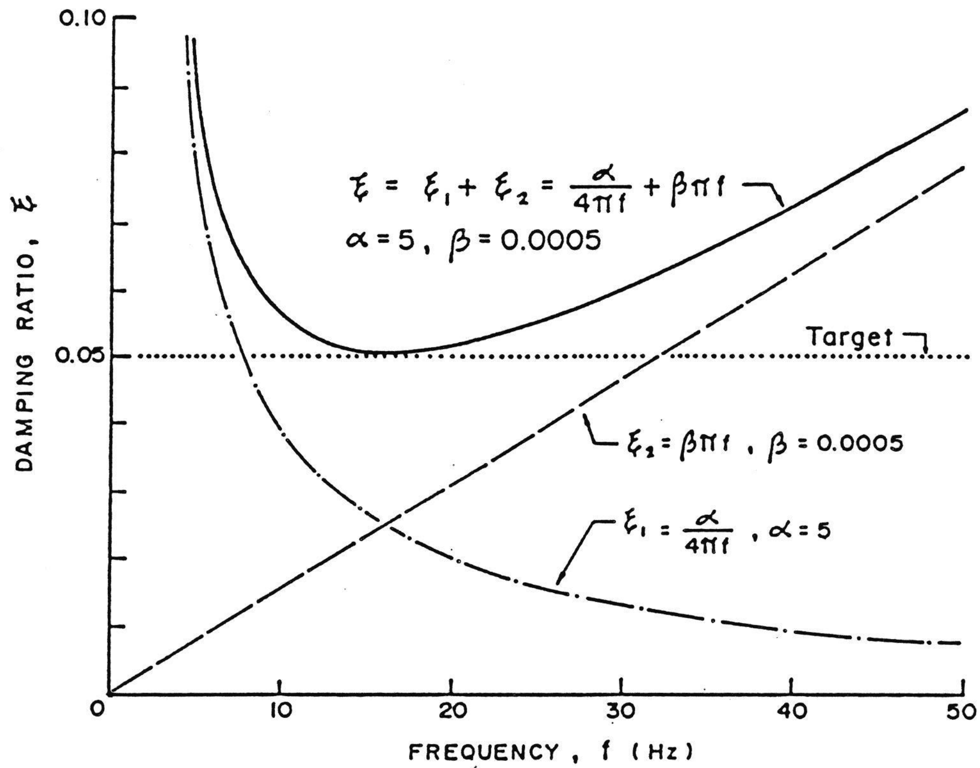

Figure 3.15 Damping Curves Corresponding to Equation 3.17.

9000 pound load was divided by 2*PI resulting in a force of 1432.4 pounds. The load was applied as a ramp function for 10 msec, held constant at the peak for 10 msec, and was released with on a ramp for 10 msec. This loading curve is compared with an approximate FWD load pulse in Figure 3.16.

3.6.2 Effect of the Static Load Assumption

Iterative back calculation programs generally use some type of layered elastic response analysis technique to synthesize deflection basins that "fit" the dynamic deflection basins obtained with a nondestructive testing device. The routines used in many programs of this type are based on elastostatic or viscoelastostatic models in which the load is assumed to be a uniformly distributed static pressure. This implies that the dynamic response of a pavement is assumed to be similar to its static response, thus discounting the inertial properties of the pavement system (73).

Each of the eight pavements were analyzed twice using the ANSYS model described in the previous sections: once for a dynamic load, and once for a static load. For the dynamic loading, the peak surface deflections were recorded along with their corresponding time value.

Rate of Loading. As in the case of an actual pavement system, the rate of loading had a significant effect on the load responses of the finite element model. For the comparisons in Figure 3.17, a trapezoidal loading curve was used, and the duration of the peak load was the varied from 0 to 1 second. A static load was also used for which the duration was considered infinite. The graph clearly shows that the peak duration (d) has a significant effect on the surface deflections, and that when (d) is greater than about one second, the depth and shape of the deflection basin approaches that of the static basin. As (d) decreases, so do the deflections.

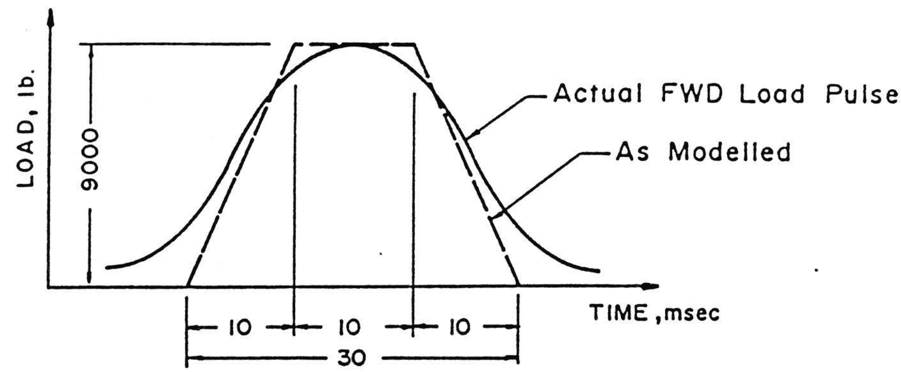

Figure 3.16 Comparison of FWD and ANSYS Model Loading Curves.

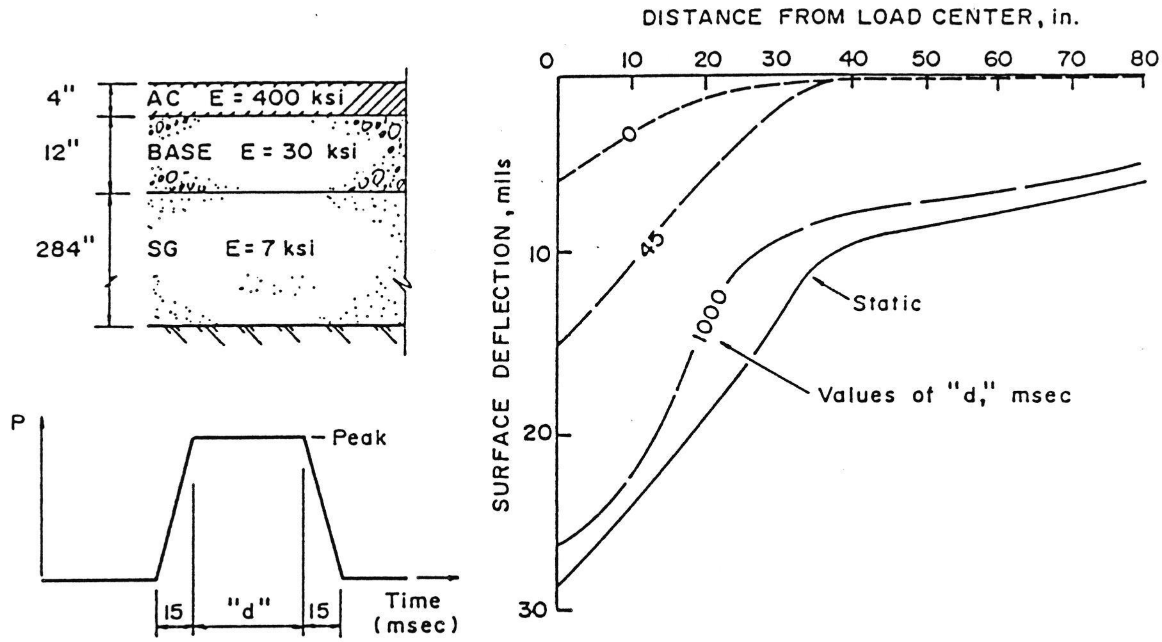

Figure 3.17 Effect of Load Duration on Surface Deflection from ANSYS Analyses.

Dynamic vs. Static Loads. Figure 3.18 clearly shows that there is a problem when trying to contrast dynamic and static deflections since the dynamic responses are sensitive to the rate of loading. The duration and shape of the loading curve shown in Figure 3.16 was used for this research and the comparisons therein.

In a static model, the load is infinitely long, enabling the pavement to continue to deform until it reaches a static equilibrium. However, a moving wheel, like the FWD, produces a short, transient load that will not allow the pavement to complete its full cycle of potential deformation. Thus, dynamic deflections are generally lower than their static counterparts.

There is significant difference between the dynamic and static deflection basins shown in Figure 3.18 for both of the pavement sections considered. This large disparity is primarily due to the inertial and damping properties of the pavement mass - properties that are totally neglected in static analyses. The effect of these differences on back calculated moduli is examined in detail in the following section.

In order to illustrate the effect of the above described phenomena on back calculated moduli, static and dynamic deflection basins were generated with the ANSYS model for the pavement section shown in Figure 3.19. Then, using FPEDD1 and BISDEF, the moduli were back calculated using both types of basin. The results are shown in Tables 3.7 through 3.10.

The actual and computed moduli are listed at the top of each table, and are followed by a brief statistical analysis. The absolute values of the percent difference between the actual and computed deflections are listed in the right-most column and are accumulated at the bottom; this value is the "absolute sum of errors" (ABSE). It is the parameter upon which the relative accuracy of the procedures is based.

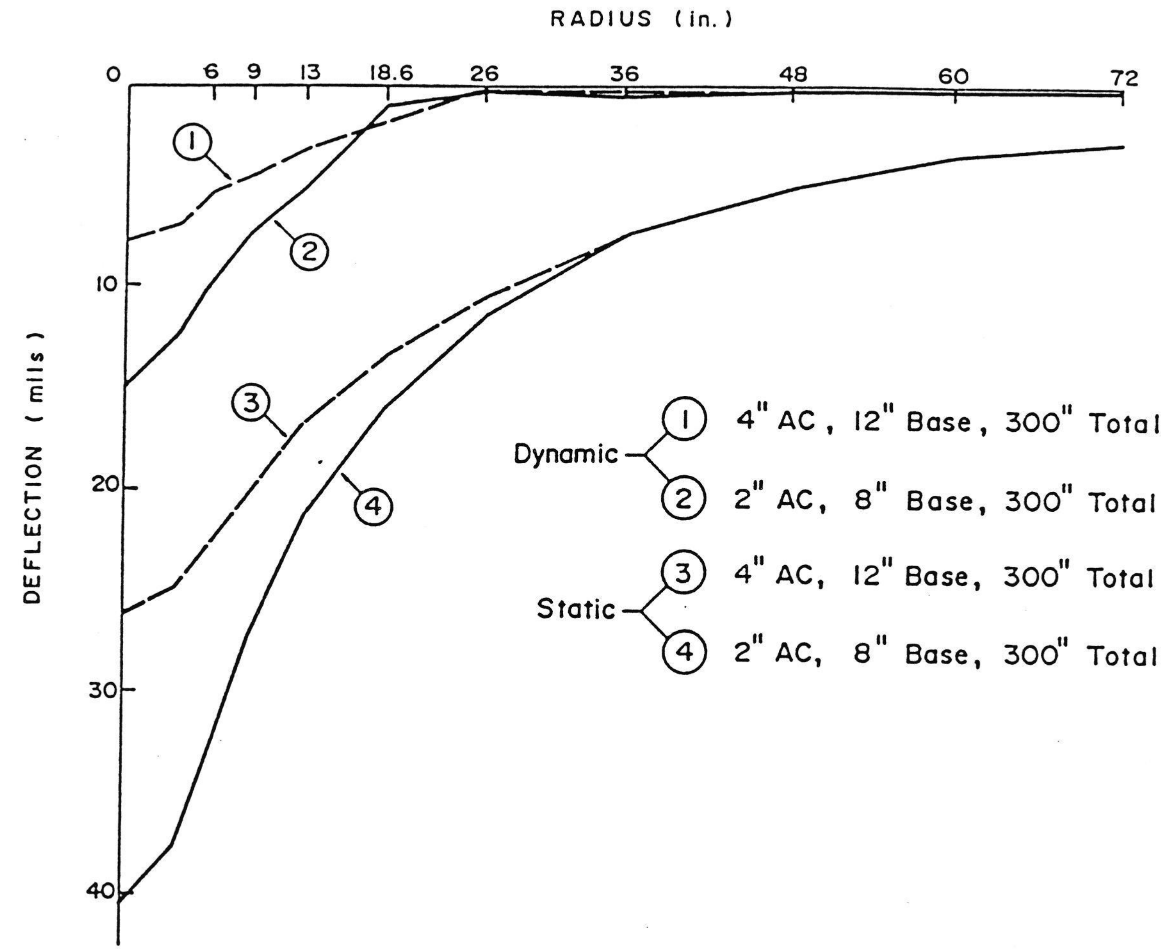

Figure 3.18 Comparison of Static and Dynamic Deflection Basins from ANSYS Analyses.

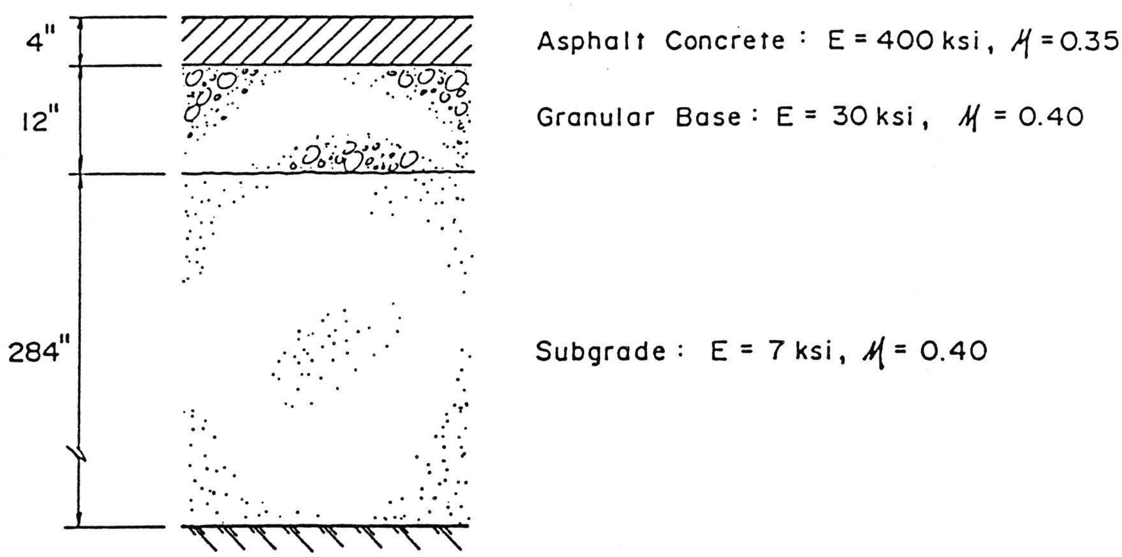

Figure 3.19 Pavement Section Used in Analyses to Evaluate Effect of Dynamic Loading on Back Calculated Pavement Moduli.

Table 3.7 Back Calculated Moduli from Static Deflections Using FPEDD1.

Actual Moduli (ksi): E1 = 400.0, E2 = 30.0, E3 = 7.0

Computed Moduli (ksi): E1 = 707.3, E2 = 23.5, E3 = 7.9

Radius	Actual Defl.	Computed Defl.	Absolute % Diff.
0"	26.24	28.46	8.46
6	22.89	25.64	12.01
13	16.93	18.40	8.68
26	10.43	10.99	5.37
36	7.51	7.67	2.13
48	5.22	5.20	0.38
60	3.72	3.72	0.00
			=====
			ABSE = 37.03

Table 3.8 Back Calculated Moduli from Dynamic Deflections Using FPEDD1.

Actual Moduli (ksi): E1 = 400.0, E2 = 30.0, E3 = 7.0

Computed Moduli (ksi): E1 = 546.4, E2 = 30.1, E3 = 172.5

Radius	Actual Defl.	Computed Defl.	Absolute % Diff.
0"	7.91	7.62	3.67
6	5.65	5.40	4.42
13	3.24	1.93	40.43
26	0.52	0.35	32.69
36	0.39	0.27	30.77
48	0.37	0.22	40.54
60	0.12	0.16	33.33
			=====
		ABSE =	185.85

Table 3.9 Back Calculated Moduli from Static Deflections Using BISDEF.

Actual Moduli (ksi): E1 = 400.0, E2 = 30.0, E3 = 7.0

Computed Moduli (ksi): E1 = 627.0, E2 = 22.4, E3 = 7.9

Radius	Actual Defl.	Computed Defl.	Absolute % Diff.
0	26.24	25.8	1.6
6	22.89	22.9	0.2
13	16.93	17.2	1.7
26	10.43	10.4	0.6
36	7.51	7.4	1.5
48	5.22	5.2	0.5
60	3.72	3.8	2.1
			====
		ABSE =	8.2

Table 3.10 Back Calculated Moduli from Dynamic Deflections Using BISDEF.

Actual Moduli (ksi): E1 = 400.0, E2 = 30.0, E3 = 7.0

Computed Moduli (ksi): E1 = 571.2, E2 = 37.0, E3 = 143.3

Radius	Actual Defl.	Computed Defl.	Absolute % Diff.
0	7.91	8.2	3.3
6	5.65	6.0	6.6
13	3.24	2.6	20.2
26	0.52	0.6	10.2
36	0.39	0.3	13.4
48	0.37	0.3	29.4
60	0.12	0.2	71.6
			====
			ABSE = 154.8

From the data that appear in Tables 3.7 through 3.10, the following conclusions may be drawn:

1. In terms of the selected statistical parameter (ABSE), the static basin gives results that are far superior to those obtained using a dynamic basin.
2. The dynamic deflections gave moduli values that were slightly closer to the actual moduli for the top two layers (surface and base) in a three layer system than the static deflections did.
3. The static deflections yielded subgrade moduli that were very close to the actual values; the moduli back calculated from the dynamic deflections were significantly higher.
4. Since the deflection data from an FWD are not static deflections, the use of dynamic (FWD) basins in a back calculation procedure such as BISDEF or FPEDD1 will yield subgrade moduli that are too high. This conclusion is based on the findings from the finite element model which showed that the dynamic deflections to be much lower than their static counterparts.
5. These comparisons show that, given the appropriate data, iterative back calculation procedures are a rational approach with which to predict the elastic moduli of layered systems using surface deflections.

Conclusion No. 3 is of particular concern since the overall goal of this research is to develop a method for estimating subgrade moduli from NDT data. It is obvious that the use of dynamic deflection data in a static based, iterative back calculation procedure will result in misleading moduli for the subgrade layer, and the use of these moduli for design will generally lead to insufficient pavement thicknesses.

3.6.3 Effect of Subgrade Thickness on Surface Deflections

The effect of the thickness of the subgrade layer (depth to a bedrock) is considered for static and dynamic loadings.

Static Loading. In this analysis, all of the parameters shown in Figure 3.19 are held constant in the finite element model except for subgrade thickness, which is varied from 100 to 700 inches in increments of 200 inches. A static point load was applied to the FWD plate, and the deflections were recorded. The results are illustrated in Figure 3.20. From this figure, it is obvious that magnitude of the surface deflections due to a static loading are quite sensitive to the subgrade thickness. This phenomenon also appears in layered elastic programs such as ELSYM5 or BISAR.

Dynamic Loading. The same type of analysis was performed as that above, but for a dynamic load of the type described in Section 4.1.2. The results are presented in Table 3.11. In all cases, the magnitude of the deflections did not change considerably from one subgrade thickness to the next. This implies that dynamic deflection occurs in, at most, the top 100 inches of the subgrade layer, and possibly less.

As pointed out previously, it takes a load duration of at least one second for the model to complete its full cycle of surface deflection. Therefore, it seems logical that the full static basin cannot be achieved with a load that is less than one thirtieth of what can be considered a "static" load.

3.7 EVALUATION OF BACK CALCULATION METHODS

The various approaches for back calculating the subgrade resilient modulus were discussed in Section 3.5. These approaches were evaluated for practical application using FWD data from numerous sites around the state. The specific procedures evaluated were: BISDEF, FPEDD1, ELMOD, MODULUS, and the ILLI-PAVE

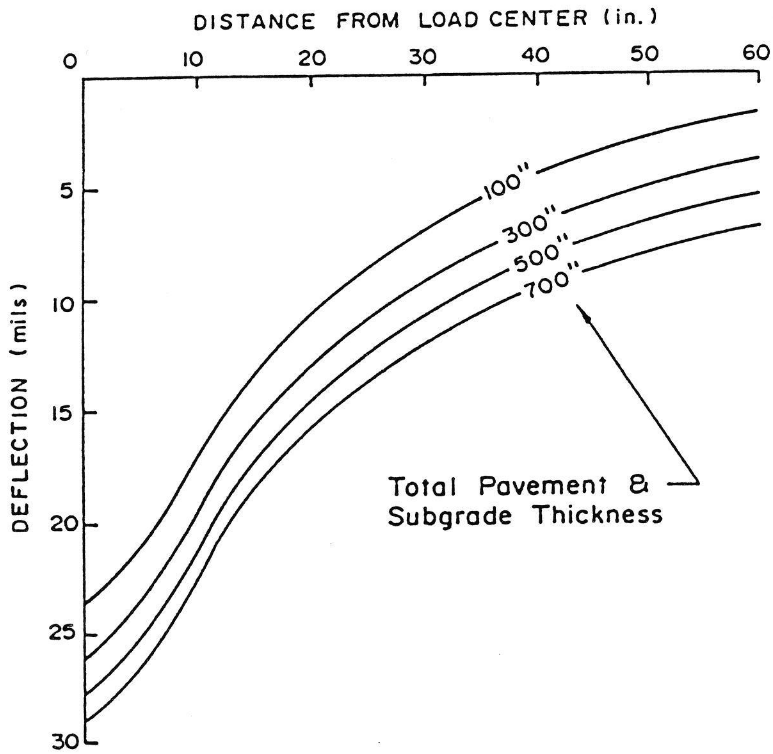

Figure 3.20 Effect of Subgrade Depth on Static Deflections.

Table 3.11 Effect of Subgrade Thickness on Predicted Deflections from a Dynamic Load Using ANSYS Model.

	Subgrade Thickness			
Radius (in.)	100	300	500	700
0	7.92	7.91	7.91	7.91
6	5.68	5.66	5.66	5.66
13	3.28	3.24	3.24	3.24
26	0.03	0.02	0.02	0.02
36	0.20	0.19	0.19	0.18
48	0.39	0.37	0.37	0.36
60	0.15	0.12	0.12	0.12

based algorithms. With the exception of the ILLI-PAVE algorithms, these procedures estimate the apparent elastic modulus (E) of all pavement layers. The ILLI-PAVE algorithms estimate only the "breakpoint" resilient modulus (E_{ri}) of the subgrade. (As will be discussed in Section 3.8, this turns out to be an advantage for use in a procedure based on the AASHTO Guide.)

Each procedure uses surface deflection data and physical data from the pavement itself to predict the moduli. Presumably, they can be expected to arrive at similar values for like conditions; it is further presumed that these values can be used for a basis on which to compare the different techniques.

All of the deflection and physical data for this portion of the research were collected by the Arkansas Highway and Transportation Department (AHTD) at the sites indicated in Figure 3.21. These particular locations were selected so that a broad range of pavement thicknesses, construction materials, and subsurface conditions in Arkansas were represented. All of the roads tested were conventional flexible pavements with the exception of Hwy. 79, which is a full-depth asphalt pavement.

Data was collected from each of the test sections in the spring, summer and fall seasons with a slight emphasis being placed on the spring period. The emphasis on testing in the spring was intended to provide data that could be used for establishing adjustments for the time of year in which the tests were made. The individual sections consisted of 25 FWD drop points spaced 25 feet apart in the outer wheel path of the traffic lane. The points were painted upon each visit so that the same spot could be tested again at a later time. On at least one of the visits, asphalt cores and soil samples (Shelby tubes, if possible) were collected at two or more drop points for laboratory testing. The thicknesses of the layers were confirmed in the field during coring.

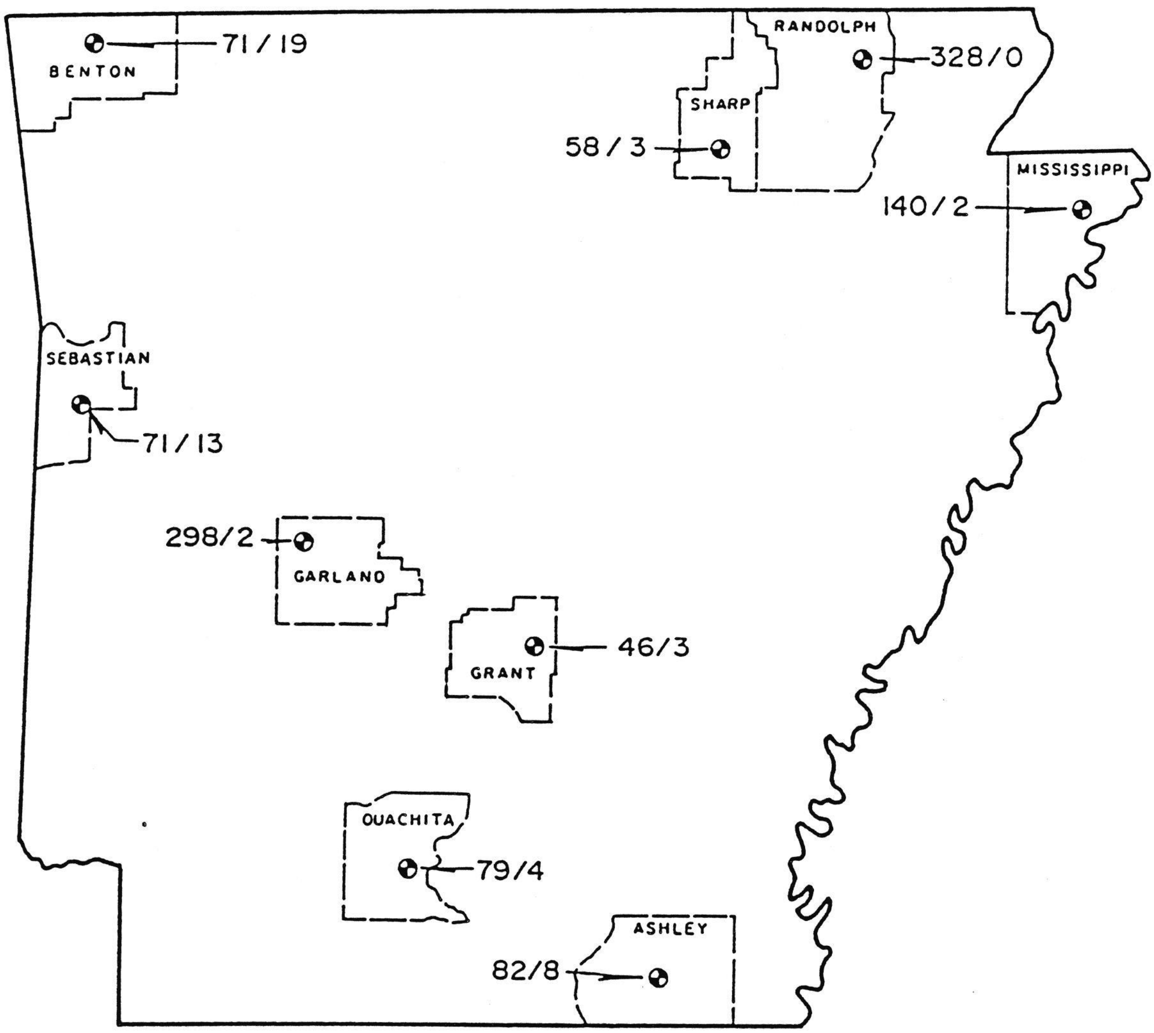

Figure 3.21 Major Test Sites for Deflection Studies.

Two sets of analyses were conducted. The first set involved comparison of values back calculated by the various methods. For these analyses, "representative" deflection basins were selected from each test site for each testing time. This set of analyses is referred to as the Representative Basin Analyses. The second set involved analyzing the only the deflection basins from which subgrade samples were taken and tested. These analyses are referred to as the Laboratory Comparison Analyses.

3.7.1 Representative Basin Analyses

For each visit to each test section one "representative" basin was selected from the 25 drop points using the computer program BASIN (76) which was developed by Al Bush at the Waterways Experiment Station in Vicksburg, Mississippi. A flowchart of the procedure for selecting the representative basin from a series of drop points is shown in Figure 3.22, and brief descriptions the steps are as follows:

1. The data required include the number of stations (N), peak load (P), number of sensors (n), deflections (d_i), and sensor radii (r_i).
2. The maximum (P_{max}) and average (P_{avg}) loads are determined.
3. All of the deflections are normalized to the maximum load level.
4. For each basin, AREA and ISM are computed.
5. The average AREA, ISM, and deflections are computed for the entire data set.
6. The sum square errors are computed for AREA, ISM, and deflections.
7. The error sums are computed for each basin, and the one having the lowest error sum is presented as the representative basin.

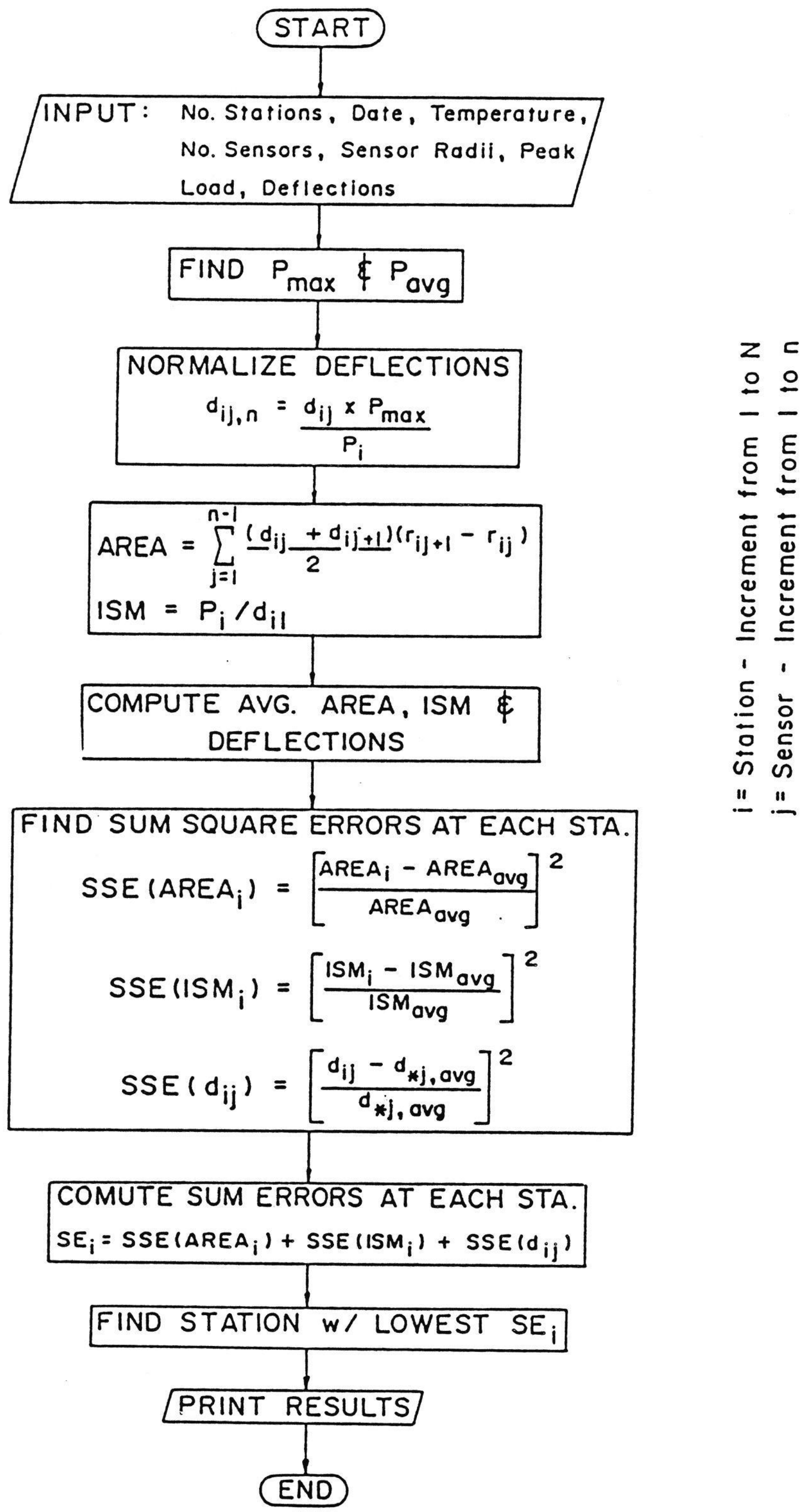

Figure 3.22 Flow Diagram for BASIN Program that Selects "Representative" Basin from a Series of Deflection Sites (Ref 76).

Due to the rather short test sections, the representative basin was very similar to most of the others in the data set. Table 3.12 lists the representative deflection data for each site visit along with physical data pertinent to the selected back calculation procedures.

As described in Section 3.6.3, the thickness of the subgrade layer has a significant effect on the moduli back calculated using static based procedures. Since no additional field testing was performed to determine the subgrade thickness, values were assumed based on general knowledge of the local soil strata. In general, the thicknesses were less in the mountainous regions of northwest Arkansas, and approaching "semi-infinite" in the alluvial plains in the south and southeast portions of the state.

The moduli that were back calculated from the data in Table 3.12 are compiled in Table 3.13. This section includes analyses and summaries of the results, and evaluations of the individual procedures. A review of the important points as established in the previous sections is presented here.

> <u>Loading Mechanism.</u> All six of the back calculation routines are based on a statically loaded model, and, when using deflection data from a dynamic testing device, one must be aware of the types of errors that will occur (see Section 3.6.2)
>
> <u>Subgrade Depth.</u> As illustrated in Section 3.6.3, the depth to the rigid boundary has a significant effect on static surface deflections, but very little on the dynamic surface deflections (according to the finite element model). In reality, it is believed that the subgrade thickness influences the FWD surface deflections - not as much as the static model suggests, but more than the dynamic one does.

Table 3.12 Representative Data from Deflection Test Sites.

Pt/Sec	Date	Temp.	Tac	Tbse	Tsb	Drop Pt.	Load	D_0	D_8	D_{12}	D_{24}	D_{36}	D_{48}	D_{60}
46/3	8-26-87	92°F	1.9"	5.0"	18.0"	18	9064	16.6	13.0	8.4	3.6	2.6	2.0	1.6
46/3	9-22-87	79	1.9	6.0	14.0	11	9144	17.4	13.3	8.5	3.5	2.6	2.0	1.6
46/3	3-15-88	80	1.9	6.0	14.0	13	8800	24.3	17.6	12.8	5.0	3.4	2.8*	2.1
58/3	6-10-87	89	2.0	6.0	--	20	8624	29.5	21.0	12.7	2.3	1.5*	0.8	0.7
58/3	8-24-87	71	2.0	6.0	--	14	8880	26.3	19.1	12.1	3.5	1.8	1.1	0.7
58/3	9-21-87	95	2.0	6.0	--	21	8640	26.7	17.0	9.2	2.4	1.7	1.1	0.8
58/3	4-21-88	108	2.0	6.0	--	22	9944	47.5	32.2	19.7	2.1*	1.6*	1.5	1.3
71/19	5-19-87	81	9.0	6.0	--	14	9056	6.9	5.5	4.5	2.5	1.5	0.7	0.5
71/19	8-17-87	88	9.0	6.0	--	21	9024	13.9	10.9	7.1	2.6	1.5	1.9	0.7
71/19	9-24-87	87	9.0	6.0	--	24	8792	13.6	10.3	7.2	2.9	1.7	1.2	0.8
71/19	4-28-88	55	9.0	6.0	--	2	9600	4.9	4.2	3.7	2.5	1.6	1.2*	0.7
71/13	4-5-87	89	8.8	6.0	--	9	9360	10.0	8.4	7.2	3.9	2.1	1.2	0.8
71/13	8-19-87	88	8.8	6.0	--	7	9272	9.5	8.1	6.8	3.8	2.1	1.2	0.8
71/13	9-29-87	78	8.8	6.0	--	14	9952	6.0	5.0	4.1	2.4	1.6	0.8	0.5
71/13	4-20-88	60	8.8	6.0	--	22	8168	7.8	6.8	6.0	3.7	2.2	1.1	0.3
79/4	7-21-87	95	9.5	---	--	16	9120	23.0	20.7	17.9	11.2	6.7	3.9	2.2
79/4	8-12-87	92	9.5	---	--	15	8936	23.0	20.6	18.0	11.6	7.6	4.7	3.1
82/8	5-7-87	75	5.8	6.0	12.0	24	8544	18.5	14.0	11.0	5.7	3.7	2.6	2.0
82/8	8-12-87	118	5.6	6.0	12.0	11	8552	19.5	15.7	11.2	5.3	3.6	2.6	2.0
82/8	3-16-88	70	5.8	6.0	12.0	25	8760	18.0	14.5	11.9	5.9	3.8	2.9*	2.0
82/8	5-2-88	97	5.6	6.0	12.0	10	8192	18.9	15.0	11.8	5.4	3.5	2.4*	1.8
140/2	8-13-87	92	3.3	12.0	10.0	10	9032	16.8	14.6	11.3	6.2	4.2	3.2	2.6
140/2	9-28-87	82	3.0	11.0	10.0	9	9344	17.5	14.6	11.4	6.1	4.2	3.2	2.7
298/2	6-1-87	83	4.0	5.0	--	13	9008	15.1	9.7	6.3	1.7	0.7	0.5	0.3
298/2	8-18-87	84	4.0	5.0	--	22	8656	12.3	7.1	4.6	1.8	1.0	0.5	0.4
298/2	5-5-88	110	4.0	5.0	--	18	9280	18.9	11.9	7.1	1.9	1.1	0.8*	0.5
328/0	5-27-87	98	4.0	8.0	--	24	8520	51.8	38.7	24.3	5.3	3.1	2.8	2.3
328/0	8-11-87	101	4.0	8.0	--	24	8608	48.8	37.6	24.3	5.4	3.2	2.9	2.3
328/0	9-21-87	89	4.3	10.0	--	12	8976	43.1	33.7	22.9	6.8	3.4	2.9	2.6
328/0	4-5-88	101	4.0	10.0	--	10	8096	35.1	26.3	13.3	5.7	3.0	2.5*	2.0

* - At the locations where a deflection sensor was not functioning, or not yeilding "decreasing deflections," the deflection was adjusted based on other basins or on adjacent deflections.

Load in Lbs; Deflections in mils (10^{-3} in.)

Table 3.13 Back Calculated Subgrade Moduli from Deflection Test Sites.

Rt./Sec.	Date	Subgrade Depth	Sta.	BISDEF	FPEDD1	ELMOD	ILLI-1	ILLI-2	ILLI-3
46/3	3-15-87	218	13	14.0	13.6	13.5	2.0	9.3	10.3
46/3	8-26-87	"	18	19.5	20.5	15.1	10.2	19.3	13.4
46/3	9-22-87	"	11	19.8	20.3	14.0	8.3	22.5	13.5
58/3	6-10-87	80	20	16.7	17.1	7.8	4.2	17.5	17.5
58/3	8-24-87	"	14	14.5	15.2	13.0	5.6	17.5	16.4
58/3	9-21-87	"	21	15.8	15.5	8.8	7.0	27.0	16.6
58/3	4-21-88	"	22	14.9	13.8	4.4	1.1	12.0	18.0
71/19	5-19-87	80	14	26.4	25.3	14.0	56.0	79.0	17.9
71/19	8-17-87	"	21	19.4	20.2	15.9	6.8	74.1	17.8
71/19	9-24-87	"	24	17.1	16.5	21.2	6.3	60.4	16.7
71/19	4-28-88	"	2	23.4	19.0	----	56.2	87.0	17.8
71/13	4-5-87	100	9	23.0	21.3	17.3	32.1	21.8	15.6
71/13	8-19-87	"	7	23.1	24.2	----	35.4	23.1	15.5
71/13	9-29-87	"	14	37.8	33.6	14.7	126.0	89.2	18.0
71/13	4-20-88	"	22	26.9	27.0	9.1	8.0	26.5	14.0
79/4	7-21-87	999	16	11.7	11.7	5.4	----	1.6	2.9
79/4	8-12-87	"	15	10.0	10.1	5.6	----	1.4	1.7
82/8	7-7-87	999	24	17.4	16.9	15.7	3.2	12.3	8.9
82/8	8-12-87	"	11	17.0	16.8	19.1	14.2	7.8	9.3
82/8	3-16-88	"	25	17.5	17.6	13.3	3.4	9.8	8.9
82/8	5-2-88	"	10	13.2	18.2	12.6	8.0	7.1	9.1
140/2	8-13-87	999	10	15.4	15.7	16.1	20.7	4.8	8.1
140/2	8-28-87	"	9	15.2	15.0	16.6	15.3	6.2	8.5
298/2	6-1-87	80	13	34.3	35.2	22.2	47.2	87.8	21.5
298/2	8-18-87	"	22	29.0	27.9	29.3	90.3	116.4	19.9
298/2	5-5-88	"	18	24.7	20.5	24.7	53.5	52.9	19.8
328/0	5-27-87	120	24	8.9	9.0	3.2	0.5	4.6	9.9
328/0	8-11-87	"	24	8.9	9.1	3.2	0.7	4.4	10.7
328/0	9-21-87	"	12	9.0	9.1	4.2	0.7	5.1	10.5
328/0	4-5-88	"	10	8.7	8.5	4.9	1.7	5.2	10.7

Factors Affecting Moduli. The parameters to which the iteratively back calculated moduli are most sensitive are the subgrade thickness (as discussed above) and the surface deflections at the outer sensors. Referring back to Figure 3.18, it can be seen that for a 300-inch thick subgrade with varying pavement thicknesses, the outer deflections are almost identical. The reason for this is the limited radius of influence of the reinforcing layers; in this case the radius of influence is approximately less than 36 inches.

Two different iterative back calculation procedures were examined: BISDEF and FPEDD1. Their operation and theoretical backgrounds are reviewed in Section 3.5.1. These two programs were more complex, difficult and time consuming to use than the other techniques. However, the iterative format is an effective method of estimating moduli, given the appropriate data (see Section 3.6.2). The other back calculation procedures evaluated by these analyses are ELMOD, which has a "black box" appearance but is believed to also follow some iterative approach, and the ILLI-PAVE algorithms, which are directly calculation approaches based on regression equations developed from finite element analyses. The following is a brief discussion of the apparent merits of each method based on these analyses.

(Note that the program MODULUS was not included in this set of analyses. MODULUS became available to the study after these were complete. MODULUS was evaluated as a part of the Laboratory Comparison Analyses.)

BISDEF. The program BISDEF, although complex, is made easier to use with the help of the interactive program BINPUT which creates correctly formatted input files. The entire process of creating a data file for one basin and back calculating the moduli takes from ten to thirty minutes on a microcomputer. The variation in computing times is mainly due to the number of layers and the quality of the seed moduli.

One important characteristic of BISDEF is that the predicted moduli of the subgrade layer are much more consistent and reproducible than the moduli for the layers above it. This is an inherent feature of the "bottom to top" approach of the iterative procedures. Such a quality lends itself to the topic of this research, since, in the proposed overlay design procedure, the structural contribution of the reinforcing layers will be included in the effective structural number parameter.

The overall performance of BISDEF can only be considered "fair" for the following reasons:

1. The time required to run a single deflection basin is considerable, and very often several runs are required to derive a set of moduli that are acceptable in terms of the absolute sum of the percent errors (ABSE). The moduli set should be refined so that the ABSE is less than about 100 percent; however, based on this criterion, some data sets will never achieve an acceptable ABSE. The default criterion is ten percent, which is unrealistic when dealing with "real world" data.
2. As discussed in Section 3.6.3, the thickness of the subgrade layer has a dramatic effect on back calculated moduli as is clearly illustrated in Figure 3.23. It is obvious that reliable subgrade thicknesses are essential to the procedure as it exists. However, such data are extremely difficult to come by since subgrade depths are so variable, and no effective means of inferring them from surface deflections has been developed.

It was observed that for the pavements that were known to be founded on extremely deep subgrade layers, the apparent performance of the program

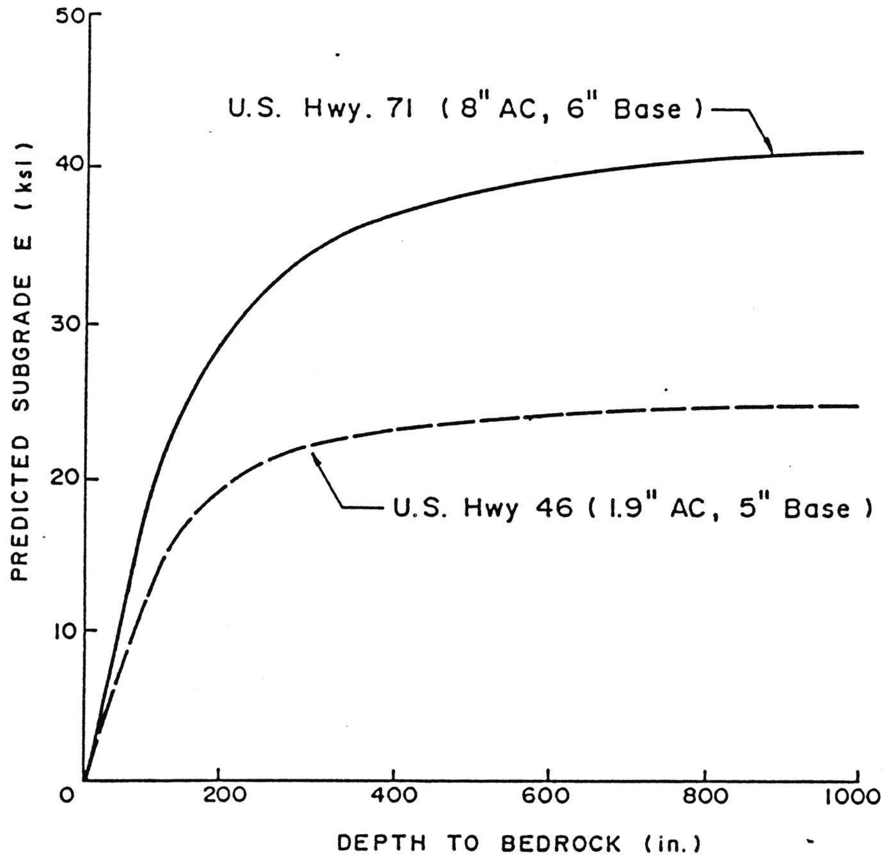

Figure 3.23 Effect of Depth to Bedrock on Back Calculated Subgrade Moduli.

increased. This notion is supported by the data in Table 3.14, and proves that reliable subgrade depths will help the program to yield more accurate moduli.

FPEDD1. The back calculation computer program FPEDD1 also uses the iterative format. The results when using this program were similar in magnitude and consistency as those derived with BISDEF. The major functional difference between the two programs is that BISDEF uses the elastic layer program BISAR, and FPEDD1 uses ELSYM5 to generate deflection basins.

Because of the lack of relative difference in the two procedures, FPEDD1 suffers from the same limitations as BISDEF. However, FPEDD1 attempts to address the problem of variable and unknown subgrade thicknesses. It uses the theory of wave propagation to estimate the depth to a rigid layer [36]. In all of the cases considered in this research, the inferred subgrade depths were consistently large, and in some cases did not appear to be realistic. This program can also be rated as "fair," because of the considerable time required to arrive at an acceptable set of moduli.

ELMOD The program ELMOD was developed, and is distributed by Dynatest, the company that manufactures the falling weight deflectometer. It is written in such a way that it is an integral part of the Dynatest FWD system, and uses deflection data in the same format as it is stored by the on board microcomputer.

The primary advantages of this program lie in its convenience and ease of use. Since the data for the entire test section comes in a format that can readily be used, data preparation time is minimal. The program itself is interactive and very simple to operate.

The time required to analyze an entire test section (25 basins in this case) takes about five minutes: very short in comparison to the manipulation

Table 3.14 Effect of Estimated Subgrade Depth on Average Absolute Sume of the Percent Error (ABSE) of Predicted Deflection.

Rt./Sec.	Subgrade Depth	Avg. ABSE (BISDEF)
46/3	218"	77.2%
58/3	80	186.4
71/19	80	102.9
71/13	100	42.2
79/4	999	91.0
82/8	999	67.5
140/2	999	31.4
298/2	80	108.7
328/0	120	169.5

time for <u>one</u> basin using an iterative program. The ELMOD program does not rely on the user for a great deal of guidance to obtain acceptable moduli. This is also looked upon as a disadvantage because the program may appear to be a "black box" approach from which input data spawns output data with very little user control. With an iterative program, the results can be controlled somewhat by the nature of the seed moduli, moduli ranges, and subgrade depths. The two iterative programs studied provide a detailed summary of the computations used to arrive at a moduli set. ELMOD, on the other hand, simply prints the final moduli.

The problem of a rigid layer at finite depth is also addressed by ELMOD. The program will query the user as to whether a rigid layer is likely to exist at shallow depth. If so, it asks for the maximum equivalent depth to said rigid layer. Then, using the specified maximum depth, it computes an estimate of the actual depth, and adjusts the layer moduli accordingly. The performance of ELMOD can be considered good with respect to both time and the quality of the predicted subgrade moduli.

<u>ILLI-PAVE Algorithms</u> The ILLI-PAVE response algorithms were developed as described in Section 3.5.3, and the results from the three selected algorithms are presented in Table 3.13. In that table, the notations ILLI-1, ILLI-2 and ILLI-3 correspond to equations 3.14, 3.15 and 3.16 respectively. Where an estimate of the modulus of elasticity of the asphalt concrete was required, that value was obtained from a curve like the one shown in Figure 3.24.

<u>ILLI-1</u>. The first of the ILLI-PAVE based algorithms, Equation 3.14, had the lowest correlation coefficient of the three, 0.889. This means that this algorithm fit the data from which it was derived more loosely than the other two. This algorithm gave results that were much more erratic than any of the other algorithms or procedures. The reason for its relatively poor perfor-

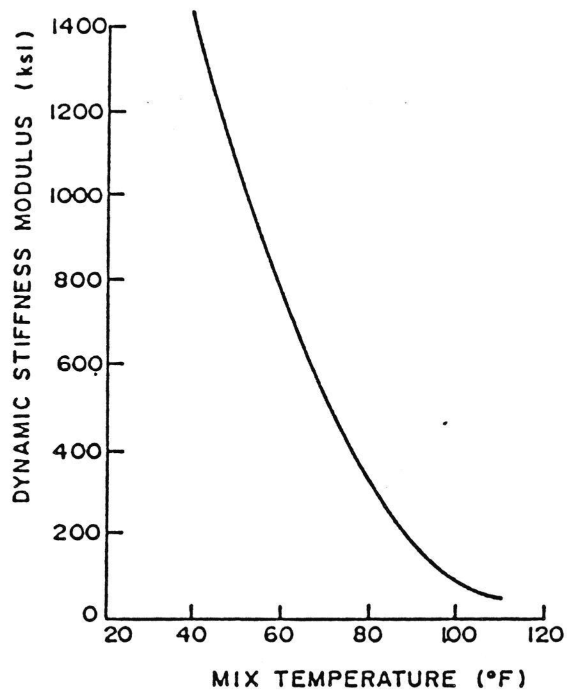

Figure 3.24 Typical Relationship between Temperature and AC Modulus.

mance is that all of the terms in the equation were directly related to the properties of the pavement layers rather than the subgrade itself. The center deflection (D_0) is the only term that has a subgrade component. As a result, the moduli shown in Table 3.13 for ILLI-1 are heavily influenced by the in-situ condition of the surface and base course.

ILLI-2. Equation 3.15 gave results that were slightly more consistent than Equation 3.14. Its apparent stability was probably due to its use of a "deflection basin parameter." This parameter (called AREA) is the area of the deflection basin normalized by the center deflection (D_0). The algorithm had a correlation coefficient of 0.984. This equation is also influenced by the material and physical properties of the asphalt and base. Therefore, the results of Table 3.13 were erratic, although less than Equation 3.14.

ILLI-3. The correlation coefficient for Equation 3.16 is 0.990, the highest of the three selected algorithms. This means that this equation yields moduli that correlate well with the finite element regression data. Another desirable feature of this algorithm is its simplicity. Equation 3.16 uses only an outer deflection sensor for back calculating the subgrade moduli. The simplicity and strong correlation clearly imply that, in this approach, there were fewer sources of error to be taken into account.

The simplistic nature of an empirical equation make the ILLI-PAVE algorithms very easy to use. However, Equations 3.14 and 3.15 (ILLI-1 and ILLI-2) did not seem to yield consistent results because of the accountability of the reinforcing layers. On the other hand, Equation 3.16 gave results that were consistent, realistic, and seemingly reliable. These qualities along with its easy application makes ILLI-3 appear to be quite an effective tool for estimating moduli.

3.7.2 Laboratory Comparison Analyses

The laboratory comparison analyses consisted of back calculating the subgrade modulus for each test site and test time for which a soil sample was obtained and tested. The samples were obtained through a core hole at the center of FWD loading using a shelby tube. Not all shelby tube samples were tested. Some samples were obviously disturbed when removed from the tube and could not be tested. Others had dried appreciable either because of inadequate sealing or long storage times so that the laboratory resilient modulus would not be representative of field conditions.

Five back calculation methods were evaluated by these analyses: FPEDD1, MODULUS, ELMOD, BISDEF, and ILLI-3. (ILLI-1 and ILLI-2 were excluded because of the inconsistent results obtained in the previously discussed analyses.) The results of these analyses are listed in Table 3.15. The analyses showed that all five methods generally produced M_r values that were higher than the laboratory test result. Except for ILLI-3, the higher values may be explained at least in part by the natural stress dependency of the soils. The resilient modulus of typical subgrade soils is higher at lower stress levels. The laboratory values were determined at a deviator stress of 6 psi. The FWD loading probably produced a lower stress on the subgrade. The back calculated M_r would be based on the lower stress except in the case of ILLI-3 which was developed to predict the M_r at a 6 psi deviator stress. The implications of this is discussed in Section 3.8, Selection of Method for Design. Also except for ILLI-3, the back calculated M_r values were frequently unrealistically high. Values of 20 ksi or greater would be expected for a granular base material but is higher than would be expected for a subgrade soil. Only ILLI-3 consistently produced values that appear to be reasonable.

Table 3-16 lists the mean, the standard deviation, and the correlation

Table 3.15 Comparison of Back Calculated and Laboratory Measured Subgrade Resilient Moduli.

Test Site	BACK CALCULATION METHOD					LABORATORY RESULT	
	FPEDD1	MODULUS	ELMOD	BISDEF	ILLI-3	Tests	Mean
Hwy 82	15.3	17.3	18.7	17.8	8.6	4.8,6.2,3.2	4.7
Hwy 113	36.4	40.4	15.4	26.2	17.4	7.0,10.0	8.5
Hwy 140	14.1	14.9	15.8	15.7	7.5	6.4,9.3	7.9
Hwy 140	18.7	18.9	19.5	20.9	9.9	8.7	8.7
Hwy 162	40.0	52.5	32.0	40.0	19.6	8.4	8.4
Hwy 46	20.9	21.0	22.4	20.5	11.5	3.5,3.9	3.7
Hwy 58	32.7	36.3	39.9	34.7	16.5	6.7	6.7
Hwy 79	6.7	8.5	5.1	7.1	1.1	9.3,8.2	8.7
Hwy 79	9.0	11.3	7.8	10.7	1.8	8.0,2.9	5.5
Hwy 201	32.7	34.9	11.2	16.8	16.1	6.0	6.0
Hwy 328	20.5	18.6	24.2	13.3	12.2	7.8	7.8

matrix of the prediction and test results. Except for ELMOD, there is a strong correlation between the various back calculation methods. However, as expected, there is very poor correlation between the test results and all of the back calculation methods. On the average, ILLI-3 comes the closest to predicting the laboratory value.

Nevertheless, the expectation of a strong correlation between shelby tube sample tests and back calculation results may not be realistic. The shelby tube provides a measure of M_r on a very small, finite sample of the subgrade. Back calculation, on the other hand, provides a gross, overall estimate of M_r for the entire depth of pavement support. As illustrated by the laboratory test data, M_r can vary significantly within a given subgrade (e.g. Hwy 82 has 3 test results of 3.2, 4.8, and 6.2 ksi). It would seem that a "reasonable" back calculation method would provide a better estimate of the overall subgrade support than would tests on a few shelby tube samples.

3.8 SELECTION OF METHOD FOR DESIGN

In all fields of engineering, there are simplifying assumptions that must be made in order to make a particular theoretical model of the real world practical. However, simplifications that significantly compromise the accuracy of the model should be avoided, and, more importantly, the model should be used in the proper applications.

All of the back calculation procedures available assume a static loading. The use of a static model to simulate the behavior of a pavement to <u>dynamic</u> loading implies that the pavement's dynamic response is similar to its static response. As demonstrated in Section 3.6.2, this assumption is in error, and when it is used in such a manner, it will compromise the accuracy of the predicted moduli. However, the current state of the art in modulus back calcula-

Table 3.16 Simple Statistics and Correlation Matrix of Back Calculated and Laboratory Measured Subgrade Resilient Moduli.

Method of Determination	Mean	Standard Deviation
FPEDD1	22.5	11.3
MODULUS	25.0	13.9
ELMOD	19.3	10.2
BISDEF	20.3	9.9
ILLI-3	11.1	6.1
Laboratory	7.0	1.8

CORRELATION MATRIX

	MODULUS	ELMOD	BISDEF	ILLI-3	LAB TEST
FPEDD1	0.977	0.798	0.840	0.975	0.128
MODULUS		0.582	0.881	0.926	0.168
ELMOD			0.821	0.676	-0.037
BISDEF				0.824	0.112
ILLI-3					0.067

tion does not allow the design engineer to properly account for these effects since it requires a great deal of computing power to do so. Therefore, the available procedures are to be used conservatively, and with informed engineering judgement. Meanwhile, research is needed to develop a dynamic pavement model and a corresponding back calculation method.

Of the back calculation procedures examined, BISDEF, ELMOD and ILLI-3 were selected as the best of their respective methodologies. The back calculated moduli from these methods are repeated in Table 3.17, and are accompanied by a brief statistical analysis. The standard deviation was not computed for the pavements that had less than three site visits. From the data that appear in Table 3.17, the following observations may be made:

1. In general, BISDEF yields higher moduli values than the other procedures.
2. The standard deviations for the individual pavement sections varied significantly between the procedures. In almost all cases, BISDEF had the highest standard deviation, ELMOD was in the middle, and ILLI-3 had the lowest.
3. BISDEF and ILLI-3 showed the same trends within the pavement blocks.
4. BISDEF and ILLI-3 did not detect the decrease of moduli that usually occurs in the spring when the subgrade soils are the wettest while ELMOD seems to have picked it up on several of the sections. However, the spring of 1988 was relatively dry and the usual decrease may well not have occurred.

Based on these observations, ELMOD and ILLI-3 seem to be the more reliable and practical procedures. In addition, BISDEF is prohibitive from the standpoints of time and ease of use. Since the selected method is to be used in an

Table 3.17 Comparison of Back Calculated Moduli from Deflection Sites.

Rt./Sec.	Date	Subgrade Depth	BISDEF	ELMOD	ILLI-3	AVG.
46/3	3-15-87	218"	14.0	13.5	10.3	12.6
46/3	8-26-87	"	19.5	15.1	13.4	16.0
46/3	9-22-87	"	19.8	14.0	13.5	15.8
AVG.			17.8	14.2	12.4	14.8
SDEV.			3.3	0.8	1.8	3.0
58/3	6-10-87	80	16.7	7.8	17.5	14.0
58/3	8-24-87	"	14.5	13.0	16.4	14.6
58/3	9-21-87	"	15.8	8.8	16.6	13.7
58/3	4-21-88	"	14.9	4.4	18.0	12.4
AVG.			15.5	8.5	17.1	13.7
SDEV.			1.0	3.5	0.8	4.4
71/19	5-19-87	80	26.4	14.0	17.9	19.4
71/19	8-17-87	"	19.4	15.9	17.8	17.7
71/19	9-24-87	"	17.1	21.2	16.7	18.3
71/19	4-28-88	"	23.4	----	17.8	20.6
AVG.			21.6	17.0	17.6	18.9
SDEV.			4.1	3.7	0.6	3.6
71/13	4-5-87	100	23.0	17.3	15.6	18.6
71/13	8-49-87	"	23.1	----	15.5	19.3
71/13	9-29-87	"	37.8	14.7	18.0	23.5
71/13	4-20-88	"	26.9	9.1	14.0	16.7
AVG.			27.7	13.7	15.8	19.5
SDEV.			7.0	4.2	1.7	7.8
79/4	7-21-87	999	11.7	5.4	2.9	6.7
79/4	8-12-87	"	10.0	5.6	1.7	5.8
AVG.			10.9	5.5	2.3	6.2
82/8	7-7-87	999	17.4	15.7	8.9	14.0
82/8	8-12-87	"	17.0	19.1	9.3	15.1
82/8	3-16-88	"	17.5	13.3	8.9	13.2
82/8	5-2-88	"	13.2	12.6	9.1	11.6
AVG.			16.3	15.2	9.1	13.5
SDEV.			2.1	2.9	0.2	3.8
140/2	8-13-87	999	15.4	16.1	8.1	13.2
140/2	8-28-87	"	15.2	16.6	8.5	13.4
AVG.			15.3	16.4	8.3	13.3
298/2	6-1-87	80	34.3	22.2	21.5	26.0
298/2	8-10-87	"	29.0	29.3	19.9	26.1
298/2	5-5-88	"	24.7	24.7	19.8	23.1
AVG.			29.3	25.4	20.4	25.0
SDEV.			4.8	3.6	1.0	4.9
328/0	5-27-87	120	8.9	3.2	9.9	7.3
328/0	8-11-87	"	8.9	3.2	10.7	7.6
328/0	9-21-87	"	9.0	4.2	10.5	7.9
328/0	4-5-88	"	8.7	4.9	10.7	8.1
AVG.			8.9	3.9	10.5	7.7
SDEV.			0.1	0.8	0.4	3.0

overlay design procedure, time efficiency will be an important factor.

Regardless of the method used to determine M_r, the design value must be consistent with the design procedure in which it is used. Since the overlay procedure developed in this study follows the AASHTO Guide approach, the design M_r needs to be consistent with the M_r value used to represent the AASHO Road Test subgrade in the design performance equation. This value is 3,000 psi. The AASHTO Guide and appendices (1) do not indicate how or why this value was selected, but it is consistent with test data reported by Thompson and Robnett (78). Their data (Figure 3.25) shows that M_r of the AASHO soil was 3,000 psi at a deviator stress of about 6 psi when it is about 1 percent wet of optimum and tested unconfined. This suggests that the design M_r should represent the soil tested at a deviator stress of 6 psi.

Of the various back calculation methods evaluated, only the ILLI-PAVE algorithms provide a value consistent with this. The other methods attempt to back calculate the "actual" M_r that duplicates the measured deflection basin. Considering the stress dependent nature of most subgrades, the back calculated M_r can be expected to be high since the deviator stress applied by the FWD will normally be much lower than 6 psi. The ILLI-PAVE algorithms, however, were developed to predict what Elliott and Thompson term E_{ri}. E_{ri} is the "break point" resilient modulus and happens to occur at approximately 6 psi. As a result, the M_r value predicted by ILLI-3 is consistent with the AASHTO Guide design equation.

Based on all of the analyses performed under this phase of the study, the ILLI-3 algorithm was selected as the method to be used for M_r determination in the overlay design procedure being developed. The following are the primary reasons for this selection:

1) ILLI-3 was the only procedure that provided reasonable M_r values

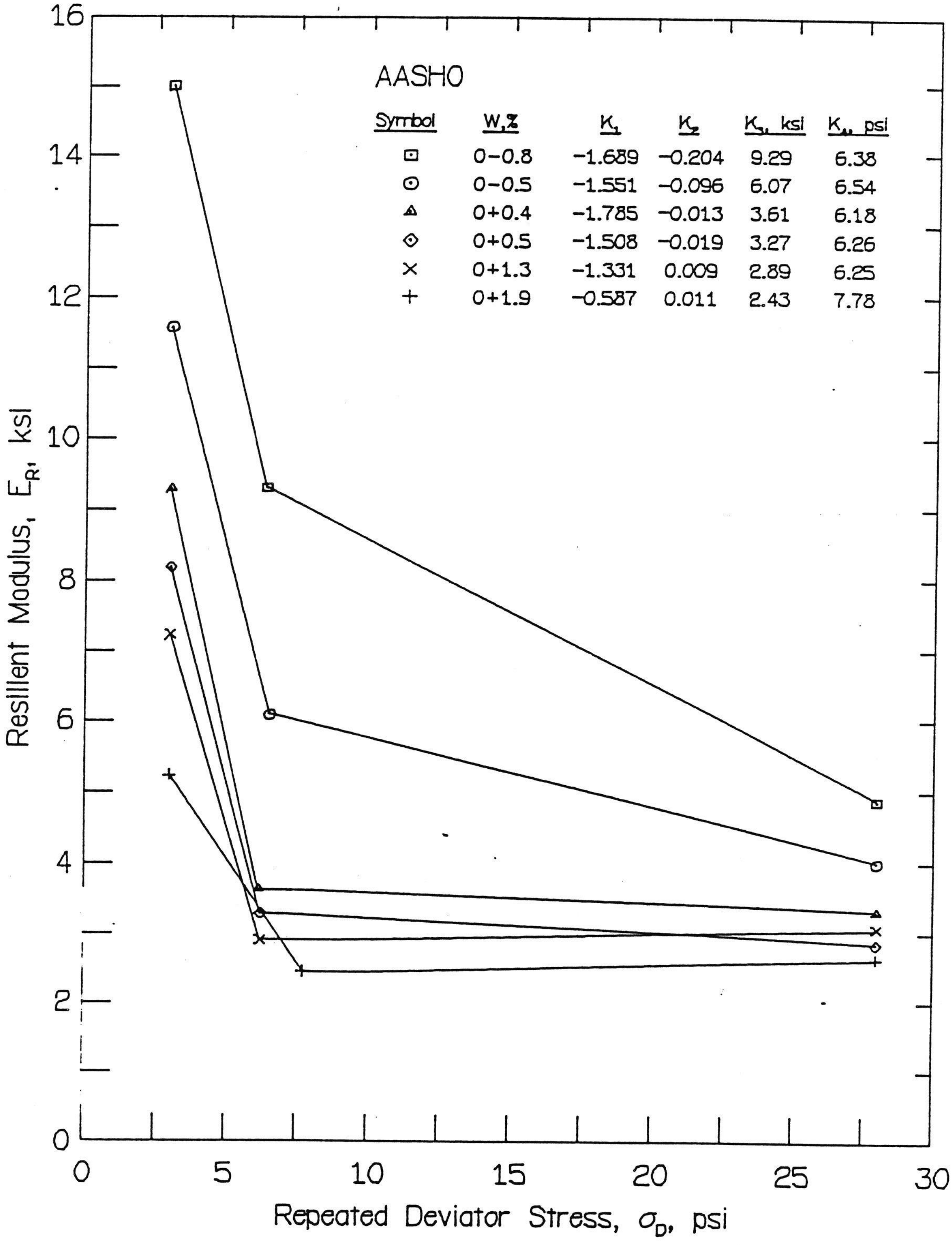

Figure 3.25 Resilient Modulus of the AASHO Road Test Subgrade (Ref 78).

in every case.

2) ILLI-3 is the fastest back calculation method, thus requiring the least computer time and permitting evaluation of every FWD test location.

3) The M_r value determined by ILLI-3 is consistent with the value used for the AASHO Road Test Subgrade in the AASHTO Guide design equation.

4) ILLI-3 is a simple, but powerful equation. It is based on a large data base and fits a wide range of pavement conditions. The specific equation evaluated (Eq 3.16) was developed for conventional flexible pavements having AC thicknesses ranging from 3 to 8 inches. However, equations were also developed for surface treatments on a granular base and for Full Depth pavements having thicknesses of 4 to 16 inches. The three equations are nearly identical and for practical purposes produce the same M_r prediction:

<u>Other ILLI-PAVE Algorithms</u>

Algorithm Developed for Surface Treatments

$$\log E_{ri} = 24.229 - 5.711\, D_3 + .351\, D_3^2 \qquad \text{(Eq 3.18)}$$

Algorithm Developed for Full Depth Pavements

$$\log E_{ri} = 24.687 - 5.411\, D_3 + .310\, D_3^2 \qquad \text{(Eq 3.19)}$$

<u>Selected Algorithm</u>

Developed for Conventional Flexible Pavements

$$\log E_{ri} = 25.035 - 5.245\, D_3 + .286\, D_3^2 \qquad \text{(Eq 3.16)}$$

CHAPTER 4

DETERMINATION OF EXISTING PAVEMENT EFFECTIVE STRUCTURAL NUMBER

4.1 AASHTO RECOMMENDED METHODS

The 1986 AASHTO Guide presents two approaches for determining the effective structural number (SN_{eff}) of the existing pavement. Both approaches use NDT data and involve backcalculation. Both procedures are also based on the assumption that SN is related to pavement (and material) stiffness. The two procedures differ in rigor and apparent sophistication. The 1986 Guide recommends the more rigorous method. The more rigorous method uses the entire deflection basin to backcalculate elastic moduli for each pavement layer. The elastic moduli are used to select layer coefficients based on assumed relationships. SN_{eff} is then calculated in the normal fashion.

The less rigorous method uses only the deflection at the center of loading and the subgrade modulus in the determination of SN_{eff}. The subgrade modulus may be either backcalculated or determined by some other means. The pavement is treated as a single layer with SN_{eff} being determined based on the effective stiffness. The 1986 Guide suggests this method for agencies that have only a Benkelman beam for deflection testing.

Neither method was considered to be satisfactory for the procedure being developed. The problems encountered in the backcalculation of subgrade modulus would obviously be compounded if the more rigorous method were used. There was also concern that with both methods the determination of SN_{eff} would be dependent upon the determination of the subgrade modulus (M_r). A more appropriate approach would allow SN_{eff} to be determined totally independent of M^r. As a result, efforts were initiated to develop a different method for determining SN_{eff} from NDT that would be independent of M_r.

4.2 CONCEPTUAL BASIS FOR THE METHOD DEVELOPED

The development of the SN^{eff} determination method began with the concept that at distances sufficiently distant from the center of loading the surface deflection is almost totally due to deformation within the subgrade. As illustrated in Figure 4.1, the zone of influence due to loading spreads with depth. Directly below the loading plate, all materials "feel" the effect of the load and deform. At locations beyond the loading plate, only those materials within the zone of influence are deformed. At some distance, only the subgrade deforms. This concept serves as the basis for most subgrade resilient modulus backcalculation methods.

Viewed from the perspective the pavement, this concept suggests that the difference between two deflections could be used as a measure of the pavement stiffness. Using the AASHTO assumption that SN_{eff} is a function of stiffness, the deflection difference becomes a measure of SN_{eff}. If the deflection at distance T in Figure 4.1 is due to subgrade deformation and the deflection at the center of loading is due to pavement and subgrade deformation, the difference between the two deflections should represent the deformation within the pavement alone. If the zone of influence spreads at an angle of about 45 degrees, the distance T would be equal to the pavement thickness.

The elastic layer theory was used to investigate the feasibility of using this concept as a basis for SN_{eff} determination. Deflection basins were generated for a variety of pavement cross-sections using the elastic layer program ELSYM5. The difference between the deflection at the center of loading and the deflection at a distance from the center equal to the pavement thickness was called "Delta D". For each cross-section, Delta D and SN were calculated. SN was calculated using layer coefficients of 0.44 for asphalt concrete and 0.14 for granular base.

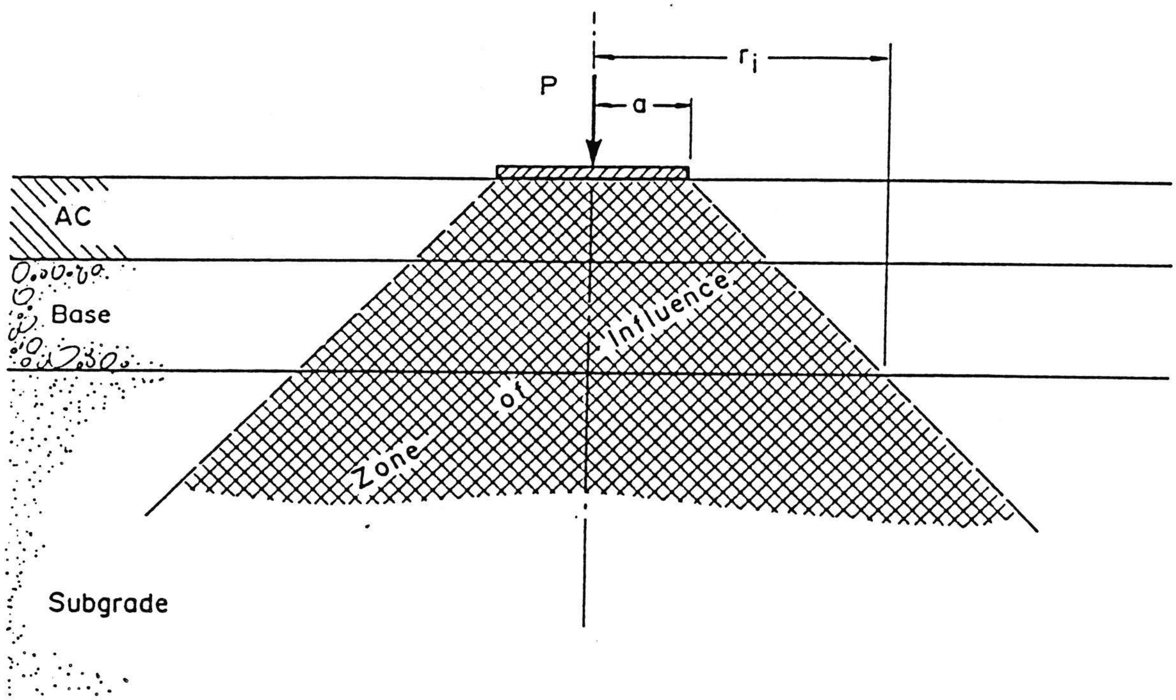

Figure 4.1 Concept of Spreading Load Zone of Influence that Serves as Basis for SN_{eff} Determination Method.

The total pavement thicknesses were 8, 12, and 24 inches. The asphalt thicknesses ranged from 1 to 7 inches with the 8 inch total thickness, 1 to 11 inches with the 12 inch total thickness, and 1 to 17 inches with the 24 inch total thickness. The elastic modulus values used in ELSYM5 to represent the asphalt and granular materials were 500 ksi and 30 ksi respectively. These represent typical values for AC at about 70^{o} F and dense graded granular base and are consistent with the layer coefficients. Subgrade resilient modulus values of 3.5 ksi, 7 ksi, 14 ksi, and 21 ksi were used for the analyses. These were selected as representative of the range of values expected for Arkansas subgrades based on TRC-94 (79). The results of the analyses (Figure 4.2) show the Delta D - SN_{eff} relationship to be reasonably independent of the subgrade modulus.

These analyses, however, incorporated the standard elastic layer assumption of a semi-infinite depth of subgrade. As discussed in Chapter 3, the subgrade depth (depth to bedrock) is believed to be one of the factors complicating the backcalculation of subgrade resilient modulus. Additional analyses were performed to determine whether this factor might also be significant relative to the Delta D - SN_{eff} relationship. Subgrade depths ranging from 8 feet to semi-infinite were considered. The Delta D - SN_{eff} relationship was also found to be reasonably independent of the subgrade depth. It was concluded that this approach would provide an practical method for the determination of SN_{eff} that would be independent of the subgrade (Figure 4.3).

4.3 TEMPERATURE ADJUSTMENT

For the method to be complete, a means was needed for temperature adjustment. Asphalt concrete is quite temperature sensitive. At higher temperatures the AC modulus decreases and at lower temperatures it increases. As a result,

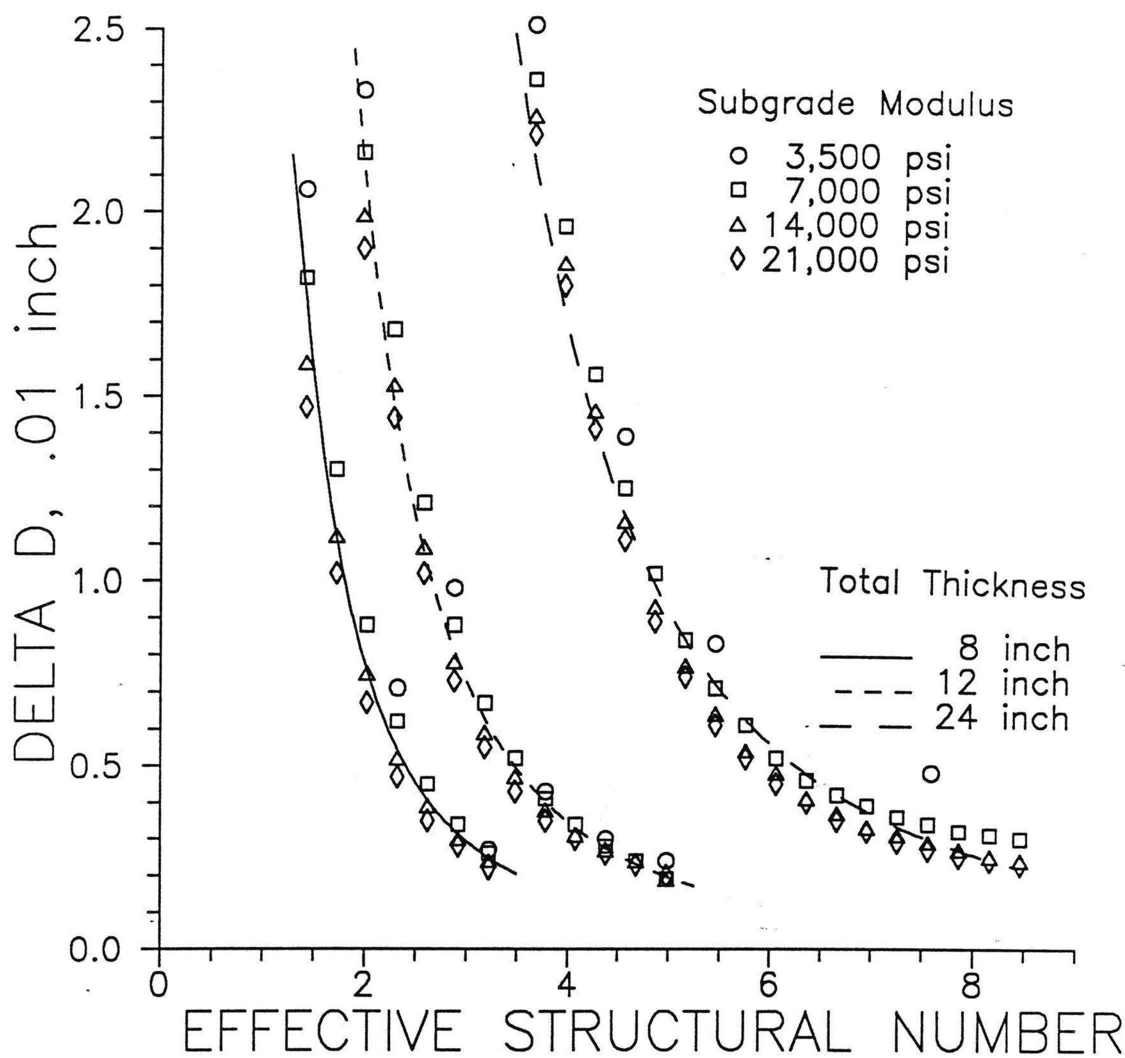

Figure 4.2 Delta D versus Effective Structural Number.

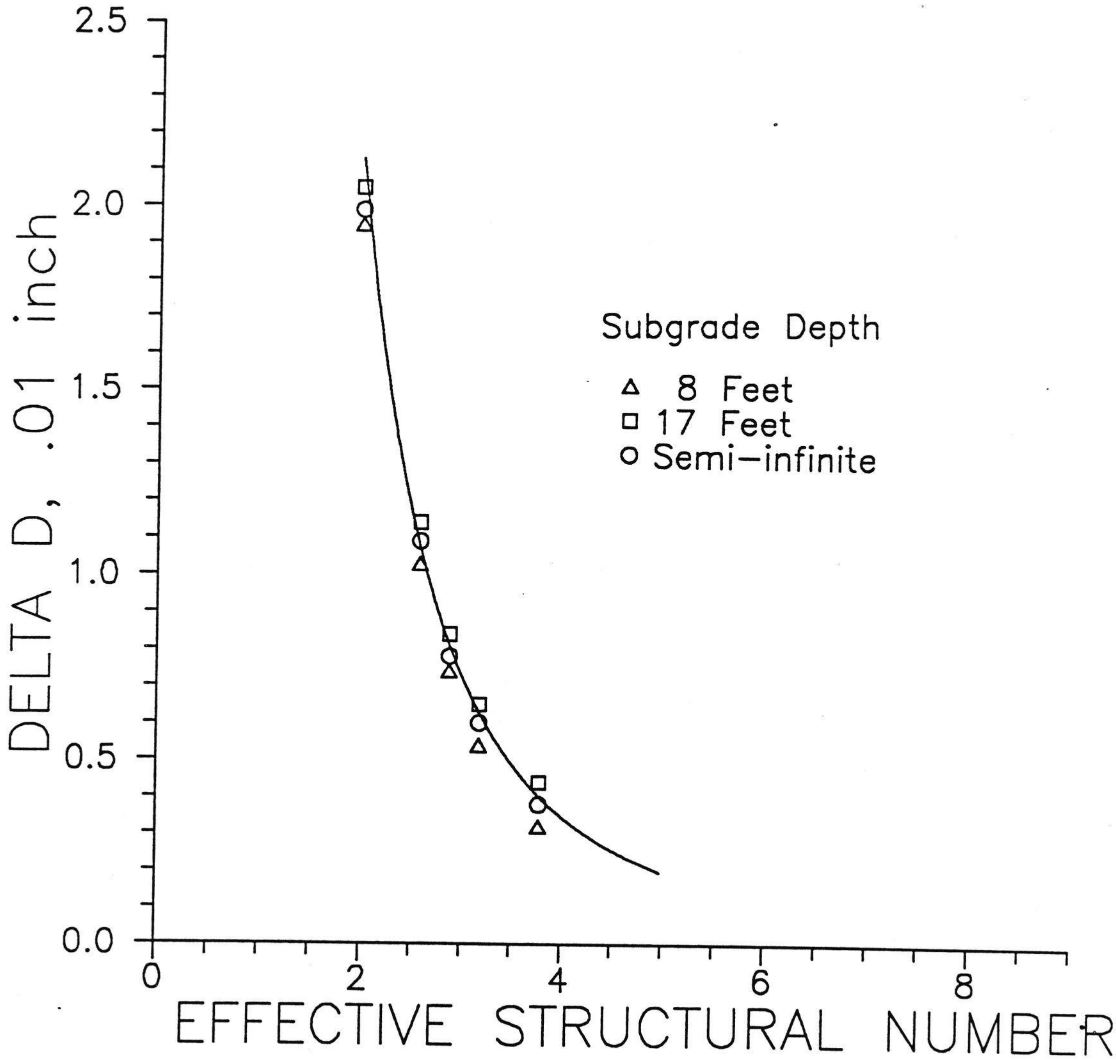

Figure 4.3 Effect of Subgrade Depth on the Delta D - SN_{eff} Relationship for a 12 inch Pavement.

Delta D is also temperature sensitive. The elastic modulus used in the above analyses was selected as typical of the resilient modulus of an Arkansas asphalt concrete at 70° F.

Additional ELSYM5 analyses were conducted to examine the effect of other AC temperatures on Delta D. The AC modulus-temperature relationship shown in Figure 4.4 was used to select modulus values for other temperatures. From these analyses temperature adjustment curves were established. The temperature adjustment was found to be reasonably independent of the subgrade but to depend on both total pavement thickness and AC thickness. The temperature adjustment factors for an 8 inch pavement is shown in Figure 4.5.

4.4 APPLICATION OF THE METHOD

The relationships identified above are used in the developed design procedure for the determination of SN_{eff}. For total pavement thicknesses other than those used in the development, Delta D - SN_{eff} relationships are established by the design program through linear interpolation. Delta D is then calculated for each deflection location using the deflection at the center of loading and the deflection at a distance (T) from the center equal to the total pavement thickness (asphalt + base + subbase). If the deflection at T was not measured, the closest measured deflections are used to estimate that deflection through straight line interpolation.

This Delta D is adjusted to a 70° F Delta D using the relationships illustrated in Figure 4.5. If the AC thickness and total pavement thickness does not match the thicknesses used in the analyses, a temperature adjustment is selected from those developed through interpolation. The adjusted Delta D is used with the relationship to establish SN_{eff} for the deflection location.

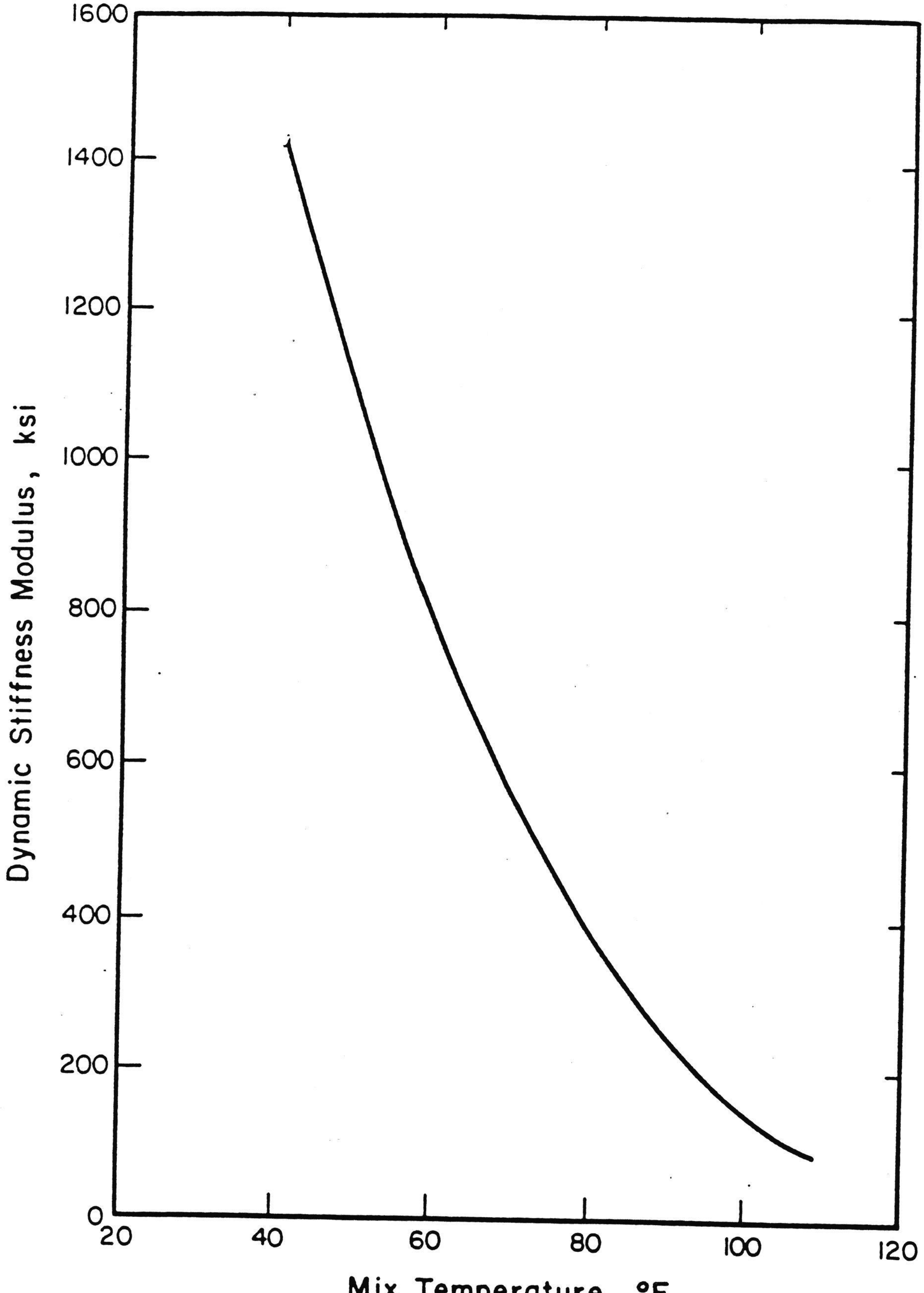

Figure 4.4 AC Modulus-Temperature Relationship Used in Development of Temperature Adjustment Method (Ref 16).

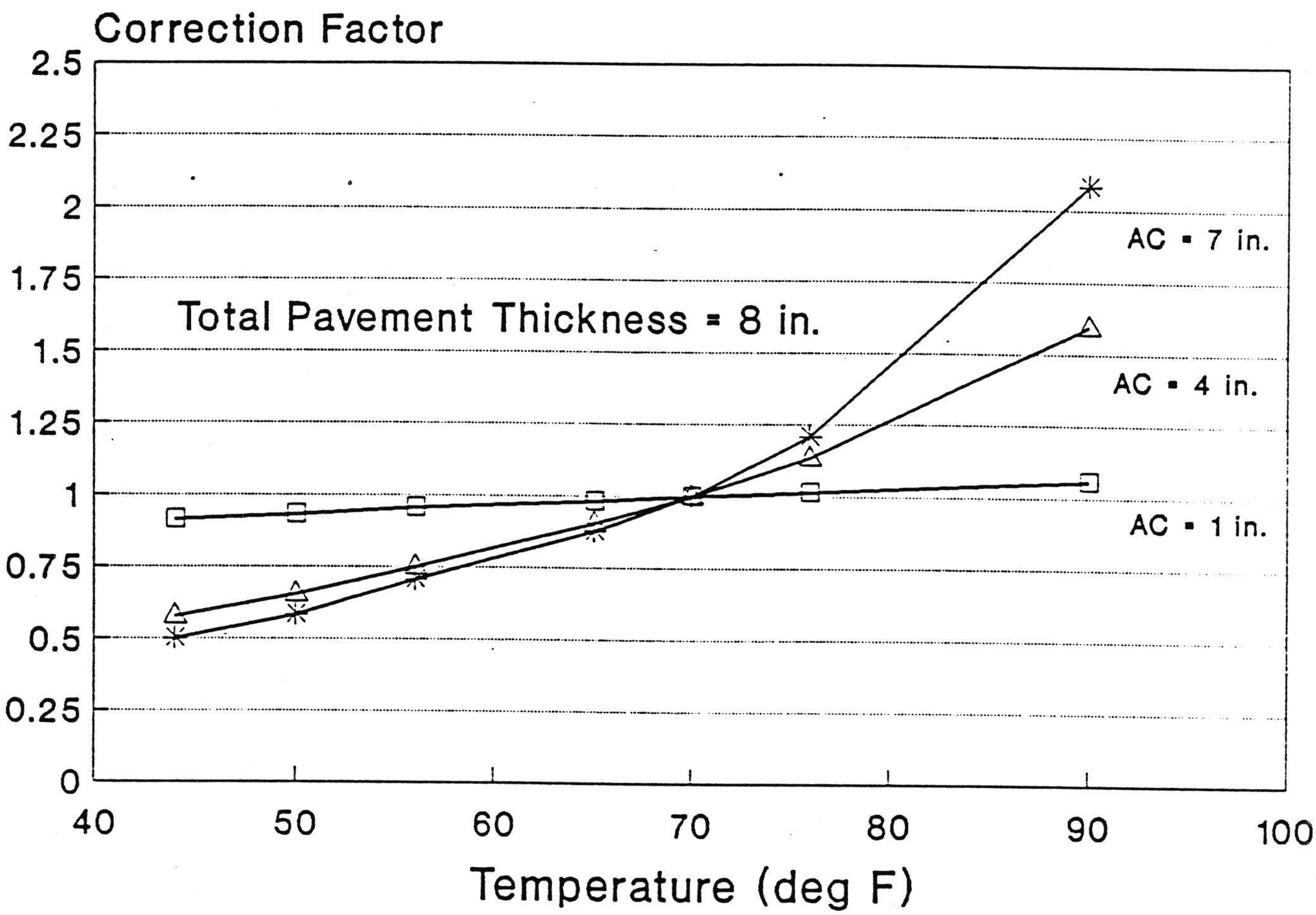

Figure 4.5 Temperature Adjustment Curves for an 8 Inch Pavement.

CHAPTER 5

EXAMINATION OF THE AASHTO REMAINING LIFE FACTOR

5.1 INTRODUCTION

A remaining life concept was introduced with the 1986 AASHTO Guide (1) that is to be applied in the design of overlays. The concept is based on the rationale that the structural capacity of a pavement decreases with load applications. For a pavement that has been overlaid, the structural capacity of the original pavement is a function of the loads applied before overlay as well as those applied after overlay. As presented by AASHTO, the remaining life concept requires that overlay thicknesses be selected considering both the "remaining" life of the pavement at the time of overlay and the expected "remaining" life when the next overlay will be applied.

The remaining life concept is applied using Equation 1.2 which was discussed in Chapter 1:

$$SN_{OL} = SN_y - F_{RL} * SN_{eff} \qquad \text{(Eq 1.2)}$$

The introduction of the remaining life concept represented a significant deviation from overlay approaches applied by many agencies using the earlier AASHTO Guide. These approaches were similar to equation 1.2 except that the F_{RL} term was not included.

The remaining life factor (F_{RL}) is determined using Figure 5.1. In this figure RLx is the remaining life factor of the existing pavement at the time of overlay and RLz is the anticipated future remaining life of the overlaid pavement when it will be overlaid. Concern has been expressed regarding the F_{RL} concept. Many have simply questioned why it was added to the approach many had previously used. However, of particular concern was the fact that at low values of RLx and RLz, the general slope of the F_{RL} curve reverses. This

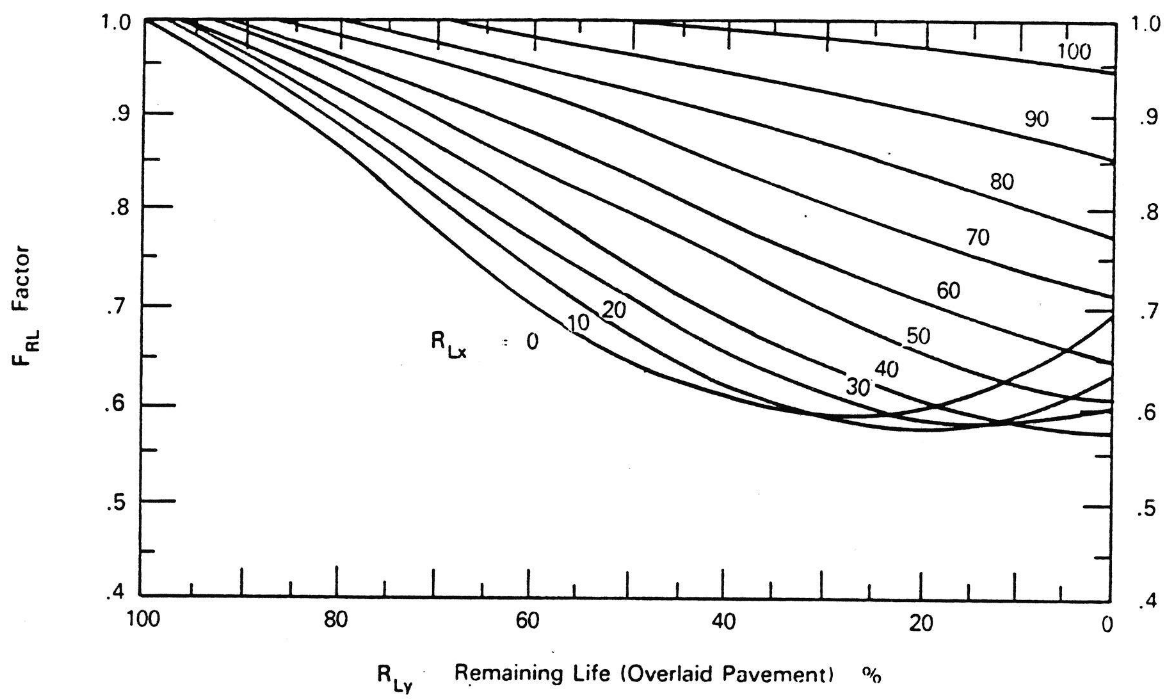

Figure 5.1 AASHTO Remaining Life Factor Curves.

investigation was initiated to study the concept and to establish a rationale for this slope reversal.

The investigation demonstrated inconsistencies in overlay designs using the AASHTO remaining life concept and suggests that for consistent designs F_{RL} should be 1.0 for all values of remaining life. This being the case, F_{RL} was not included in the overlay design developed.

5.2 CONCEPT OF REMAINING LIFE

The AASHTO remaining life concept is discussed in detail in reference 80. The following is an abbreviated discussion of that material to aid the reader in following the investigation conducted under this study.

The remaining life concept was developed to be used in a structural deficiency approach to overlay design. In the structural deficiency approach, the structural requirement for the overlay (SN_{OL}) is determined as the difference between the structure needed to support future (design) traffic (SN_y) and the structural capacity of the existing pavement (SNeff). F_{RL} was added to the basic structural deficiency equation to account for future structural damage to the existing pavement.

The fundamentals of remaining life are illustrated in Figure 5.2 using the flexible pavement structural number as the measure of structural capacity. The serviceability of a pavement decreases with time and traffic from an initial value, Po. Without rehabilitation, the serviceability would eventually reach a "failure" level, Pf. The total number of traffic applications to "failure" is shown as Nf.

However, at some point prior to failure, an overlay is placed. The traffic applications to that point is x. The remaining life (RLx) is defined as the additional applications that could have been applied to "fail-

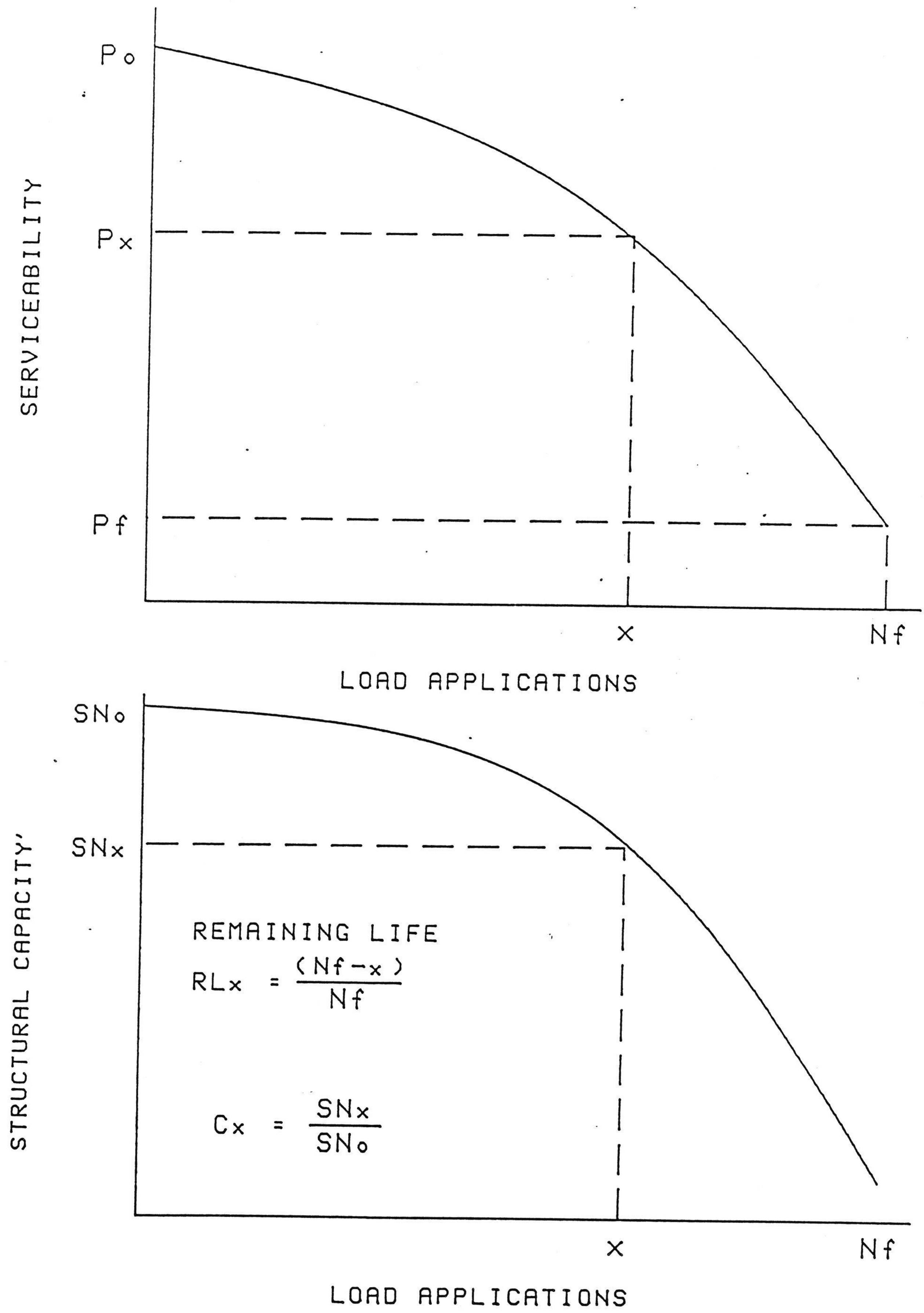

Figure 5.2 Illustration of the Remaining Life Concept.

ure" expressed as a fraction of the total possible applications. That is:

$$RLx = (Nf - x) / Nf \qquad \text{(Eq 5.1)}$$

The structural capacity of the pavement decreases similarly from SNo to SNf. At the time of overlay, the pavement structural capacity is SNx. A pavement condition factor (Cx) can be defined as:

$$Cx = SNx / SNo \qquad \text{(Eq 5.2)}$$

Since SNx is also the effective structural capacity (SN_{eff}) of the pavement at the time of overlay, SN_{eff} can be expressed as a function of Cx and SNo.

$$SN_{eff} = Cx * SNo \qquad \text{(Eq 5.3)}$$

For the AASHTO Guide, a relationship between Cx and RLx was developed using the AASHTO flexible pavement design equation. Cx and RLx values were computed for various designs based on present serviceable indices at "failure" (Pf) of 1.5 to 2.5. These produced a "best fit" relationship:

$$Cx = RLx^{0.165} \qquad \text{(Eq 5.4)}$$

A first step in this investigation was to attempt to reproduce this relationship. Cx and RLx values were computed for structural numbers ranging from 6.0 to 2.5 with Pf equal to 1.5 and 1.0. As shown on Figure 5.3, these values fit the AASHTO relationship reasonably well.

The AASHTO remaining life concept, however, does not use the "best fit" relationship. Although the CX values produced by the relationship were viewed as being realistic to RLx values as low as 0.005, the relationship was abandoned by AASHTO because Cx goes to zero at "failure" (RLx = zero). A modified relationship was used by AASHTO. The modified relationship (80) is:

$$Cx = 1 - 0.7 * e^{-(RLx + 0.85)^2} \qquad \text{(Eq 5.5)}$$

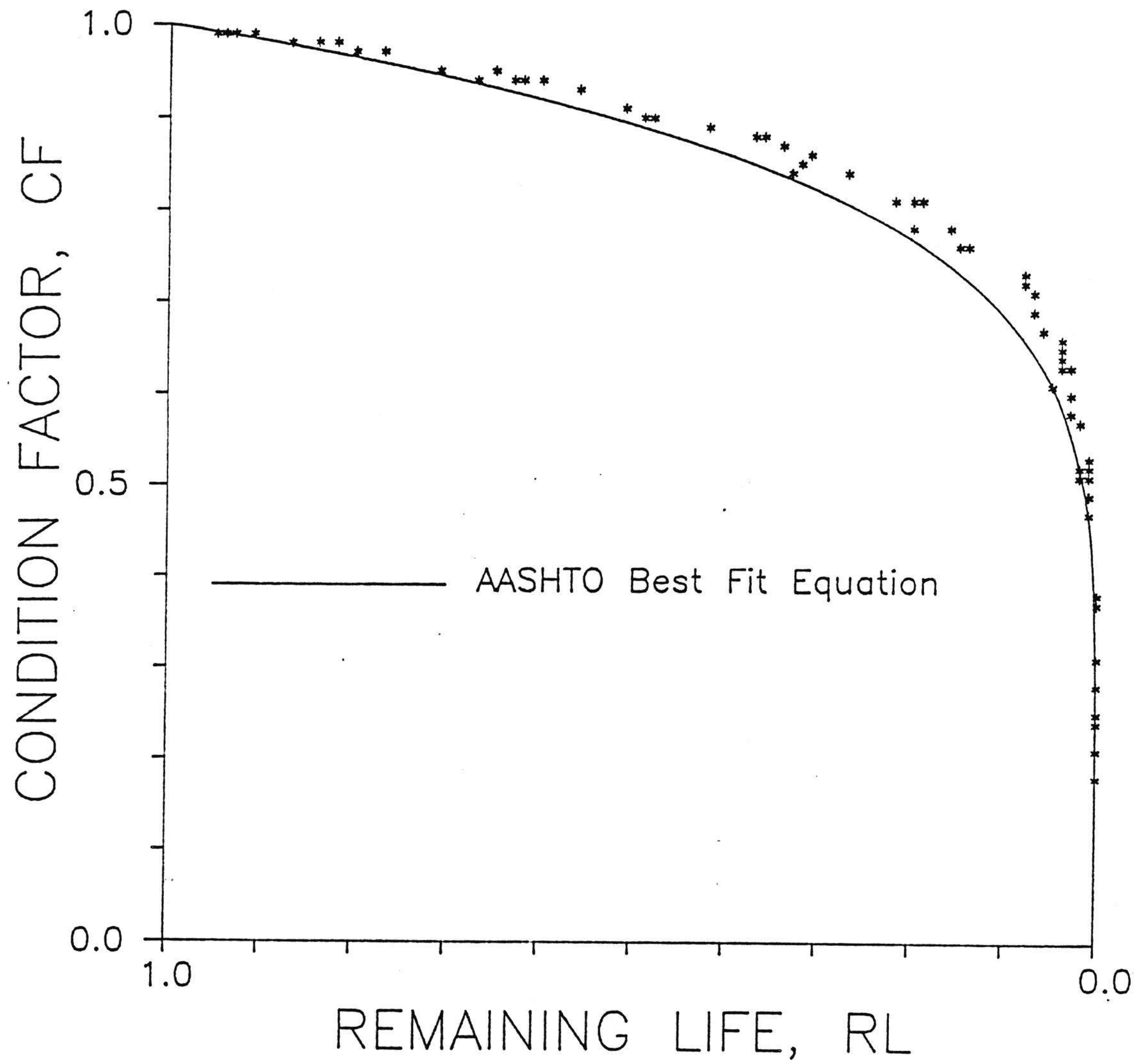

Figure 5.3 Comparison of CF Values from This Study with the AASHTO "Best Fit" Equation.

The best fit and modified relationships are compared in Figure 5.4. In addition to Cx not going to zero at "failure", the modified relationship provides a Cx values for a negative remaining life. Although the meaning of a negative remaining life is not clear, this feature of the modified relationship is a necessary (although perhaps erroneous) part of the AASHTO application of remaining life.

5.3 APPLICATION OF REMAINING LIFE TO OVERLAYS

The reduction in structural capacity of the overlaid pavement is similar to that shown in Figure 5.2. Thus, if SNn and z were used in place of the SNo and x used previously, the structural capacity of the overlaid pavement after z load applications would be:

$$SNz = Cz * SNn \qquad \text{(Eq 5.6)}$$

Without the remaining life factor (F_{RL}), SNn is SN_{OL} + SNeff. Thus, equation 5.6 can be written:

$$SNz = Cz * SN_{OL} + Cz * SNeff \qquad \text{(Eq 5.7)}$$

AASHTO (1) argued that this equation is incorrect since the existing pavement (SNeff) would lose structural capacity at a greater rate than would the overlay (SN_{OL}). To "correct" the equation, AASHTO stated that Cz * SNeff should be replaced by a similar function that includes the original (new) structural number of the existing pavement (SNo) and a condition factor (Czx) that is a function of the traffic applications (or remaining life) both before and after the overlay. That is:

$$Czx = f(RLx, RLz) \qquad \text{(Eq 5.8)}$$

and

$$SNz = Cz * SN_{OL} + Czx * SNo \qquad \text{(Eq 5.9)}$$

From these, AASHTO developed a relationship for F_{RL} in terms of Czx,

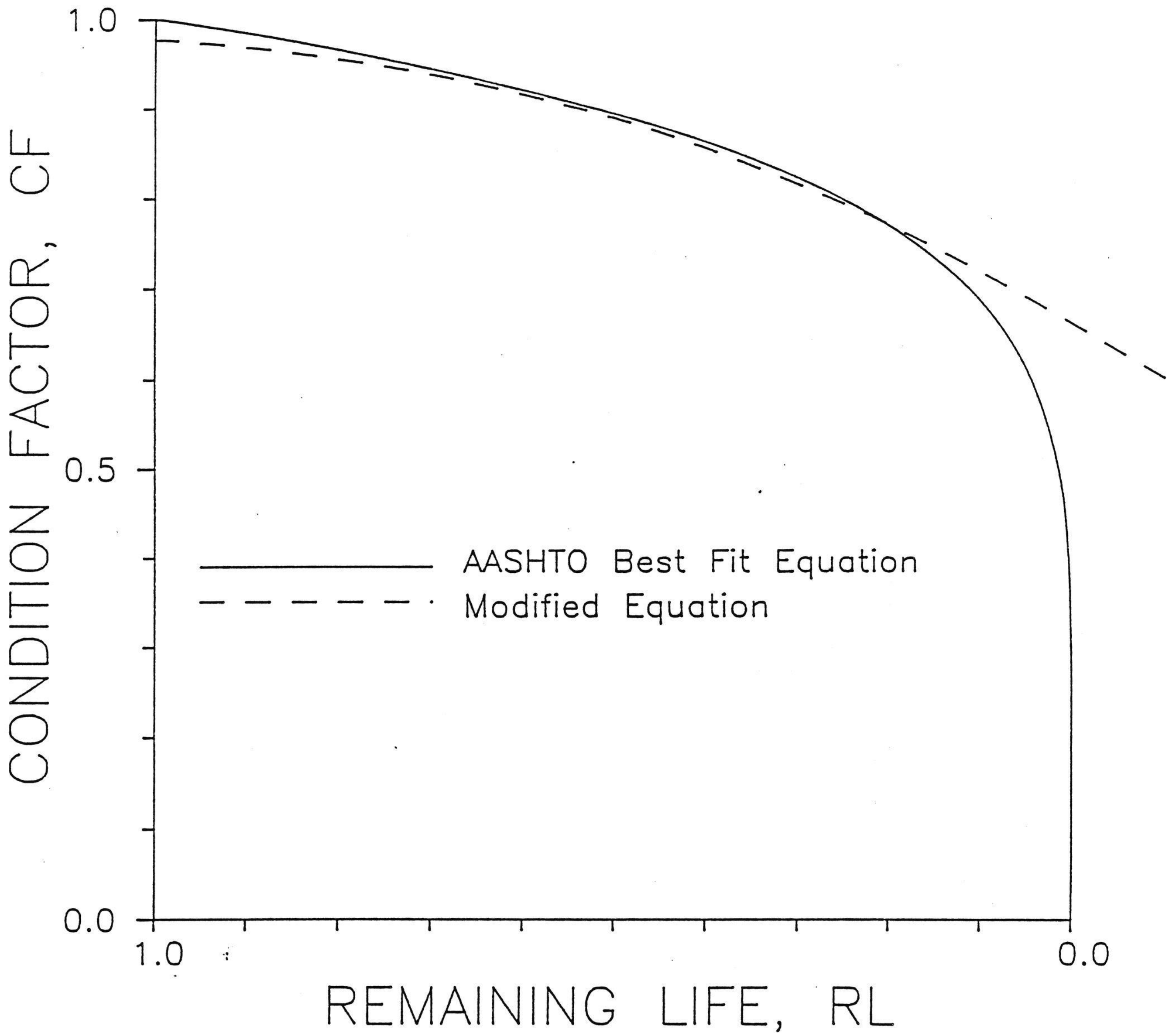

Figure 5.4 Comparison of the AASHTO "Best Fit" and Modified Equations.

Cz, and Cz:

$$F_{RL} = Czx / (Cx * Cz) \qquad \text{(Eq 5.10)}$$

At this point, it should be noted that Equation 5.7 already included SNo and a function of the traffic before and after overlay (Cx * Cz). Using Equation 5.3, SNeff in Equation 5.7 may be replaced by Cx * SNo resulting in :

$$SNy = Cz * SN_{OL} + Cx * Cz * SNo \qquad \text{(Eq 5.11)}$$

Nevertheless, the introduction of Czx might be viewed as an advance since Cx * Cz specifies the structural loss relationship for the existing pavement while Czx does not. Yet, in order to apply F_{RL}, it was necessary to assume an arbitrary relationship (Equation 5.12 below).

5.4 REMAINING LIFE FACTOR CURVES

The second step in this investigation was to verify the remaining life factor curves (Figure 5.1). These curves were developed using equations 5.5 and 5.10. However, because Czx is a function of RLx and RLz, AASHTO has to assume a relationship between the two in order to apply equation 5.5. The relationship assumed was that the combined remaining life (RLxz) would be equal to the remaining life at the time of overlay (RLx) minus the damage done (dz) during the period of overlay. That is:

$$RLxz = RLx - dz \qquad \text{(Eq 5.12)}$$

Since dz is 1 - RLz, this equation may be written:

$$RLxz = RLx + RLz - 1 \qquad \text{(Eq 5.13)}$$

Initially, this assumption seems reasonable. However, it produces an uneasiness that grows with further reflection. By subtracting the full damage done after overlay, there seems to be no accounting for the reduction in the rate of damage that results from the lower load stresses due to the overlay. Also, because both RLx and RLz generally will be less than 0.5, the combined remaining life will be negative. A negative remaining life has no meaning. Finally, because the condition factor relationship itself (Eq 5.5) is assumed, this assumption (Eq 5.12) results in a compounding of assumptions.

Nevertheless, application of this assumption together with equations 5.5 and 5.10 verified the mathematical accuracy of Figure 5.1 including the slope reversals at the lower values of RLx and RLz.

5.5 INCONSISTENCIES IN APPLICATION

The third step in the current investigation involved application of the F_{RL} factors to a hypothetical design situation to see if reasonable values and trends were produced. The design situation selected involved a design traffic ESAL of 5,000,000 and an effective structural number for the existing pavement (SN_{eff}) of 4.5. The required overlay structural numbers (SN_{OL}) were determined for terminal Present Serviceability Indices (PSI) ranging from 3.5 to 1.55. The remaining life of the existing pavement (RLx) was also varied using values of 0.0, 0.2, and 0.4.

The total structural number required (SN_y) and remaining life of the overlay (RLz) was computed using the AASHTO design equation (1) with a "failure" PSI of 1.5. A reliability to 50% and subgrade resilient modulus of 3000 psi were used to reduce the equation to the original AASHO Road Test equation and eliminate any potential effects resulting from assumptions involved in adding reliability and subgrade modulus to the equation. To assure accuracy in application, the F_{RL} values were calculated in lieu of being taken from Figure 5.1.

The results of the analyses are listed in Table 5.1 and displayed graphically in Figure 5.5. The slope reversals seen in Figure 5.5 clearly illustrate an inconsistency. However, the major inconsistency is the general negative

Table 5.1 Overlay Computations Using Remaining Life Factors.

Design ESAL = 5,000,000 SNeff = 4.5

Terminal PSI	Required SNn	RLy	RLx = 0.0 Frl	SNol	RLx = 0.2 Frl	SNol	RLx = 0.4 Frl	SNol
3.5	6.65	.904	.988	2.20	.999	2.15	1.00	2.15
3.25	6.02	.904	.945	1.77	.967	1.67	.987	1.58
3.00	5.59	.827	.881	1.63	.919	1.45	.955	1.29
2.50	5.03	.603	.711	1.83	.773	1.55	.848	1.21
2.25	4.84	.465	.633	1.99	.689	1.74	.776	1.35
2.00	4.69	.317	.589	2.04	.616	1.92	.703	1.53
1.75	4.57	.167	.605	1.85	.576	1.98	.642	1.68
1.60	4.50	.062	.665	1.51	.578	1.90	.615	1.73
1.55	4.48	.029	.694	1.36	.586	1.84	.610	1.74

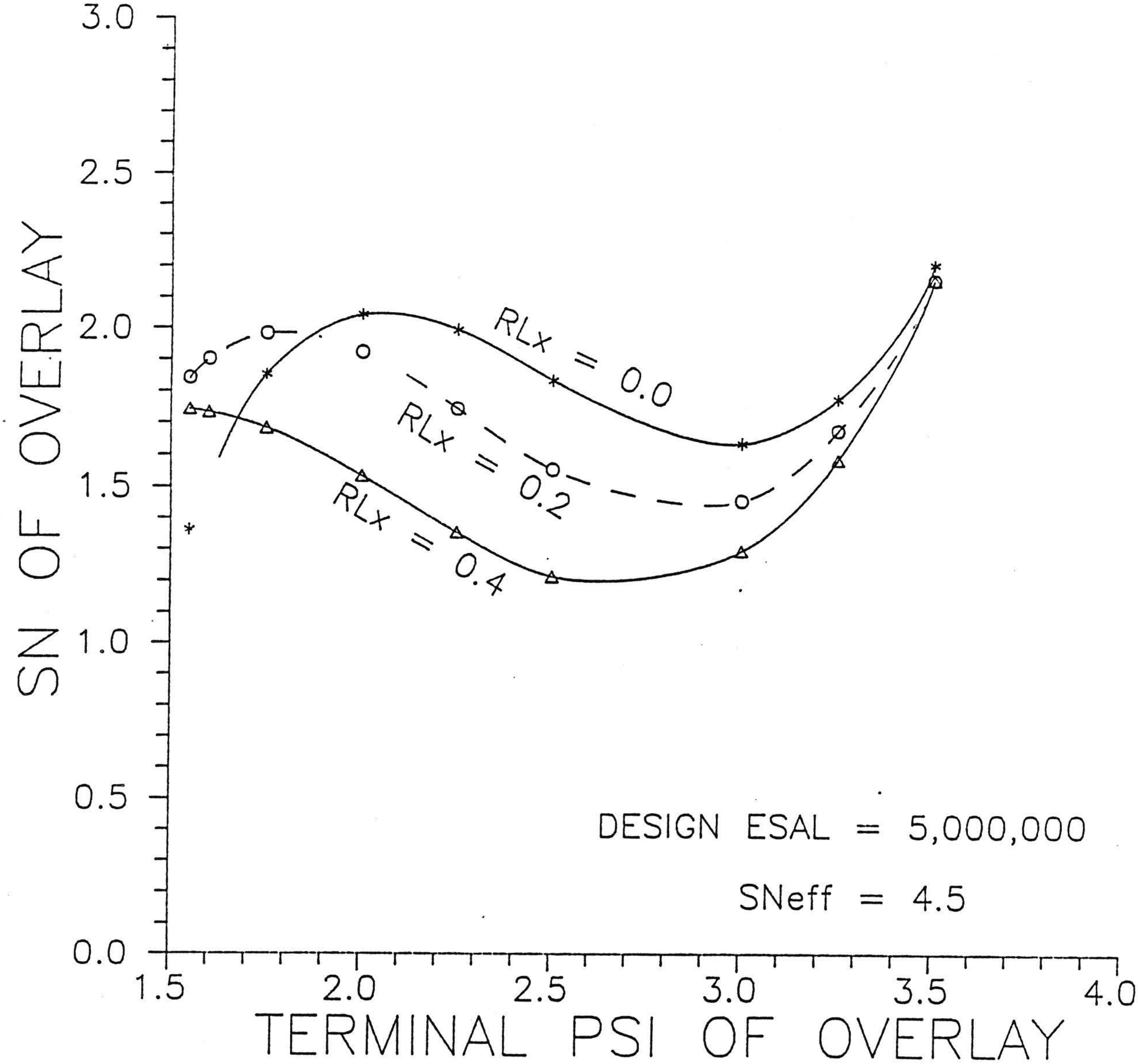

Figure 5.5 Results of Overlay Analyses Using the AASHTO Remaining Life Factor.

slope of the curves between terminal PSI's of 2.0 to 3.0. For a given design situation, design to a lower terminal PSI should result in a lower required structural number. This is correctly illustrated by the trend of the SNy values in Table 5.1. However, after F_{RL} is applied to establish the overlay requirement, the general trend for SN_{OL} is reversed.

Quite obviously, something is wrong with the AASHTO remaining life approach.

5.6 MODIFICATION OF THE REMAINING LIFE APPROACH

The final step in the investigation was to identify the problem with the concept and to develop a recommended correction. The apparent source of the problem is in the compounding of assumptions, first with the modification of the Cx-RLx relationship (Equations 5.4 and 5.5) and secondly with the combined remaining life relationship (Equation 5.13).

As an alternative to Equation 5.13 the following development is suggested. The curve in Figure 5.6 represents some as yet undefined relationship between C and RL. At some point (x), the pavement is overlaid and the existing pavement values are Cx and RLx. After the overlay, C of the existing pavement will continue to decline from Cx but RL will now be 100. This is represented on Figure 5.6 by the revised RL scale.

At the time of the second resurfacing (y), the respective values are Czx and RLz. A simple scale transformation of RLz from the revised scale to the original scale shows that:

$$RLxz = RLx * RLz \qquad \text{(Eq 5.14)}$$

This equation for RLxz eliminates the need for a negative remaining life. The philosophy behind it is similar to the concept of the man that each day walks halfway to his destination. He never arrives. As long as

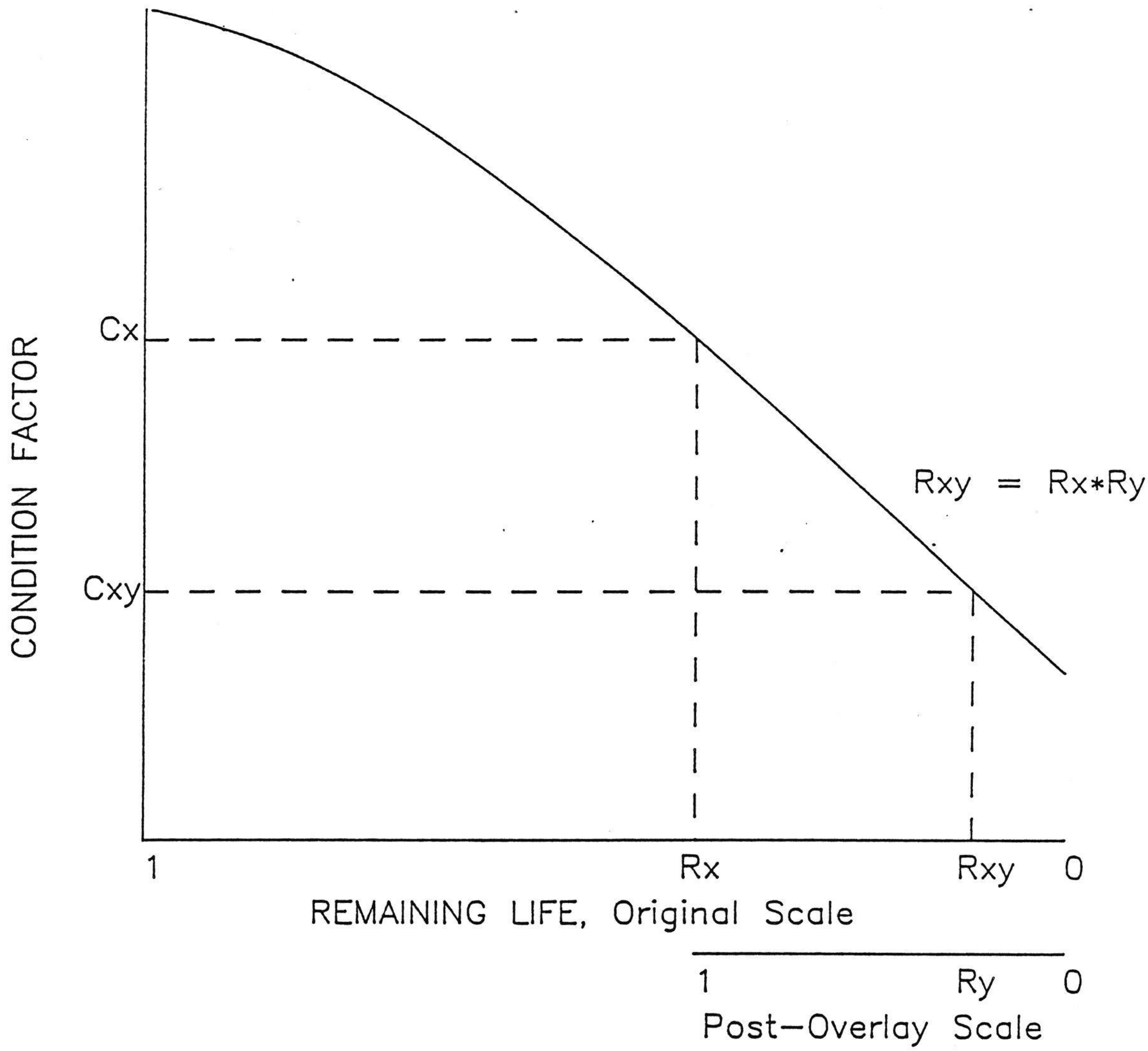

Figure 5.6 Modified Approach for Determining Cxy.

the pavement is overlaid prior to "failure", "failure" is not reached in any component. The existing damage condition remains in the existing materials and progresses. However, the overlay is designed to slow the rate of additional damage so that the "failure" condition is reached for the entire pavement.

Equations 5.14 and 5.10 were used to determine F_{RL} values with both the original C-RL relationship (Eq 5.4) and the modified version (Eq 5.5). With the original relationship, F_{RL} is always 1.0:

$$F_{RL} = (RLxz)^{.165} / (RLx^{.165} * RLz^{.165} =$$
$$= (RLx * RLz)^{.165} / (RLX * RLY)^{.165} = 1.0 \quad \text{(Eq 5.15)}$$

With the modified AASHTO relationship (Eq 5.5) the equation is more complicated. However, except for very low values of both RLx and RLz, F_{RL} is generally about 1.0. At very low RL values, F_{RL} becomes greater than 1.0. (At RLx and RLz equal to 0.0, F_{RL} is 1.5)

5.7 OTHER DIFFICULTIES

Inconsistency in application is not the only difficulty with the AASHTO remaining life concept. There are other difficulties that need to be recognized and researched. The first of these is the application of the AASHTO Road Test performance equation to establish a remaining life-condition relationship.

The Road Test equation is an empirical relationship selected to provide a means of predicting the performance of the research pavements at the Road Test. It is not a theoretical or fundamental performance relationship and may, in fact, not even be the "best fit" prediction relationship. It is simply the best relationship found by the researchers involved in the Road Test using the analysis tools that were available at that time. To apply the equation in the fashion used relative to remaining life represents a very significant extrapolation beyond the data and original intent of the equation.

Secondly, as it is being applied the remaining life concept assumes that all materials will experience damage and structural loss at the same rate. It is conceivable that at "failure" a stabilized layer will be reduced to the equivalency of a granular layer while a granular layer may experience little loss.

The third difficulty is with the reliance on structural number. Many pavement engineers and researchers have expressed concern with the structural number approach to pavement design since it was first introduced. The structural number approach assumes that each incremental thickness of a material provides an equal contribution to the structural capacity of the pavement regardless of the total thickness or total pavement configuration. Several studies have shown that this assumption is erroneous (81,82,83,84).

5.8 CONCLUSION AND RECOMMENDATION

This investigation demonstrated that the AASHTO remaining life concept produced inconsistent overlay design thicknesses. The inconsistencies appear to be caused by a compounding of assumptions used to produce the remaining life factor (F_{RL}) curves (Figure 5.1). An alternative approach developed as a part of this investigation found that the appropriate value for F_{RL} is 1.0. As a result, the AASHTO remaining life factor was not included in the overlay design procedure developed under this project.

CHAPTER 6

DELINEATION OF PROJECT ANALYSIS UNITS

The overlay design procedure program developed under this project was named ROADHOG. This name was selected to designate that the program is a roadway design tool that was developed at the University of Arkansas, the Razorbacks. As a design tool, ROADHOG forms one part of the overall process of overlay design. Various other procedures such as traffic analyses and a detailed materials and environmental study are included in the design process. The first step in the AASHTO design process is Analysis Unit Delineation, some form of which should be included in any comprehensive overlay design process.

Analysis Unit Delineation is a process by which a length of pavement slated for rehabilitation (e.g. overlay) is subdivided into "homogeneous" sections. Homogeneous sections or "analysis units" have been defined as "sections of pavement that can be considered nearly alike in terms of performance, age, traffic, structural capacity, etc., and for which a single treatment is appropriate" (85). Subdividing a project into analysis units can greatly increase the efficiency and cost-effectiveness of an overlay design. The use of analysis units can help to insure the optimum amount of overlay is placed where it is needed.

Due to the importance of analysis unit delineation to the design process, ROADHOG was given the capability to aid designers in this task. The unit delineation function is contained in the program module UNIDEL. Like the thickness selection function of ROADHOG, unit delineation by UNIDEL is a design tool. The decision of how to use the tool, or indeed, whether to use the tool at all, remains an administrative judgement. UNIDEL provides one means of analysis unit delineation. The extent of its use resides with the designer, dependent upon economics and practicality.

6.1 UNIT DELINEATION METHODS

A number of methods have been suggested to subdivide rehabilitation projects into homogeneous units (85). In general terms, a designer could use a qualitative or a quantitative approach to unit delineation. The approach taken may depend a great deal on the type of data a designer has available.

6.1.1 Qualitative Approach

A designer using a qualitative approach identifies homogeneous sections based on historical evidence such as construction data (cross-section, soil type, etc.) and traffic history. This approach assumes that similar pavements constructed on similar foundations with similar traffic histories are in similar condition. Many times current measurements of serviceability or condition surveys will be used to supplement historical records. The 1986 AASHTO Guide (1) gives an example of this type of analysis, which it calls an "idealized method", reproduced here as Figure 6.1.

In the example, five factors: Pavement Type, Construction History, Cross Section, Subgrade, and Overlay Traffic, are considered in subdividing the project into six analysis units. Each unit is in some way unique from the others and requires a different level or possibly a different type of rehabilitation. This method is especially effective for making a preliminary identification of analysis units, but it should be supplemented with some type of field verification (i.e. condition survey, NDT testing). The designer in this case is totally dependent on the amount and reliability of available data.

Another type of qualitative method for unit delineation involves the use of a pavement rating system. One example of a rating system is AASHTO's Pre-

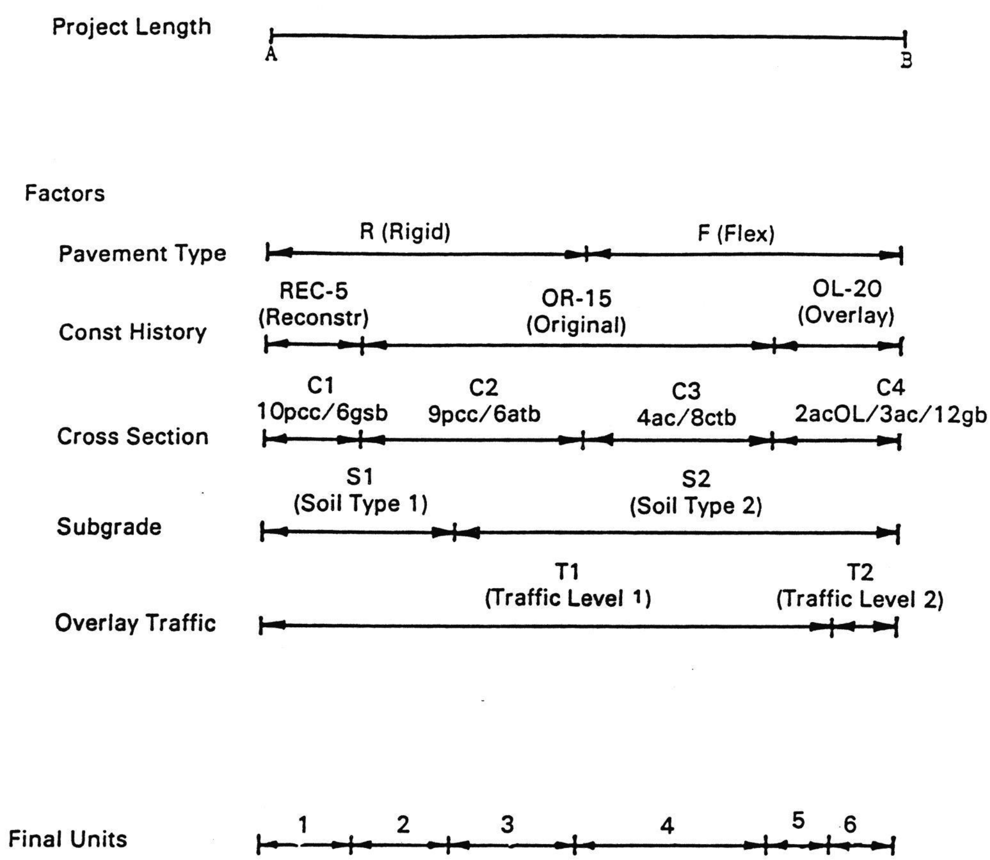

Unit Attributes:

Unit No.	1	2	3	4	5	6
Pavement type	R	R	R	F	F	F
Construction Hist	REC-5	OR-15	OR-15	OR-15	OL-20	OL-20
Cross Section	C1	C2	C2	C3	C4	C4
Subgrade	S1	S1	S2	S2	S2	S2
Overlay Traffic	T1	T1	T1	T1	T1	T2

Figure 6.1 Idealized Method for Analysis Unit Delineation (Ref 1).

sent Serviceability Index scale, ranging from five to zero (in descending order) with intervals of "very good", "good", "fair", "poor", and "very poor". Another example is the Pavement Condition Index (PCI) used by the U.S. Army Corps of Engineers in its PAVER pavement management procedure (86). PCI ranges from zero to 100 and is divided into seven intervals with 100-86 described as "excellent" and 10-0 described as "failed". A drawback to using this type of system to subdivide a project is that these procedures are primarily concerned with functional deficiencies rather than the structural condition of the pavement. Another disadvantage is that the nature of actual pavement distress is lost when the pavement is described by a rating number or adjective (85).

6.1.2 Quantitative Approach

Quantitative procedures for unit delineation involve the use of some type of measured pavement response to determine consistent differences in pavement condition. A number of criteria can be used as the response variable, but the most popular is surface deflection measured during a non-destructive test. The use of NDT data for unit delineation is also convenient when used in conjunction with a deflection-based thickness design procedure.

Prevalent methods of evaluating response data for unit delineation include visual/graphical methods and statistical methods. These methods are demonstrated using "real-life" data obtained from the Arkansas Highway and Transportation Department. The data are taken from a section of Arkansas Highway 165 slated for rehabilitation by overlay. For demonstration purposes, the NDT maximum deflection at the center of loading is used as the response variable.

Figure 6.2(a) is a plot of maximum deflection along the project length. The data is somewhat erratic; however, the project can be visually divided

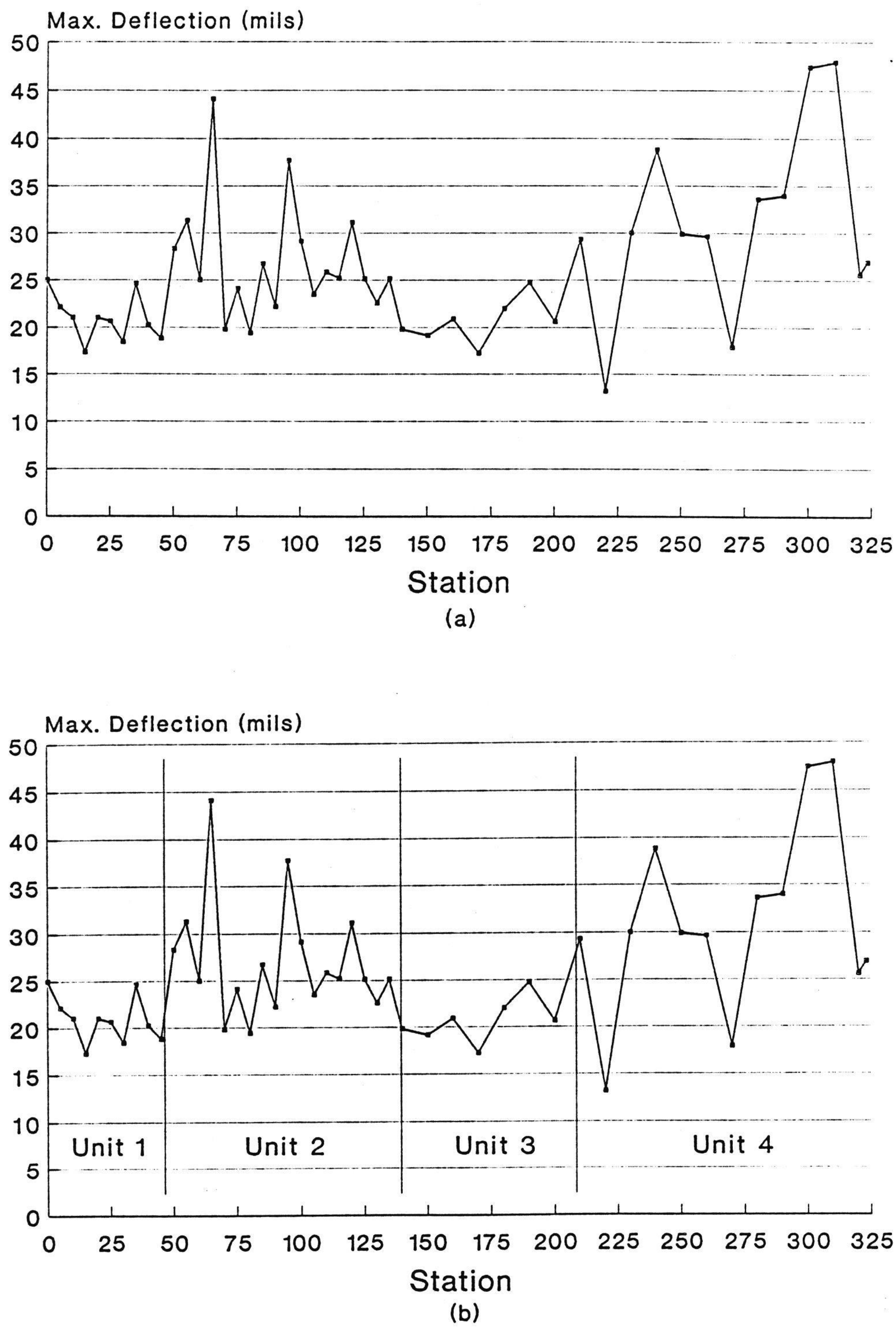

Figure 6.2 Example Visual/Graphical Selection of Analysis Units Using Maximum Deflections.

into analysis units as shown in Figure 6.2(b). This example illustrates one disadvantage of using a visual/graphical method to determine analysis units. Many times response data do not fit into easily definable patterns. The designer's judgement becomes tantamount to efficient design.

In the field of statistics, a number of methods exist to subdivide an ordered group of data into statistically homogeneous units. One method is a hypothesis test for equal means using the Student-t distribution. Reference 85 outlines this approach, which was suggested for use in unit delineation by ARE, Inc. The equal means test is used after preliminary analysis units are established. Two preliminary units are compared using this procedure to determine whether the units are significantly different. If the units are not significantly different, they are combined and compared against the next preliminary unit. For example, units 1 and 2 shown on Figure 6.2(b) were compared using the equal means test and found to be "not significantly different". Therefore, units 1 and 2 would be combined for comparison against unit 3. A statistical procedure such as the equal means test provides a method for confirming analysis units previously chosen by visual or other means.

Another statistical approach to unit delineation is the cumulative difference method. The 1986 AASHTO Guide recommends this method for use when a statistical method is desirable. The ROADHOG overlay design procedure uses the cumulative difference approach in the UNIDEL module. A full discussion of this method is presented in Appendix J of the AASHTO Guide. A brief outline of the procedure is given with an example in the next section.

6.2 UNIT DELINEATION IN ROADHOG

The cumulative difference approach to unit delineation used in ROADHOG is a powerful statistical procedure that is easily adaptable to a computerized process. Similar to the equal means test, the cumulative difference approach uses a response variable along the project length. ROADHOG uses the required overlay thickness as the response variable. (The module OVLTHICK generates a required overlay thickness for each NDT test site. UNIDEL uses the required thickness as the response variable.) Using.the required overlay thickness as the response variable is reasonable since the thickness is the best indication of the overlay required at a point.

The cumulative difference approach is demonstrated using NDT data from Arkansas Highway 165 (used in an earlier example). The data have been used in the ROADHOG design procedure to generate required overlay thicknesses. Figure 6.3(a,b,c) and Table 6.1 are used to help illustrate the unit delineation process.

Figure 6.3(a) is a plot of the required overlay thickness along the project length. The area under the response (thickness) versus distance plot can be determined by multiplying the average value of the required thickness over an interval by the interval length. The cumulative area to a point is found by summing the interval areas to that point. Figure 6.3(b) is a plot of the cumulative area (of the response-distance plot) along the project. The dashed line in Figure 6.3(b) was generated by connecting the origin with a point corresponding to the average thickness-distance area for the entire project (the project average thickness multiplied by the project length). The dashed line represents the overall average project thickness.

The cumulative difference variable Z_x is the difference between the actual cumulative area (the solid line in 6.3(b)) and the overall average cumulative area (the dashed line in 6.3(b)) for any given point along the project. Figure 6.3(c) is a plot of the Z_x value along the project length. Unit boundaries coincide with the location along the project where the slope of the Z_x curve

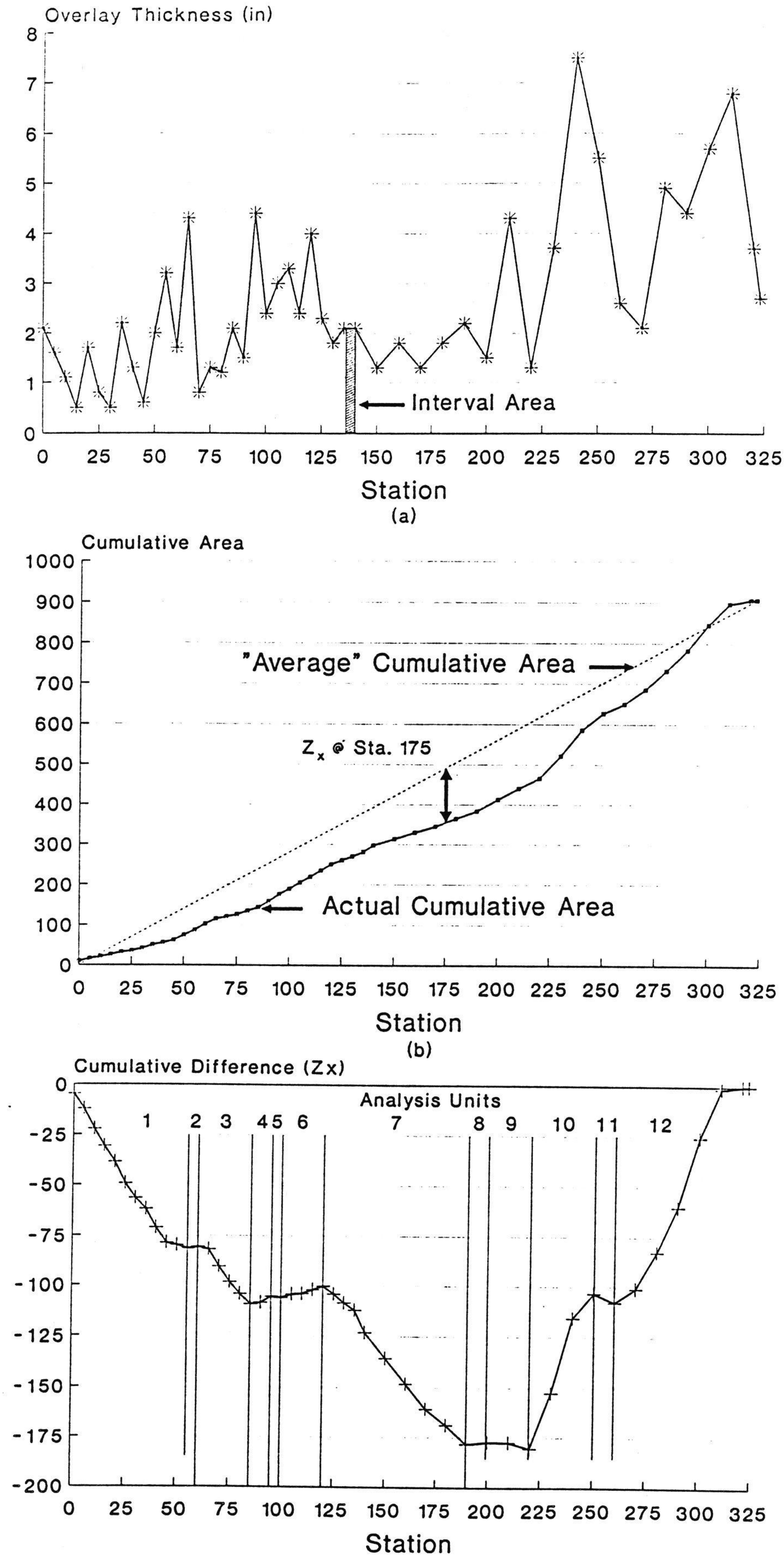

Figure 6.3 The Cumulative Difference Approach to Unit Delineation.

changes algebraic sign. Thus for the example shown, unit boundaries occur at Stations 55, 60, 85, 95, 100, 120, 190, 200, 220, 250, and 260.

Table 6.1 shows the calculations necessary to determine unit boundaries. UNIDEL performs these calculations in ROADHOG. One advantage of this procedure is that boundaries can be determined mathematically, with no visual judgement required of the designer.

The UNIDEL module allows the designer to set the minimum length of an analysis unit. For long projects, a recommended minimum length of analysis unit is 1000 feet (85). The minimum length should be based on economics and/or practicality. UNIDEL establishes "calculated analysis units" based solely on the statistical procedure outlined above. "Recommended analysis units" are determined by combining calculated units shorter than the minimum with adjacent units. After recommended units are determined, UNIDEL assigns each station along the project a unit number. Output of results according to analysis units is based on the assigned unit numbers.

Table 6.1 Calculations for the Cumulative Difference Approach.

Station	Pavement Response Value	Interval Number	Interval Distance	Cumulative Interval Distance	Average Interval Response	Actual Interval Area	Cumulative Area	Zx Value
0.00	2.10							
		1.00	5.00	5.00	1.85	9.25	9.25	-4.78
5.00	1.60							
		2.00	5.00	10.00	1.35	6.75	16.00	-12.07
10.00	1.10							
		3.00	5.00	15.00	0.80	4.00	20.00	-22.10
15.00	0.50							
		4.00	5.00	20.00	1.10	5.50	25.50	-30.64
20.00	1.70							
		5.00	5.00	25.00	1.25	6.25	31.75	-38.42
25.00	0.80							
		6.00	5.00	30.00	0.65	3.25	35.00	-49.20
30.00	0.50							
		7.00	5.00	35.00	1.35	6.75	41.75	-56.49
35.00	2.20							
		8.00	5.00	40.00	1.75	8.75	50.50	-61.77
40.00	1.30							
		9.00	5.00	45.00	0.95	4.75	55.25	-71.06
45.00	0.60							
		10.00	5.00	50.00	1.30	6.50	61.75	-78.59
50.00	2.00							
		11.00	5.00	55.00	2.60	13.00	74.75	-79.62
55.00	3.20							
		12.00	5.00	60.00	2.45	12.25	87.00	-81.41
60.00	1.70							
		13.00	5.00	65.00	3.00	15.00	102.00	-80.44
65.00	4.30							
.	.	.	.	.	.	.	.	.
.	.	.	.	.	.	.	.	.
.	.	.	.	.	.	.		
.	.	.	.	.	.	.		
320.00	3.70							
		47.00	3.00	323.00	3.20	9.60	906.60	0.00
323.00	2.70							

CHAPTER 7

CONCLUSIONS, RECOMMENDATIONS, AND IMPLEMENTATION

7.1 COMPARISON OF ROADHOG AND ELMOD

The Arkansas Highway and Transportation Department (AHTD) has been using the ELMOD computer program for overlay design. ELMOD is a deflection-based, quasi-mechanistic procedure that selects overlay thickness based on estimates of allowable versus actual stresses and strains in a pavement system. The procedure was developed by the manufacturers of the Dynatest Falling Weight Deflectometer. A comparison of the overlay thicknesses determined by ELMOD and ROADHOG (the procedure developed for AHTD under this study) is given for the data used in previous examples (Arkansas Highway 165).

Design data used in the comparison includes a design period of 10 years, design traffic (which includes all growth factors) of 350 ESAL's per day, allowable change in serviceability index (delta PSI) of 2.2, design standard deviation of 0.48, minimum length of an analysis unit of 2500 feet, and design reliability levels as shown on the comparison graphs and discussed in the text. The existing pavement on Hwy. 165 consists of 4 inches of asphalt concrete surface over 7 inches of gravel base course. No estimate of subgrade thickness (depth to bedrock) is given; AHTD standard procedure is to use an equivalent maximum depth to bedrock equal to 160 inches in the ELMOD program.

Figure 7.1 is a direct station-by-station comparison of the required overlay thicknesses determined by ELMOD and ROADHOG. The reliability levels used in ROADHOG are shown on the figure. The reliability level used by ELMOD is not known but is believed to be 50 percent. Figure 7.1 shows that ROADHOG generally tends to yield more conservative (thicker) estimates of required overlay thickness. One interesting aspect of the plot concerns the similarity of

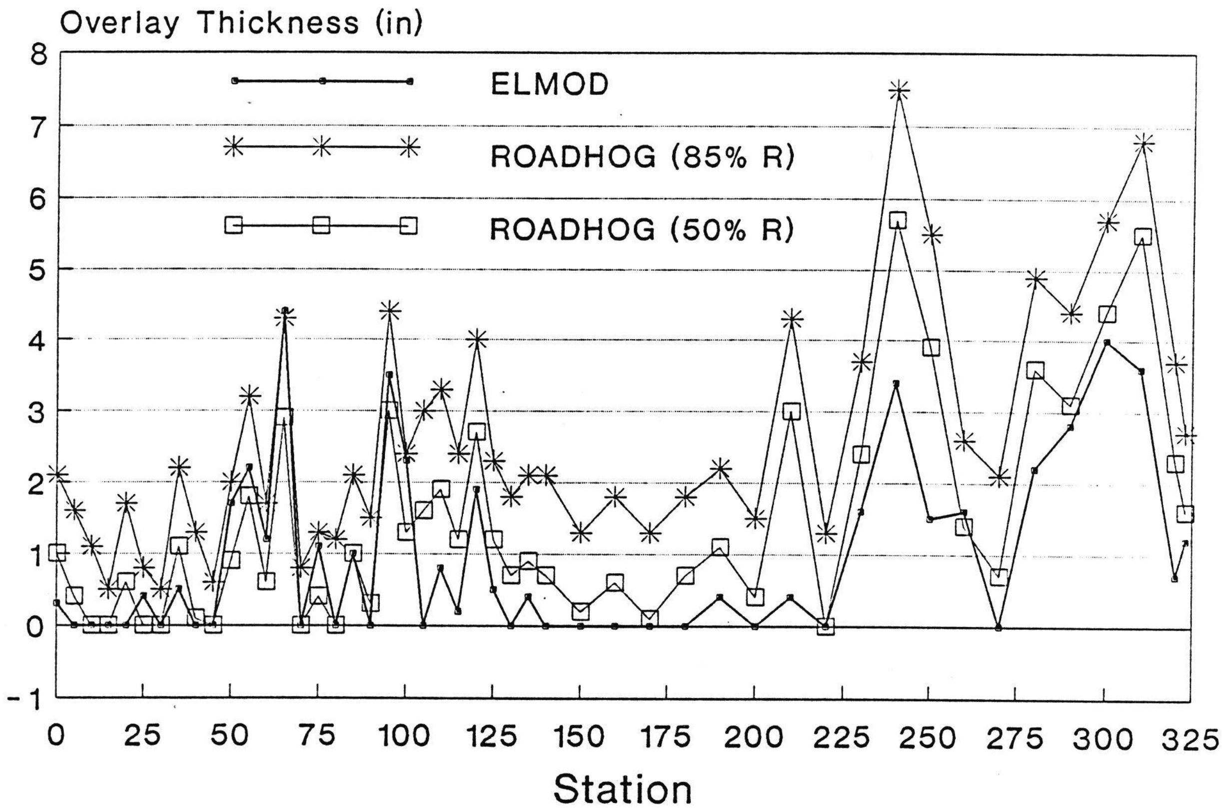

Figure 7.1 Station-by-Station Comparison of ROADHOG and ELMOD.

the shape of the curves between ELMOD and ROADHOG. Both procedures show similar deviations in thickness along the project in response to changes in the deflection basin.

Figure 7.2 depicts the overlay thickness(es) required for two levels of reliability, assuming the project is designed with a single overlay thickness for its entire length. Design thicknesses were calculated using the relationship shown as Equation 7.1.

$$OL = X + S*Z \qquad \text{(Eq 7.1)}$$

where

OL = design overlay thickness

X = average required overlay thickness for station-by-station thicknesses determined using 50% reliability

S = standard deviation of required overlay thicknesses

Z = standard normal deviate corresponding to a given design reliability level

Figure 7.2 shows ROADHOG to be the more conservative of the procedures. For this project, ROADHOG recommended required overlay thicknesses 0.6 and 0.7 inches thicker that ELMOD for 85% and 70% reliability levels, respectively. The difference in required overlay thickness between ROADHOG and ELMOD is project-specific. A large database of comparisons is necessary to draw conclusions regarding the level of conservatism gained by using ROADHOG.

Chapter 6 discussed the advantages gained in terms of efficiency and cost-effectiveness of subdividing a project into homogeneous analysis units. Figure 7.3 shows design overlay thicknesses along the project, subdivided into analysis units, determined by ROADHOG as opposed to the single-thickness design concept currently used by the AHTD. This figure graphically illustrates the optimization of design that can be accomplished using analysis

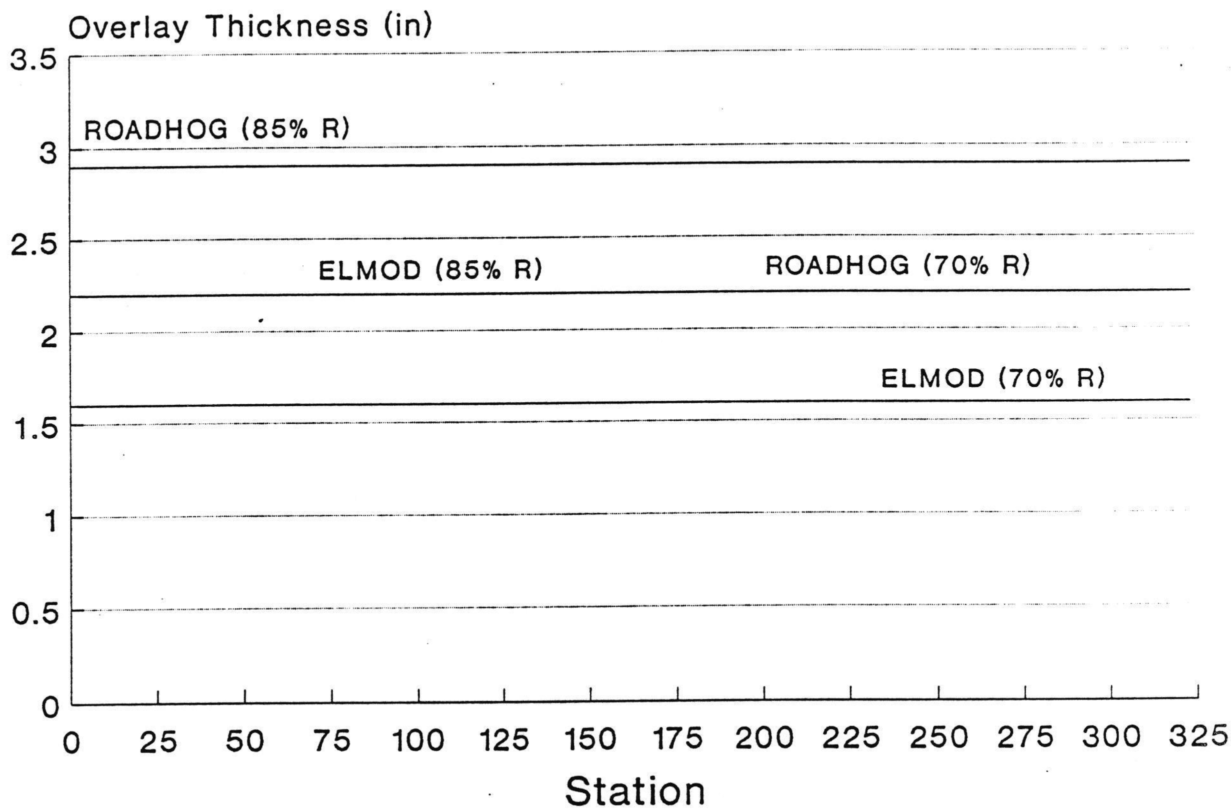

Figure 7.2 Comparison of ROADHOG and ELMOD for a Single-Thickness Design.

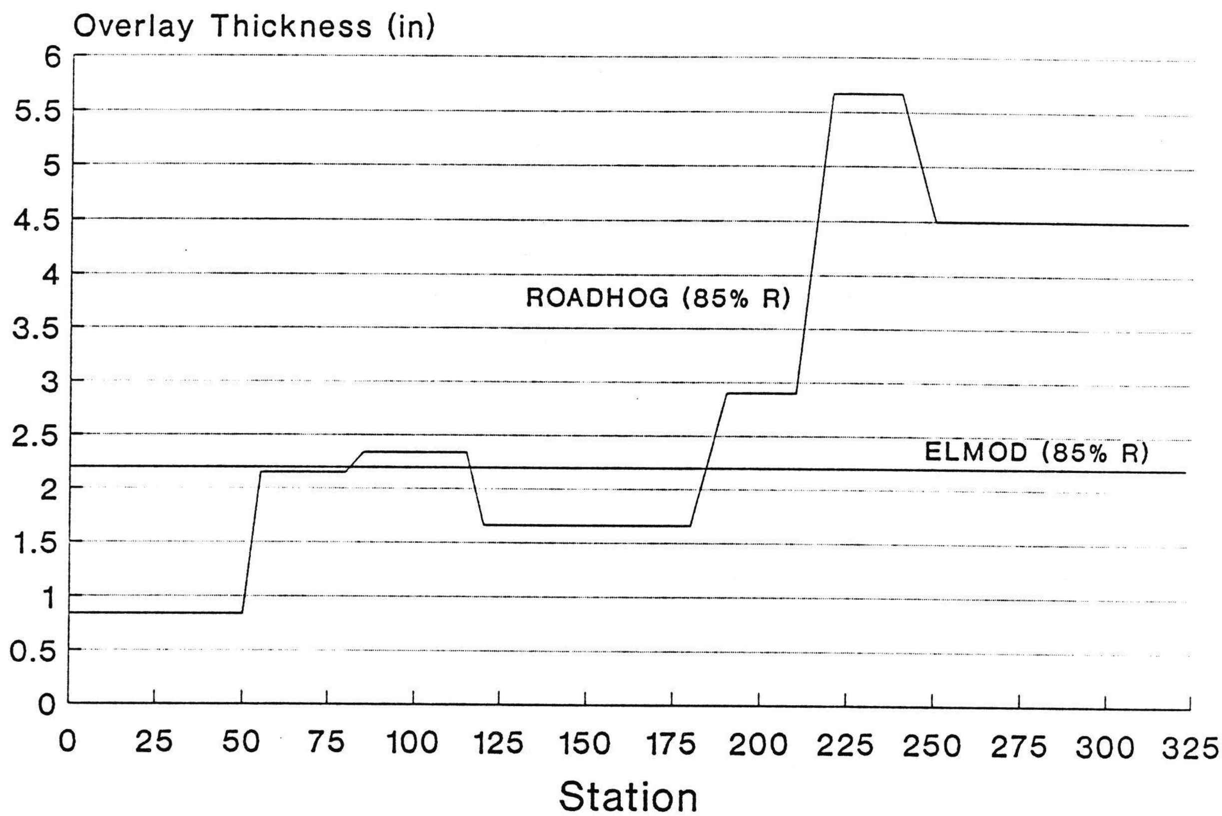

Figure 7.3 ROADHOG Analysis Unit Design versus ELMOD Single-Thickness Design.

units. ROADHOG remains conservative in some areas, but compensates in terms of the overall project by optimizing the design in areas that do not require the full structural overlay thickness.

7.2 DESIGN RELIABILITY

One difficulty in making meaningful comparisons between the ELMOD and ROADHOG procedures is the method of applying a reliability level to the design. Reliability is the probability that a design will perform as intended for the design period. Thus a design with "50 percent reliability" has a 50 percent chance of performing satisfactorily; conversely, the design has a 50 percent chance of failing during the design period. In this respect, the use of the term "Reliability" as applied to the ELMOD design and as applied in Figure 7.2 to the ROADHOG design is not technically correct. Nevertheless, that term will continue to be used in this discussion for lack of a better term.

In NDT overlay design, a level of reliability can be applied to the required thickness at each individual NDT test point (referred to as "station-by-station" in earlier sections), to the overall average required thickness, or to both. However, the meaning of applying a reliability to the average required thickness from thicknesses already determined at a reliability level is unclear. An intensive, in-depth study is needed to determine a meaningful method of handling reliability in overlay design.

Until such a method becomes available, using a reliability level of 50 percent to generate station-by-station thicknesses and then applying a design reliability level to the average required thickness (e.g. Equation 7.1) should produce realistic overlay designs. If the project is being designed with analysis units, this procedure should be applied to each individual unit; the units are then "connected" to form the overlay project.

7.3 CONCLUSIONS

The ROADHOG overlay design procedure provides a method for selecting reasonable overlay thicknesses based on the structural deficiency approach. ROADHOG is straightforward, easy to use, and yet is a powerful analytical tool. Its major advantages are speed, extreme flexibility, and ability to aid the designer in optimizing a design through analysis unit delineation. Primary disadvantages include the lack of refinements to existing pavement and subgrade modulus characterization, such as provisions for testing time of year and past performance data. Also, the present lack of clear understanding of design reliability for overlays may be detrimental.

In addition to this general conclusion relative to the ROADHOG procedure, numerous more specific conclusions were made during the course of this study. Most of these have been expressed through out this report in the various chapters. For the reader's convenience, the more prominent of these are restated here.

BACK CALCULATION OF SUBGRADE M_r

1. Major sources of error in back calculating the moduli of pavement layers from NDT data are lack of knowledge relative to subgrade depth to bedrock and the fact that the back calculation schemes are based on static loading theroies.
2. Of these, the static loading assumption may be the more critical since depth to bedrock does not effect the surface deflection casued by a dynamic load as much as the static theory suggests (Figure 3.20 and Table 3.11).
3. Of the various back calculation methods evaluated, only ILLI-3 consistently provided reasnonable values of M_r.
4. The ILLI-PAVE algorithms (including ILLI-3) are the only back calcula-

tion methods that provide a subgrade modulus that is consistent with the value used in the used for the AASHO Raod Test Subgrade in the AASHTO Guide design equation.

EFFECTIVE STRUCTURAL NUMBER

1. The effective structural number of the existing pavement (SN_{eff}) should be determined independent of the subgrade modulus.
2. The difference between the deflection at the center of loading and the deflection at a distance from the center equal to the total pavement thickness (surface+base+subbase) is relatively independent of the subgrade modulus.
3. This deflection difference can be used as the measure of SN_{eff}.

AASHTO REMAINING LIFE FACTOR

1. The remaining life cocept as presently contained in the AASHTO Guide is flawed. Its use in overlay design produces incosistencies indesign thicknesses.
2. An alternative approach to remaining life deveoped in this study was found to produce F_{RL} values of 1.0 in all pracitcal cases. As a result, the AASHTO remaining life factor was not included in ROADHOG.

TRANSFER FUNCTIONS

1. Transfer Functions for mechanistic design of asphalt pavements should represent the two most predominate load related failure modes - fatigue cracking in the AC layer and surface rutting due to overstressing the subgrade.
2. The two failure modes can be represented adequately by a single Transfer Function based on surface deflection.
3. The general form of the fatigue transfer function is:

$$\log N = K + n \log (1/eac) + b \log (1/Eac) \quad \text{(Eq 2.2)}$$

Reasonable and practical values for the n and b coefficients are 3.0 and 0.0 respectively.

4. For practical design purposes, it may be necessary to develop two fatigue functions, one for Full Depth AC pavements and another for conventional (AC over granular base) flexible pavements.
5. A subgrade stress ratio transfer function was found to be at least as reliable as the more commonly use subgrade strain function and, from a practical standpoint, may be preferred.

7.4 IMPLEMENTATION STATEMENT

The overlay design procedure developed under this study is ready for immediate implementation. ROADHOG was prepared to be a user friendly program that can be directly incorporated into routine AHTD engineering design practice. Also, to aid in the implementation, a user's guide was prepared under the project to assist the designer. The user's guide is reproduced in this report as Appendix A.

Nevertheless, the project staff recommends that for at least the first year of use careful scrutiny be given to all design thicknesses determined by ROADHOG to see if they are reasonable. This probably can be accomplished best by AHTD's research staff who currently perform most overlay thickness design analyses for AHTD using ELMOD.

The project staff also recommends that a short training program (1 day) be conducted for the design staff prior to complete implementation of ROADHOG to routine design. Because ROADHOG is designed to be very user friendly, problems in the operation and use of the program are not expected. However, because of its ease of use, there is always a danger that gross misuse and serious design errors may be made due to a lack of understanding of the basic principles behind the procedure.

7.5 RESEARCH RECOMMENDATIONS

Successful research efforts always uncover questions for which there is no adequate answer. As a result, all research projects end with recommendations for further research. This study is no exception; and some of those questions are painfully obvious.

For example, comparison of Figures 1.2 and 1.3 show that ROADHOG does not contain all of the features envisioned for a complete AASHTO based overlay design procedure; there is no consideration of the time of year of the NDT testing and no consideration of past traffic and current pavement condition. Also from Chapter 3, it should be clear that many questions remain to be answered relative to the back calculation of the subgrade resilient modulus. The following is a listing of research needed to improve and complete the overlay design process.

1. TIME OF YEAR ADJUSTMENT - The spring thaw and seasonal variations in subgrade moisture are generally believed to cause seasonal variations in the subgrade resilient modulus. This effect is typically accounted for in overlay design by adjusting the subgrade modulus to some "standard time of year". One of the objectives of this study was to establish time of year adjustments for Arkansas. It was envisioned that the adjustment would include consideration of three factors: 1) time of testing, 2) area within the State, and 3) soil type. However, none of the data available to the study provided justification for establishing an adjustment method. NDT data from this study, from TRC-94, and from the load limit study being conducted by AHTD were reviewed in an attempt to identify patterns of seasonal variations. No consistent

pattern was found. However, this does not necessarily mean that no seasonal adjustment is needed. Most of the available data were collected during years that had relatively dry springs and mild winters.

2. OVERLAY PERFORMANCE REVIEW - A significant weakness of most overlay design procedures is the lack of an adequate data base of past performance. ROADHOG is no exception. The comparison discussed earlier in this chapter between ROADHOG and ELMOD showed ROADHOG to be somewhat more conservative by requiring a slightly greater overlay thickness. Unfortunately, however, this does not tell which thickness is "right". They may both be conservative or may both be inadequate. The performance of overlays that have been designed using NDT should be closely monitored; and, when sufficient data is available, the procedure should be adjusted to fit that performance.
3. IMPROVED PAVEMENT MODEL - The efforts to select a method for determining the subgrade resilient modulus (Chapter 3) revealed that there are many problems with the currently available back calculation methods. One major problem was shown to be the fact that the pavement structural models are based on static loading. A pavement model is needed that is based on structural dynamics. Although the development of such a model appears to be fundamental and theoretical, the dynamic analyses performed as a part of this study show that use of the model could have very significant practical implications.
4. DESIGN RELIABILITY - The concept of design reliability was introduced to routine pavement design with the 1986 AASHTO Guide (1). While the concept is valid and useful, there are many questions regarding its application in overlay design. Major questions that need to be answered pertain to the overall standard deviation of overlay performance and

the effect of the point-by-point design approach used by ROADHOG. The point-by-point approach (i.e. determining a required thickness for each NDT test location) is considered to be a strong point of the ROADHOG procedure; however, it invalidates some of the assumptions of the AASHTO reliability approach to design. A study is needed to identify a proper approach for considering reliability within ROADHOG and for giving the designer guidance on the appropriate reliability level to use in selecting overlay thicknesses.

5. EFFECT OF PAVEMENT CONDITION - The condition of the existing pavement at the time the overlay is placed has a pronounced effect on how well the overlay performs. The AASHTO Guide attempted to consider this effect by the incorporation of a remaining life factor in the overlay design. Unfortunately the AASHTO remaining life approach was found to be flawed (Chapter 5). Nevertheless, some method for considering the current condition and past performance of the existing pavement is needed to make the design process complete.

REFERENCES

1. "AASHTO Guide for Design of Pavement Structures", American Association of State Highway and Transportation Officials, Washington, D.C., 1986.

2. Clipper™, a dBASE™ compiler, product of the Nantucket Corporation, Los Angeles, California.

3. "Predictive Design Procedure, VESYS Users Manual", Federal Highway Administration, Report No. FHWA-RD-77-154, 1978.

4. Finn, F., Saraf, C.L., Kulkarni, R., Nair, K., Smith, W., and Abdullah, A., "Development of Pavement Structural Subsystems", Final Report, Project 1-10B, National Cooperative Highway Research Program, 1977.

5. "Thickness Design - Asphalt Pavements for Highways and Streets", Manual Series No. 1, The Asphalt Institute, 1981.

6. "Shell Pavement Design Manual", Shell International Petroleum Company Limited, London, 1978.

7. "Asphalt Overlays for Highway and Street Rehabilitation", Manual Series No. 17, Second Edition, The Asphalt Institute, 1983.

8. Thompson, M.R. and Elliott, R.P., "ILLI-PAVE Design Algorithms for Flexible Pavements", Transportation Research Record 1043, Transportation Research Board, 1985.

9. Gomez-Achecar, M. and Thompson, M., "Mechanistic Design Concepts for Full-Depth Asphalt Concrete Pavements", Illinois Cooperative Highway and Transportation Series No. 207, University of Illinois at Urbana-Champaign, 1984.

10. Pell, P.S., "Dynamic Stiffness and Fatigue Strength of Bituminous Materials", Lecture notes presented in a course at the University of Nottingham, England, March 1982.

11. Bonnaure, F., Gravois, A., and Udron, J., "A New Method for Predicting the Fatigue Life of Bituminous Mixes", Proceedings of the Association of Asphalt Paving Technologists, 1980.

12. Kingham, R.I., "Failure Criteria Developed from AASHO Road Test Data", Third International Conference on the Structural Design of Asphalt Pavements, London, England, 1972.

13. Witczak, M.W., "Design of Full-Depth Asphalt Airfield Pavements", Research Report 72-2, The Asphalt Institute, 1972.

14. Finn, F.N., "Factors Involved in the Design of Asphaltic Pavement Surfaces", NCHRP Report 39, 1967.

15. Pell, P.S., "Characterization of Fatigue Behavior", Special Report 140, Highway Research Board, 1973.

16. Elliott, R.P. and Thompson, M.R., "ILLI-PAVE Mechanistic Analysis of AASHO Road Test Flexible Pavements", Transportation Research Record 1043, Transportation Research Board, 1985.

17. Van Dijk, W., "Practical Fatigue Characterization of Bituminous Mixes", Proceeding of the Association of Asphalt Paving Technologists, 1975.

18. "Research and Development of The Asphalt Institute's Thickness Design Manual (MS-1) Ninth Edition", Research Report No. 82-2, The Asphalt Institute, 1982.

19. Elliott, R.P. and Thompson, M.R., "Mechanistic Design Concepts for Conventional Flexible Pavements", Illinois Cooperative Highway and Transportation Series No. 208, University of Illinois, 1985.

20. Elliott, R.P. and Herrin, M., "Asphalt Q.A. Specifications - Influence of Significant Material Factors and Development of a Rational Payment Schedule", Illinois Cooperative Highway and Transportation Series No. 203, University of Illinois, 1983.

21. Maupin, Jr., G.H., and Freeman, Jr., J.R., "Simple Procedure for Fatigue Characterization of Bituminous Concrete", Report No. FHWA-RD-76-102, Federal Highway Administration, 1976.

22. Pell, P.S. and Cooper, K.E., "The Effect of Testing and Mix Variables on the Fatigue Performance of Bituminous Mixes", Proceedings of the Association of Asphalt Paving Technologists, 1977.

23. Sharma, M.G. and Larson, T.O., "Mechanical Characterization of Materials", Volume 4, Report PTI 7509, The Pennsylvania Transportation Institute, The Pennsylvania State University, 1971.

24. Knutson, R.M., Thompson, M.R., Mullin, M.R., and Tayabji, S.D., "Material Evaluation Study - Ballast and Foundation Materials Research Program", U.S. Department of Transportation, Federal Railroad Administration, Report No. FRA-OR&D-77-02, 1977.

25. Poulsen and Stubstadt, "Laboratory Testing of Cohesive Subgrades: Results and Implications Relative to Structural Design and Distress Models", Transportation Research Record 671.

26. Barker, W.R., Brabston, W.N., and Chou, Y.T., "A General System for the Design of Flexible Pavements", Volume I, Proceedings of the Fourth International Conference on the Structural Design of Asphalt Pavements, University of Michigan, 1977.

27. Walker, R.N., Patterson, W.D.D., Freeme, C.R., and Marais, C.P., "The South African Mechanistic Pavement Design Procedure", Fourth International Conference on the Structural Design of Asphalt Pavements, Ann Arbor, Michigan, 1977.

28. Maree, J.H. and Freeme, C.R., "The Mechanistic Design Method Used to Evaluate the Pavement Structures in the Catalogue of Draft TRH4 1980", Technical Report P/2/81, National Institute for Transport and Road, CSIR, South Africa, 1981.

29. Chou, Y.T., "Assess Subgrade Rutting Potential by Stress Factor", Journal of Transportation Engineering, Volume 109, No.3, May, 1983.

30. "The AASHO Road Test, Report 5 - Pavement Research", Special Report 61E, Highway Research Board, 1962.

31. Lister, N.W. and Kennedy, C.K., "A System for the Prediction of Pavement Life and Design of Pavement Strengthening", Proceedings of the Fourth International Conference on Structural Design of Asphalt Pavements, University of Michigan, 1977.

32. Brown, S.F., Pell, P.S., and Stock, A.F., "The Application of Simplified, Fundamental Design Procedures for Flexible Pavements", Volume I, Proceedings of the Fourth International Conference on the Structural Design of Asphalt Pavements, University of Michigan, 1977.

33. Kingham, R.I., "Development of the Asphalt Institute's Deflection Method for Designing Asphalt Concrete Overlays for Asphalt Pavements", Research Report 69-3, The Asphalt Institute, 1969.

34. Brabston, W.N., Barker, W.R., and Harvey, G.G., "Developement of Structural Design Procedure for All-Bituminous Concrete Pavements for Military Roads", Technical Report S-75-10, Waterways Experiment Station, 1975.

35. Chou, Y.T., Hutchinson, R.L., and Ulery, H.H., Jr., "A Design Method for Flexible Airfield Pavements", Transportation Research Record 521, 1974.

36. Claussen, A.I.M., Edwards, J.M., Sommer, P., and Uge, P., "Asphalt Pavement Design - The Shell Method", Volume I, Proceedings of the Fourth International Conference on the Structural Design of Asphalt Pavements, University of Michigan, 1977.

37. Dorman, G.M. and Metcalf, C.T., "Design Curves for Flexible Pavements Based on Layered System Theory", Highway Research Record 71, 1965.

38. Edward, J.M. and Valkering, C.P., "Structural Design of Asphalt Pavement for Heavy Aircraft", Koninklijke/Shell Laboratorium, Amsterdam.

39. Finn, F.N., Nair, K., and Monismith, C.L., "Applications of Theory in the Design of Asphalt Pavements", Proceedings of the Third International Conference on the Structural Design of Asphalt Pavements, London, 1972.

40. Finn, F., Saraf, C.L., Kulkarni, R., Nair, K., Smith, W., and Abdullah, A., "The Use of Distress Prediction Subsystems for the Design of Pavement Structures", Proceedings of the Fourth International Conference on Structural Design of Asphalt Pavements, University of Michigan, 1977.

41. Peattie, K.R., "A Fundamental Approach to the Design of Flexible Pavements", Proceedings of the International Conference on the Structural Design of Asphalt Pavements, University of Michigan, 1962.

42. Santucci, L.E., "Thickness Design Procedure for Asphalt and Emulsified Asphalt Mixes", Volume I, Proceedings of the Fourth International Conference on the Structural Design of Asphalt Pavements, University of Michigan, 1977.

43. Southgate, H.F., Deen, R.C., Havens, J.H., and Drake, Jr., W.B., "Kentucky Research: A Flexible Pavement Design and Management System", Volume I, Proceedings of the Fourth International Conference on the Structural Design of Asphalt Pavements, University of Michigan, 1977.

44. "Pavement Management Guide", Roads and Transportation Association of Canada, 1977.

45. Boussinesq, J., "Application des Potentials a L'Etude de L'Equilibre et du Mouvement des Solides Elastiques," Paris, 1883.

46. Love, A. E. H., "Treatise on the Mathematical Theory of Elasticity," Cambridge University Press, 1923.

47. Burmister, D.M., "The Theory of Stresses and Displacements in Layered Systems and Applications to the Design of Airport Runways," Highway Research Board, Proceedings of the Twentieth Annual Meeting, 1943.

48. Burmister, D.M., "The General Theory of Stresses and Displacements in Layered Systems," Journal of Applied Physics, Volume 16, 1945.

49. Whiffin, A.C., and Lister, N.W., "The Application of Elastic Theory to Flexible Pavements," Proceedings of the International Conference on the Structural Design of Asphalt Pavements, " University of Michigan, 1962.

50. Schiffmam, R.L., "General Analysis of Stress and Displacements in Layered Elastic Systems," Proceedings of the International Conference on the Structural Design of Asphalt Pavements," University of Michigan, 1962.

51. Uddin, W., Meyer, A.H., and Hudson, R., " A User's Guide for Pavement Evaluation Programs RPEDD1 and FPEDD1," Research Report 387-2, University of Texas at Austin, August, 1985.

52. Weaver, W. and Johnson, P.R., "Finite Elements for Structural Analysis," Prentice-Hall, 1984.

53. "Standard Method for Nondestructive Static Plate Load Tests of Soils and Flexible Pavement Components, For Use in Evaluation and Design of Airport and Highway Pavements," 1966 Book of ASTM Standards, Part 11, Philadelphia, 1966.

54. Heft 1-6 Veroffentlichungen des Instituts der Dettschen Forschungsgesellschaft fur Bodenmechanik (Degebo) as referenced in [56].

55. Jones, R. and Whiffin, A.C., "A Survey of Dynamic Methods of Testing Roads and Highways," Highway Research Board, Bulletin No. 277, 1960.

56. Nijboer, L.W., and Van der Poel, C., "A study of Vibration Phenomena in Asphaltic Road Construction," Proceedings of the Association of Asphalt Paving Technologists, Volume 22, 1953.

57. Heukelom, W., and Klomp, A.J.G., "Dynamic Testing as a Means of Controlling Pavements During and After Construction," Proceedings of the International Conference on the Structural Design of Asphalt Pavements, University of Michigan, 1962.

58. Jones, R., "Measurement and Interpretation of Surface Vibrations on Soil and Roads," Highway Research Board, Bulletin No. 277, 1960.

59. Bohn, A.O., "Danish Experiments with the French Falling Ball Deflectometer," Proceedings of the Second International Conference on the Structural Design of Asphalt Pavements, University of Michigan, 1967.

60. Bohn, A.O., Ullidtz, P., Stubstad, R., and Sorensen, A., "Danish Experiments with the French Falling Weight Defloctometer," Proceedings of the Third International Conference on the Structural Design of Asphalt Pavements, London, 1972.

61. Dynatest Consulting, Inc., Dynatest 8000 FWD Test System, General Equipment Booklet, Ojai CA, 1986.

62. Larsen, H.J.E., and Stubstad, R.N., "The Use of Nondestructive Testing in Flexible Pavement Rehabilitation Design," International Symposium on Bearing Capacity of Airfields, Trondheim Norway, 1982.

63. Kilareski, W.P., and Anani, B.A., "Evaluation of In-Situ Moduli and Pavement Life from Deflection Basins," Proceedings of the Fifth International Conference on the Structural Design of Asphalt Pavements, University of Michigan, 1982.

64. Tholen, O., Sharma, J., and Terrel, R.L., "Comparison of Falling Weight Deflectometer with Other Deflection Testing Devices," Transportation Research Board, 1007, 1985.

65. Lindly, J.K., Pumphrey Jr., N.D., White, T.D., and Andersen, V.L., "Evaluation and Comparison of Various NDT Devices in Side-by-Side Testing on Indiana Highways," Proceedings of the Sixth International Conference on the Structural Design of Asphalt Pavements, University of Michigan, 1987.

66. Irwin, Lynne H., "Determination of Pavement Layer Moduli from Surface Deflection Data for Pavement Performance Evaluation," Proceedings of the Fourth International Conference on the Structural Design of Asphalt Pavements, University of Michigan, 1977.

67. Uddin, W., Meyer, A.H., and Hudson, W.R., "A Flexible Pavement Structural Evaluation System Based on Dynamic Deflections," Proceedings of the Association of Asphalt Paving Technologists, 1985.

68. Uddin, W., Meyer, A.H., and Hudson, W.R., "Rigid Bottom Considerations for Nondestructive Evaluation of Pavements," Transportation Record 1070, Transportation Research Board 1986.

69. Bush, Albert J. and Alexander, Don R., "Pavement Evaluation Using Deflection Basin Measurements and Layered Theory, " Transportation Research Record 1022, Transportation Research Board, 1985.

70. Bush, Albert, J., BISDEF Computer Code, Version DRA-11.87.30.

71. Raad, L. Figueroa, J.L., "Load Response of Transportation Support Systems," Transportation Engineering Journal, 1980.

72. Duncan, J.M., Monismith, C.L., and Wilson, E.L., "Finite Element Analyses of Pavements," Highway Research Record, 1968.

73. Mamlouk, M.S., "Use of Dynamic Analysis in Predicting Field Multilayer Pavement Moduli," Transportation Research Record 1043, Transportation Research Board, 1986.

74. Desalvo, Gabriel J., and Gorman, Robert W. Ansys Engineering Analysis System User's Manual for ANSYS Revision 4.3, Houston PA, 1987.

75. Hoffman, M.S., and Thompsom, M.R., "Nondestructive Testing of Flexible Pavements - Field Testing Program Summary," Transportation Engineering Series 31, University of Illinois at Urbana-Champaign, Illinois Cooperative Highway and Transportation Research Program Series 188, June 1981, as Referenced in [73].

76. Bush, Albert J., BASIN Computer Code, Version DRA-11.87.09.

77. Uddin, Waheed, "A Structural Evaluation Methodology for Pavements Based on Dynamic Deflections," Ph.D. Dissertation, University of Texas, 1984, as Referenced in [67].

78. Thompson, M.R., and Robnett, Q., "Final Report - Data Summary, Resilient Properties of Subgrade Soils," Transportation Engineering Series No. 14, University of Illinois, Urbana, Illinois, 1976.

79. Elliott, R.P., et al, "Final Report, TRC-94, Resilient Properties of Arkansas Subgrades," Report No. UAF-AHTRC-88-002, Arkansas Highway and Transportation Research Center, University of Arkansas, Fayetteville, 1988.

80. "Remaining Life Considerations in Overlay Design," Appendix CC, Vol.2, AASHTO Guide for Design of Pavement Structures, American Association of State Highway and Transportation Officials, Washington, D.C., 1986.

81. Gomez, M. and Thompson, M., "Structural Coefficients and Thickness Equivalency Ratios," Transportation Engineering Series 38, University of Illinois, Urbana-Champaign, 1983.

82. Dunn, Jr., H.D., "A Study of Four Stabilized Base Courses," Ph.D. Dissertation, Department of Civil Engineering, Pennsylvania State University, University Park, 1974.

83. Elliott, R.P., "Rehabilitated AASH(T)O Road Test - Analysis of Performance Data Reported in Illinois Physical Research Report 76," QIP-101, National Asphalt Pavement Association, Riverdale, MD, 1981.

84. Wang, M.C., and Larson, T.D., ""Performance Evaluation of Bituminous Concrete Pavements at the Pennsylvania State Test Track," Transportation Research Record 632, TRB, National Research Council, Washington, D.C., 1977. pp. 21-27.

85. Finn, F.N., and C.L. Monismith, "Asphalt Overlay Design Procedures," NCHRP Synthesis No. 116, TRB, National Research Council, Washington, D.C., 1984.

86. "Pavement Maintenance Management," Technical Manual TM 5-623, Headquarters, Department of the Army, Washington, D.C., November 1982.